DESIGN, SYNTHESIS, AND EVALUATION OF CYSTEINE PROTEASE INHIBITORS

A Dissertation
Presented to
The Academic Faculty

By

Sylvia Shadinger Bridges

In Partial Fulfillment
Of the Requirements for the Degree
Doctor of Philosophy in Chemistry

Georgia Institute of Technology

August, 2008

DESIGN, SYNTHESIS, AND EVALUATION OF CYSTEINE PROTEASE INHIBITORS

Approved by:

Dr. James C. Powers, Advisor
School of Chemistry and Biochemistry
Georgia Institute of Technology

Dr. Donald Doyle
School of Chemistry and Biochemistry
Georgia Institute of Technology

Dr. Jonathan Glass
Department of Neurology
Emory University

Dr. Wendy L. Kelly
School of Chemistry and Biochemistry
Georgia Institute of Technology

Dr. Sheldon May
School of Chemistry and Biochemistry
Georgia Institute of Technology

Date Approved: May 23, 2008

DEDICATION

For my husband, Ben T. Bridges,

and

For my son, Wilson Bridges.

ACKNOWLEDGEMENTS

There are many people I have to thank for gifting me the tools necessary to complete this journey. First and foremost is Dr. James C. Powers, my advisor. Dr. Powers expertly walked the fine line between giving me the advice I needed to successfully complete my projects and prodding me to figure out my dilemmas myself. Both teaching methods have left me with skills that will serve me for a lifetime. His demonstration of how to develop and carryout a research project has been vital to my education.

I would also like to thank my thesis committee members, Dr. Donald Doyle, Dr. Jonathan Glass, Dr. Wendy Kelly, and Dr. Sheldon May. Their comments and thoughtful evaluation of my work were vital to my success. For their time and energy spent reading and reviewing my work, I am grateful.

To my co-workers in the lab, my day-to-day helpers and companions, I thank you for the hours spent teaching me and allowing me to teach you in turn. Juliana Asgian, Karen Ellis James, Brian Rukamp, Karrie Rukamp, Özlem Doğan Ekici, Marion Götz, and Amy Campbell were all essential in shaping both my research and who I am as a scientist. I am also thankful for research scientist Zhao Zhao Li for her excellent advice and knowledge in organic synthesis. For the many hours of commiseration, advice, training, and friendship I am very grateful.

My success is in large part due to the loving support of my family. For my parents, Dr. and Mrs. Richard and Marilyn Shadinger, who raised me to believe that I could achieve anything I set my mind to, and proudly supported my dream of becoming a chemist, I am eternally grateful. My husband, Ben T. Bridges has been my constant supporter during this academic journey. His belief in me and my abilities has been the motivation that has pushed me past the bumps in the road to be the best that I can be. For his loving support I will always be thankful. And to my son, Wilson Bridges, whose sunny smile and joy for life has given me extra incentive to make this world a better place, Mommy loves you.

TABLE OF CONTENTS

LIST OF TABLES

LIST OF FIGURES

LIST OF ABBREVIATIONS

Å	angstrom
AA	amino acid
AArg	aza-arginine
AAsp	aza-aspartic acid
Abu	aminobutyric acid
Ac	acetate
AHph	aza-homophenylalanine
ALeu	aza-leucine
ALys	aza-lysine
AMC	aminomethylcoumarin
AOrn	aza-ornathine
Arg	arginine
Asp	aspartic acid
Bis-Tris	Bis(2-hydroxyethyl)iminotris(hydroxymethyl)methane
Boc	*t*-butyloxycarbonyl
Brij	polyoxyethylene lauryl ether
Bzl	benzyl
^{o}C	degrees Celsius
C-terminal	carboxy-terminal
Ca	calcium

Casp	caspase
Cbz	benzyloxycarbonyl
$CDCl_3$	deuterated chloroform
CDI	carbonyldiimidazole
CHAPS	3-[(3-cholamidopropyl)dimethylammonio]propanesulfonic acid
CMK	chloromethylketone
CNS	central nervous system
Cys	cysteine
DIC	diisopropylcarbonyldiimidazole
d_6-DMSO	deuterated dimethylsulfoxide
DMF	dimethylformamide
DMSO	dimethylsulfoxide
DTT	dithiothreitol
EDC	1-ethyl-3-(3-dimethylaminopropyl)carbodiimide hydrochloride
EDTA	ethylenediaminetetraacetic acid
EP	epoxide
EPS	epoxysuccinate
eq	equivalents
ESI	electron spray ionization
Et	ethyl
EtOAc	ethyl acetate

EtOH	ethanol
FAB	fast atom bombardment
FMK	fluoromethylketone
Fmoc	9-fluorenylmethyloxycarbonyl
g	gram
Gln	glutamine
Glu	glutamic acid
Gly	glycine
^{1}H NMR	proton nuclear magnetic resonance
HEPES	4-(2-hydroxyethyl)-1-piperazineethanesulfonic acid
His	histidine
HOBT	1-hydroxybenzotriazole
hr	hour
HRgpA	Gingipain R, catalytic and hemagglutinin adhesion domains, from the gene *rgpA*
HRMS	high resolution mass spectrometry
I	inhibitor
IBCF	isobutylchloroformate
IC_{50}	concentration of I at 50% inhibition
ICE	interleukin-1β converting enzyme
Ile	isoleucine
k_2	second order rate constant
Kgp	gingipain K

K_I	inhibition equilibrium constant
K_M	Michaelis constant
k_{obs}	observed rate constant
KRH	Krebs-Ringer-Hepes solution (125 mM NaCl, 5 mM KCl, 1.2 mM $MgSO_4$, 1.2 mM KH_2PO_4, 2 mM $CaCl_2$, 6 mM glucose and 25 mM Hepes, pH 7.4)
λ	wavelength
Leu	leucine
Lys	lysine
M	molar
Me	methyl
MeOH	methanol
min	minute
mg	milligram
MHz	megahertz
mL	milliliter
mM	millimolar
mmol	millimole
m/z	mass to charge ratio
µL	microliter
µM	micromolar
MS	mass spectrometry
N	normal

N-terminal	amino-terminal
p-NA	*para*-nitroanaline
NaAc	sodium acetate
ND	not determined
NI	no inhibition
nm	nanometers
NMM	*N*-methylmorpholine
$[P]_{\infty}$	product at time ∞
$[P]_t$	product at time t
PBS	phosphate buffered saline
PDB	protein data bank
Phe	phenylalanine
PhPr	phenylpropyl
Pipes	1,4-Piperazinebis(ethanesulfonic acid)
Pro	proline
RgpB	Gingipain R, catalytic domain, from the gene *rgpB*
s	seconds
SAR	structure-activity relationship
sat	saturated
Suc	succinate
t	time

*t*Bu	*tert*-butyl
TFA	trifluoroacetic acid
THF	tetrahydrofuran
Thr	threonine
TIPS	triisopropylsilane
TLC	thin layer chromatography
TNFα	tumor necrosis factor alpha
TRIS-HCl	2-amino-2-hydroxymethyl-1,3-propanediol hydrochloride
Trp	tryptophan
p-TsOH	para-toluenesulfonic acid
Tyr	tyrosine
u	units
Val	valine
v_o	velocity at time 0
VS	vinyl sulfone
v_t	velocity at time t
Z	benzyloxycarbonyl

SUMMARY

Proteases are enzymes that cleave protein amide bonds. Proteases are involved in a myriad of biological processes and are considered favorable targets for drug design. The proteases described herein are cysteine proteases, which utilize a cysteine residue thiol to attack the amide carbonyl, leading to amide bond cleavage. Irreversible inhibitors of cysteine proteases react with the active site cysteine, forming a covalent bond and rendering the enzyme inactive.

The first project involved the design and synthesis of aza-peptide epoxide inhibitors for calpain, a clan CA, ubiquitous, calcium-activated human enzyme involved in neurodegeneration. These inhibitors proved to be poor inactivators of calpain, demonstrating that the aza-peptide epoxide is a warhead specific to clan CD cysteine proteases (caspases, gingipains). Subsequently, a known epoxide inhibitor of calpain was optimized to create a more potent inhibitor. Several of these inhibitors were more potent than the parent, and all were demonstrated to inhibit calpain in a breast cancer cell line which was treated with paclitaxel to spike calpain activity.

The second project involved the design and solid phase synthesis of aza-peptide Michael acceptor caspases inhibitors. The two goals of this project were to develop a solid phase method for synthesis of inhibitors that are tedious to synthesize in solution phase, and to use a variety of amino acid residues to determine the optimal interactions in

the P3' position for various caspases. The synthesis was successful, and the optimal P3' residues were determined.

The third project involved the kinetic evaluation of aza-peptide epoxide and Michael acceptor inhibitor designed for the gingipains. Gingipains K and R are virulence factors in the pathology of *Porphyromonas gingivalis* involved in gingivitis and periodontal disease. These inhibitors proved to be extremely potent inactivators of gingipains, with some of the highest rates of inhibition measured in the Powers laboratory. Gingipain K preferred larger, aromatic moieties in the P1' position, while gingipain R preferred the Michael acceptor inhibitors, with the P1' substituent having less of an impact on potency.

CHAPTER ONE

INTRODUCTION

Proteases. Proteases are enzymes that hydrolyze amide bonds of peptide substrates. These enzymes are present in all living organisms, and comprise more than 2% of the human genome.[1] Proteases are involved in a large number of biological regulatory processes and systems, such as simple food digestion, protein activation, and protein synthesis. Proteases are involved in inflammation, fertilization, allergic reactions, cell growth and death, blood clotting, tumor growth, and bone remodeling. Because of the ubiquitous nature of proteases in biological processes, they have been prime targets of inhibitor design and have been identified as therapeutic targets for many diseases and conditions.

Protease Clans. Proteases have been divided into classes, clans, and families based on their mechanism of action and overall structural fold (Figure 1.1).[2,3] The first division of proteases is made based on the active site catalytic residue. Aspartate proteases catalyze hydrolysis through an aspartic acid residue side chain in complex with a water molecule. Metallo-proteases contain a metal cation, for example zinc, which complexes with a water molecule, rendering the water molecule nucleophilic enough to perform the hydrolysis. Serine proteases catalyze hydrolysis through reaction of the serine side chain hydroxyl moiety with the substrate carbonyl. Threonine and tyrosine proteases react

similarly to serine proteases. Lastly, cysteine proteases catalyze peptide bond hydrolysis through nucleophilic reaction of the cysteine thiol with the substrate carbonyl.

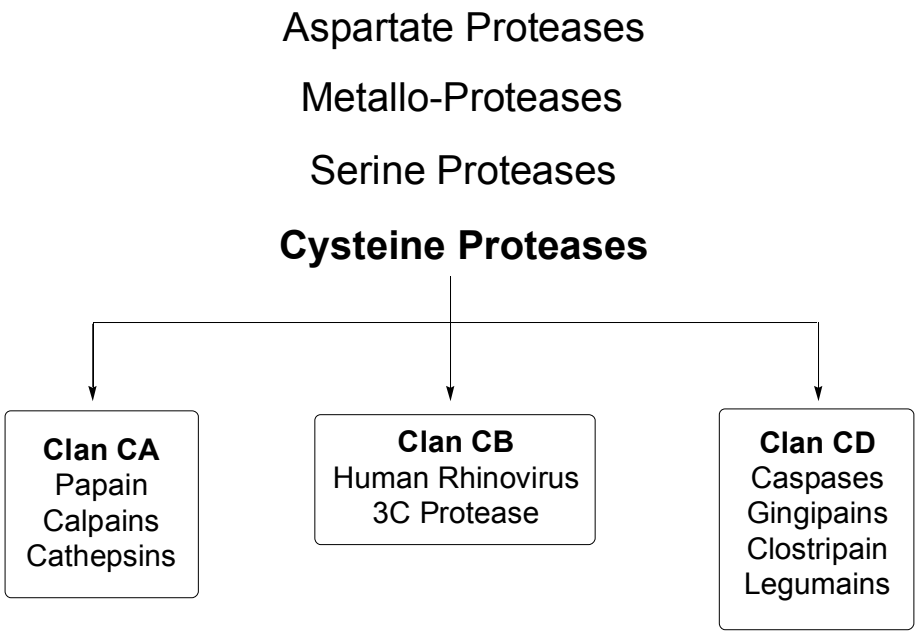

Figure 1.1. Cysteine Protease Clans.

Each of these types of proteases is further partitioned into clans based on the overall structural fold. The clans are given the names AX, SX, MX, and CX, with the first letter delineating the catalytic residue. The second letter is arbitrary, and divides the proteases by structure and fold. All of the work presented herein involves cysteine proteases.

Protease Nomenclature. Substrate peptides bind with proteases along the active site cleft. The substrate residue side chains interact with various enzyme pockets on both sides of the scissile amide bond. Proteases have varying substrate sequence specificity based on the size, shape, and position of these subsite pockets. Protease nomenclature was developed by Schecter and Berger in 1967 and can be seen in Figure 1.2.[4] This system allows for clear discussion of protease active site pockets and substrate residues, as well as their interaction with each other. All protease subsites and substrate residues are named based on their proximity to the scissile bond. The enzyme pockets that interact with substrate residue side chains are named S1, S2, S3, and so on increasing from the scissile bond towards the *N*-terminus of the substrate. The enzyme subsites towards the *C*-terminus are named S1', S2', S3', and so on, increasing away from the scissile bond. Substrate and inhibitor amino acid residues are named P1, P2, P3, and so on, increasing away from the scissile bond towards the N-terminus. The C-terminal residues are names P1', P2', P3', and so on, increasing away from the scissile bond.

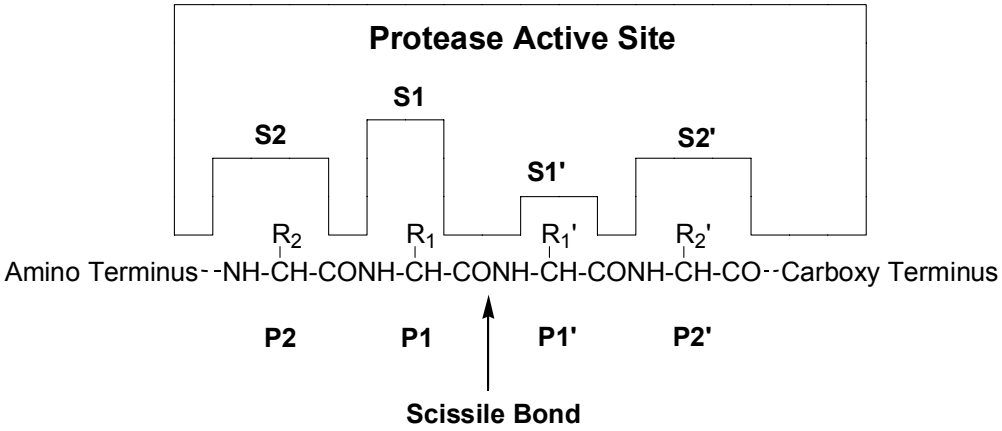

Figure 1.2. Protease Nomenclature.

Cysteine Proteases. Cysteine proteases catalyze hydrolysis through reaction of the cysteine thiol with the substrate amide carbonyl, as shown in Figure 1.3. The thiol is rendered nucleophilic through acid/base coordination with a histidine imidazole ring, which constitutes the catalytic dyad. In some proteases a third residue is involved in the positioning of the histidine residue, in which case a catalytic triad exists. The thiol attacks the carbonyl carbon generating a tetrahedral oxyanion intermediate. This intermediate is generally stabilized through interaction with an oxyanion hole in the active site containing positively charged residues. The oxyanion then collapses back to a carbon-oxygen double bond, cleaving the amide bond and releasing the *C*-terminal end of the substrate, leaving the acylated enzyme. The *N*-terminal end of the substrate is then hydrolyzed from the cysteine residue by a water molecule, regenerating the active enzyme.

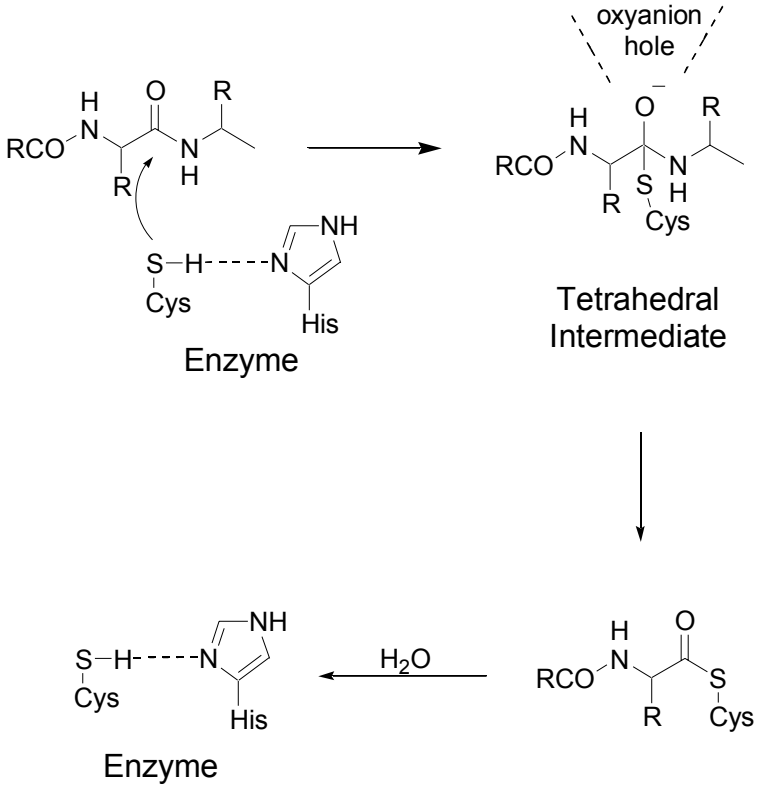

Figure 1.3. Cysteine Protease Hydrolysis Mechanism.

Clan CA Proteases and Specificity. Most cysteine proteases are members of the clan CA or the papain family of proteases. Clan CA cysteine proteases have a deep and narrow active site cleft. The representative protease of this class is papain.

Papain. Papain is the most extensively studied protease, and the first one for which a crystal structure was determined.[5] Papain is isolated from the tropical papaya fruit. Papain is considered to have a broad specificity relative to other cysteine proteases.

The S2 subsite mainly determines the substrate specificity.[5] Papain prefers bulky non-polar side chains in the S2 subsite.[5] The S1 subsite will accommodate a wide variety of residues, with a small preference for Arg or Lys.[5] The S1' subsite has a very broad specificity.[5]

Calpains. The calpains are members of the clan CA which require Ca^{2+} for protease activity. They are ubiquitous mammalian enzymes believed to be involved in neurodegeneration.[6] There are as many as 10 calpains, however the major forms present in mammals are calpain I and calpain II, which require μM and mM concentrations of Ca^{2+} for activation, respectively.[7] The calpains exist in an inactive form in the absence of Ca^{2+}, with the active site closed and a loop blocking the binding of a substrate. Calpains bind Ca^{2+} at multiple binding sites, causing a conformational change which opens the active site and swings the loop away.[8] Calpains have narrow specificity, with the preference determined by the S2 subsite. Calpains prefer an S2 Leu or Val residue.[9] The S1 subsite of the calpains can accommodate a range of aromatic and branched or unbranched aliphatic side chains.[10]

Cathepsin B. Cathepsin B is a lysosomal cysteine protease which is implicated in muscular dystrophy, bone resorption, pulmonary emphysema, and tumor metastasis.[11] Cathepsin B displays an S2 specificity for Arg due to a Glu residue in the S2 pocket, however it will also tolerate hydrophobic residues in this position.[12] Generally, hydrophobic residues are well tolerated in the S1 and S3 subsites.[11] Cathepsin B is also known to bind inhibitors with large hydrophobic sequences in the S1' to S2' region.[11]

Clan CD Proteases and Specificities. Clan CD is a much smaller group of proteases but contains some very important members. Clan CD proteases tend to have a wider, flatter active site cleft than clan CA proteases. Clan CD protease specificity is generally determined by the S1 subsite.

Caspases. Caspases compose the larger portion of clan CD proteases. As many as 11 human caspases have been identified.[13] Caspases are involved in cytokine processing, apoptosis, and inflammation.[14] All caspases require a P1 Asp residue in substrates and inhibitors for efficient binding.[14] Most caspases recognize a tetrapeptide sequence in the non-prime side of substrates and inhibitors.[14] Differences in tetrapeptide preferences provide modest differentiation between caspases.

Gingipains. Gingipains R and K are bacterial proteases isolated from *Porphyromonas gingivalis* and are important virulence factors in the progression of periodontitis.[15] The specificity of the gingipains is determined almost exclusively by the S1 subsite.[15] Gingipains R and K have a stringent requirement for a P1 Arg and Lys, respectively. Both gingipains accept a wide variety of amino acid side chains in the S2 position.[15]

Clostripain. Clostripain is a cysteine protease isolated from the Gram-positive bacterium *Clostridium hystolyticum*, which is associated with gas gangrene syndrome. Clostripain, like other clan CD proteases, determines its specificity by the S1 pocket.[16] Clostripain prefers P1 Arg or Lys residues, with a slight preference for Arg over Lys.[16]

Inhibitor Design. Inhibitors for cysteine proteases usually involve a combination of a peptide sequence preferred by the target protease along with a "warhead" moiety. The

peptide sequence binds with the protease active site, while the warhead reacts either reversibly or irreversibly with the active site cysteine thiol. When a lead compound inhibitor is discovered, the structure is usually refined through SAR studies to find the most potent and selective inhibitor analog. Reversible inhibitor warheads include aldehydes, α-ketoamides, α-ketoesters, and α-ketoacids. These inhibitors interact with the protease active site, forming the tetrahedral intermediate, but are eventually hydrolyzed, regenerating enzyme and inhibitor in an equilibrium reaction. Irreversible inhibitors of cysteine proteases have been extensively reviewed by Powers et al,[17] and include halomethylketones, epoxides, vinyl sulfones, and acyloxymethylketones. These inhibitors inactivate their protease target through alkylation of the active site cysteine thiol, permanently disabling enzyme function. As more and more protease crystal structures become available, inhibitor design can be directed through modeling and docking of potential inhibitors in the enzyme active site. There are also efforts to replace the peptide portion of inhibitors with a peptidomimetic in order to make an inhibitor that is more bioavailable and less susceptible to metabolic elimination. Such inhibitors would have increased therapeutic value.

Irreversible Inhibitor Kinetics. Irreversible inhibitors react with their target enzymes through the formation of a non-covalent enzyme-inhibitor intermediate E·I, where K_I is the dissociation constant. A covalent bond is then formed yielding E-I, with k_2 designating the first-order rate constant of the bond formation.

$$E + I \underset{}{\overset{K_I}{\rightleftharpoons}} E{\cdot}I \xrightarrow{k_2} E\text{-}I$$

In 1962 Kitz and Wilson[18] developed a method for the determination of K_I and k_2 by incubating enzyme with a large excess of inhibitor and subsequently diluting the sample into a buffer solution containing an appropriate peptide substrate with measurable cleavage properties. The residual enzyme activity v_t is hereby measured at time t of the incubation. This method is described by the following equation

$$\ln(v_t/v_o) = -k_{obs}t$$

where v_o is the initial rate of substrate hydrolysis in the absence of inhibitor and k_{obs} is the pseudo-first order rate constant. The parameter k_{obs} is defined by the following equation:

$$k_{obs} = k_2[I]/(K_I + [I])$$

When inhibitor concentration is less then 10-fold excess of enzyme concentration, the pseudo-first order rate constant no longer accurately describes the inhibition rate, as the inhibitor concentration can no longer be assumed to be a steady state. In this case, second order kinetics must be applied as defined in the following equation:

$$k_{2nd}t = [1/(i - e)]\ln[e(i - x)/i(e - x)]$$

where *i* and e are initial inhibitor and enzyme concentrations, respectively, and e – x and *i*-x account for the changing enzyme and inhibitor concentration over the course of the experiment.

Faster reacting inhibitors are logistically difficult to measure by the incubation method, and in this case the Progress Curve Method provides a convenient alternative. Developed by Tian and Tsou,[19] the progress curve method involves monitoring the substrate hydrolysis of the enzyme in the presence inhibitor over time until the enzyme is completely inhibited. In this method the substrate and inhibitor compete for the enzyme active site, which slows down the inhibition reaction. This method follows an exponential time course where the accumulated substrate hydrolysis product P approached a limited concentration $[P]_\infty$:

$$[P]_t = [P]_\infty[1 - e^{-A[I]t}]$$

or,

$$\ln([P]_\infty - [P]_t) = -A[I]t$$

where A is the apparent rate constant of inhibition, and can be determined by the plot of $\ln([P]_\infty - [P]_t)$ versus time. The apparent rate constant is converted to a second order rate constant using the following equation:

$$k_2 = A(1 + [S]/K_M)$$

This conversion accounts for the slowing of inhibition due to substrate competition. The progress curve method is convenient for fast inhibitors, and for enzymes, such as calpain, which require high enzyme concentrations for hydrolysis detection, and therefore high inhibitor concentrations.

CHAPTER TWO

AZA-PEPTIDE EPOXIDE AND EPOXIDE INHIBITORS OF CALPAINS AND OTHER CLAN CA PROTEASES

Introduction

Calpains are calcium activated ubiquitous cysteine proteases that are members of the clan CA papain family. Calpains I and II are distinguished by the requirement of micromolar and millimolar concentrations of calcium respectively. A current hypothesis is that cellular injury leads to elevated intracellular calcium and provokes the pathologic activation of calpains.[20] The activation of calpains is believed to be responsible for the cell death and axonal degeneration seen in ischemic stroke,[21] spinal cord injury,[22] closed head injury,[23] and Wallerian degeneration.[24] The calpains are also shown to be involved in a number of diseases that involve neurodegeneration, including Alzheimer's disease,[25,26] Parkinson's disease,[27] muscular dystrophy,[28] and diabetes.[29,30] Calpain inhibitors have been shown to be therapeutic agents against many conditions including Parkinson's disease,[27] spinal cord injury,[31] brain injury,[32] and other CNS injuries and diseases.[6]

Calpain Structure. The structure of calcium-free, inactive calpain I has been solved,[7] as well as the crystal structure of calcium-bound, active calpain I.[8] The authors mainly investigated the mechanism by which Ca^{2+} binding induces structural repositioning around the active site to produce proteolytic activity, however they did note that the active site of calpain aligned very well with the active site of papain. A more recent paper by the same group investigates the active site structure of calpain through its interactions with the aldehyde inhibitor leupeptin and the epoxide inhibitor E64.[33] The authors conclude that while the active sites of calpain and papain are highly similar, the active site cleft of calpain is deeper and narrower, requiring substrates and inhibitors to adopt an extended conformation. There are also two mobile loops present in calpain on each side of the active site cleft, which seem to both widen the active site for inhibitor binding and to swing around a bound inhibitor. The S1 and S2 pocket structures of calpain are highly conserved with papain, however the S3 subsite of calpain seems to be more solvent exposed. This S3 difference could be an artifact of the truncated protease core of calpain used in this study. The publishing of these structure studies will lead to greater structure-based design of calpain inhibitors in the future.

Calpain Inhibitors. Calpastatin is an endogenous polypeptide that specifically inhibits calpain. This polypeptide is present *in vivo* and is part of a calpain activity regulatory system. Calpastatin is the only specific calpain inhibitor known, and has no activity toward papain and other cysteine proteases. Calpastatin is a large polypeptide that binds calpain at an allosteric region, inducing a conformation change that renders calpain

inactive. The fact that calpastatin inhibits through a mechanism that does not include the calpain active site results in selectivity.

Synthetic inhibitors developed for calpains have been well reviewed and include peptide aldehydes, α-ketoamides, halomethylketones, and acyloxymethylketones.[9,17] While some of these inhibitors are potent deactivators of calpain, few are selective inhibitors for calpain over other cysteine proteases. An overview of several potent calpain inhibitors can be seen in Table 2.1.

Table 2.1. Representative Calpain Inhibitors From the Literature.

No.	Inhibitor	Calpain 1 Inhibition	Ref
	Irreversible		
1	HO-EPS-Leu-$(CH_2)_4$-NH-C(=NH)-NH_2 **(E64)**	$k_{obs}/[I]$ = 7,450 $M^{-1}s^{-1}$	34
2	HO-EPS-Leu-$(CH_2)_4$-NH-CO_2-benzyl **(EP460)**	$k_{obs}/[I]$ = 15,000 $M^{-1}s^{-1}$	self tested
3	Z-Leu-Leu-Phe-CH_2F	$k_{obs}/[I]$ = 290,000 $M^{-1}s^{-1}$	9
4	Z-Leu-Phe-CH_2OPO(O-2-methylbenzyl)$_2$	$k_{obs}/[I]$ = 365,000 $M^{-1}s^{-1}$	9
5	Z-Leu-Leu-Tyr-VS-phenyl	$k_{obs}/[I]$ = 24,300 $M^{-1}s^{-1}$	9
	Reversible		
6	Z-Val-Phe-H	IC_{50} = 0.01 μM	9
7	Z-Leu- Abu-CONH-$(CH_2)_3$-morpholino **(AK295)**	K_I = 0.041 μM	35

The ketoamide calpain inhibitor AK295, Figure 2.1, has been studied extensively in cells and has been shown to protect cells from death following brain ischemia.[23,36] We have recently demonstrated that AK295 has the ability to inhibit calpain activity in PC12 cells following calpain activation by paclitaxel.[37] However, AK295 has a charged

morpholino group which could limit its potency in cells. Because of these issues, we turned our attention to epoxide inhibitors.

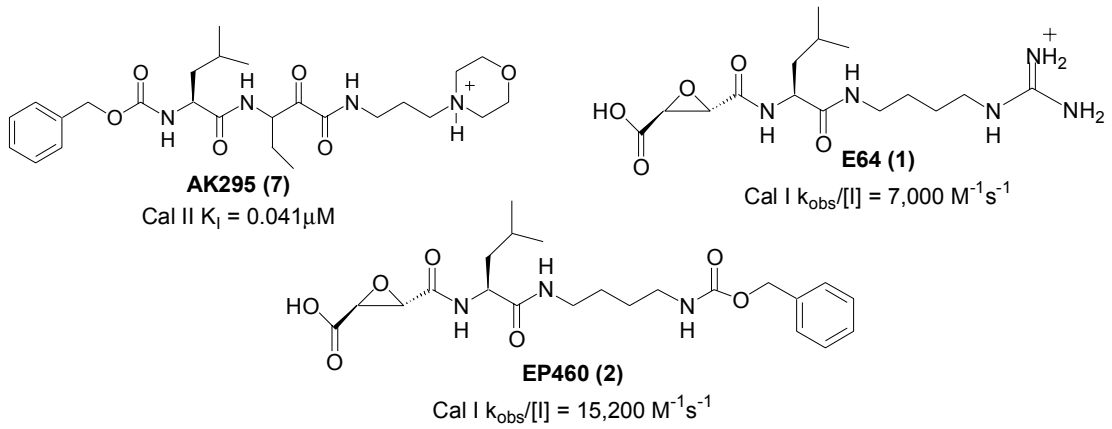

Figure 2.1. Structures of AK295, E64 and EP460.

The naturally occurring epoxide inhibitor E64, Figure 2.1, isolated from *Aspergillus japonicus* is known to be an general inhibitor of clan CA proteases.[38] The epoxide analog EP460 is the most potent epoxide inhibitor for calpain in the literature (k = 15,200 $M^{-1}s^{-1}$).[34] The epoxides inhibit through an irreversible reaction with the active site cysteine thiol, resulting in permanent alkylation of the catalytic cysteine residue.

The mechanism of inhibition by epoxide inhibitors can be seen in Figure 2.2. The cysteine thiol can theoretically attack on either the C2 or C3 carbon of the epoxide, resulting in the epoxide ring opening. Crystal structures of clan CD proteases (caspase-3,

SARS coronavirus main protease) with epoxides synthesized in the Powers laboratory elucidated that the cysteine attacks the C3 epoxide carbon.[39-41]

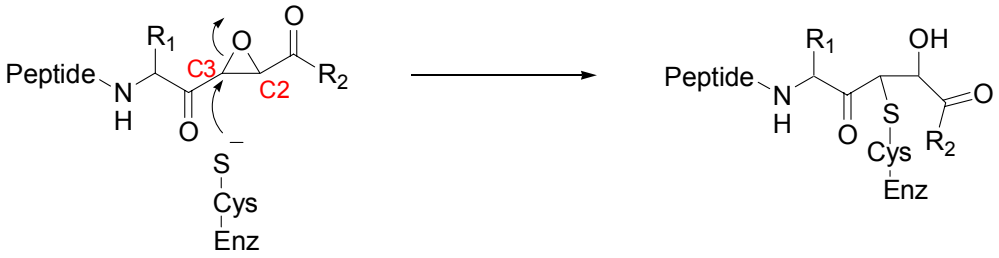

Figure 2.2. Mechanism of Inhibition of Cysteine Proteases By Epoxide Inhibitors.

Epoxide inhibitors have several advantages over other types of calpain inhibitors. Epoxides are generally not as reactive as halomethylketones and aldehydes, so they have the potential to be more selective towards a single target and could cause fewer toxicity problems *in vivo*. Since epoxide inhibitors are irreversible and the enzyme is permanently inactivated, this class of inhibitors could be delivered less frequently than reversible transition-state inhibitors, which are only effective until they are cleared from the circulation. Epoxides were put through human trials in Japan in the 1980's for muscular dystrophy, and while they were shown to be non-toxic, the particular inhibitors tested were not effective enough against the disease to warrant further investigation.[42]

Inhibitor Design

The Aza-Peptide Epoxide Design. The Powers laboratory has recently developed the aza-peptide epoxide warhead for clan CD proteases with great success.[43] The aza-peptide epoxide design involves replacing the α-carbon of an amino acid residue with a nitrogen, and using this nitrogen as a connection point for the epoxysuccinate moiety. An example of an aza-peptide epoxide can be seen in Figure 2.3. Some possible advantages of the aza-peptide epoxide design include: a) the loss of stereochemistry at the aza-amino acid residue resulting in a planar geometry, b) the ease of synthesis of the amide bond between the nitrogen of the aza-residue and the epoxysuccinate, c) the ability to easily extend the inhibitor to the prime side, varying prime side residues to create a more potent and selective inhibitor.

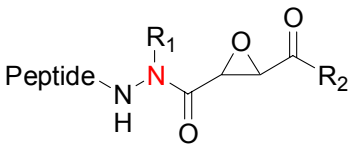

Figure 2.3. Aza-Peptide Epoxide Design.

An initial design to create aza-peptide epoxide inhibitors of calpain included aza-peptide epoxides of the sequences Z-Leu-AHph and Z-Leu-ALeu as seen in Figure 2.4.

The Leu residue was chosen because calpain requires a P2 leucine. The ALeu and AHph were also chosen to be compatible with calpain. The inhibitors were synthesized with an ethyl ester in the P1' position for simplicity of synthesis and structure. These inhibitors were also tested with the clan CA enzymes cathepsin B and papain, which have potential to be inhibited by these aza-peptide epoxides.

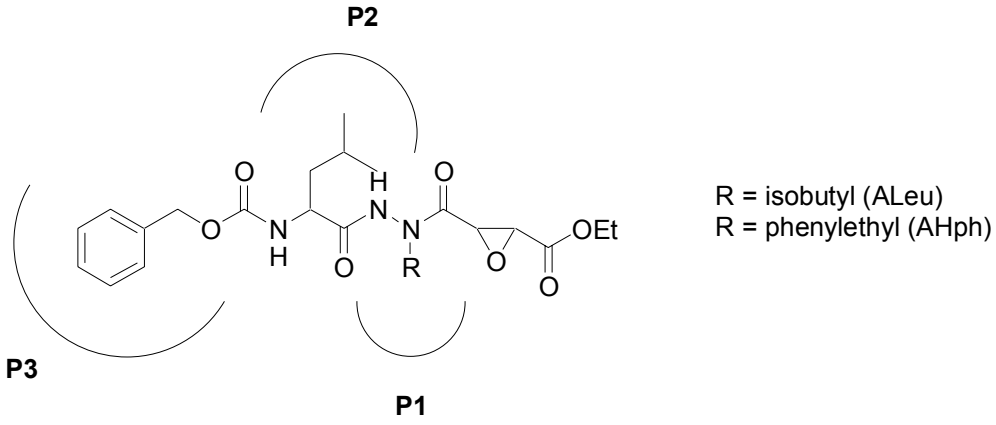

Figure 2.4. Aza-Peptide Epoxide Design for Calpains.

In another design, the aza-peptide epoxide analog of EP460 was explored as a potential calpain inhibitor, as seen in Figure 2.5. EP460 is the most potent of the known epoxide inhibitors for calpain. The aza-version of EP460 would be a "reverse" inhibitor compared to the first design, given that EP460 binds in the active site in the C → N peptide direction, opposite of the N → C direction of the previous design. The

conversion of the inhibitor to an aza-peptide involved the substitution of a nitrogen atom for the Leu α-carbon. This modification is expected to alter the geometry of the inhibitor and the positioning of the EP460 inhibitor in the calpain active site.

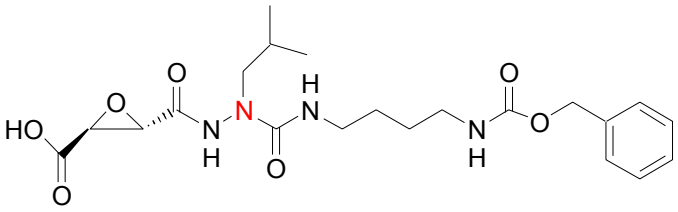

Aza-EP460

Figure 2.5. Aza-EP460 Design.

Epoxide Stereochemistry. The epoxide moiety has two stereocenters, with the possibility of 4 different epoxide isomers: two "*trans*" isomers (2*S*, 3*S* and 2*R*, 3*R*) and two "*cis*" isomers (2*S*, 3*R* and 2*R*, 3*S*). The literature on epoxide inhibitors comes to the consensus that the trans (2*S*, 3*S*) isomer tends to be the most potent for clan CA enzymes. However, due to our unique design, we synthesized versions of the inhibitors containing the two trans isomers stereospecifically, along with a version containing a mixture of the cis isomers, with the idea that if the cis isomers were potent they could also be synthesized stereospecifically.

Synthesis

The synthesis of the AHph derivatives is shown in Figure 2.6. The methyl ester of Z-Leu-OH was synthesized by treatment with $SOCl_2$ in MeOH. Z-Leu-OMe was treated with hydrazine to yield **10**. Z-Leu-$NHNH_2$ (**10**) was condensed with phenylacetaldehyde to yield the hydrazone **11**. The hydrazone was reduced with $NaBH_3CN$ under acidic conditions to yield the hydrazide **12**. The hydrazide was coupled to the epoxysuccinates by the EDC/HOBT coupling method to yield the final inhibitors **13a-c,** each differing in epoxide stereochemistry. The stereospecific epoxysuccinates were synthesized by method of Mori,[44] starting from the D or L diethyltartarate. The ALeu inhibitors were synthesized similarly, substituting isobutyraldehyde for phenylacetaldehyde.

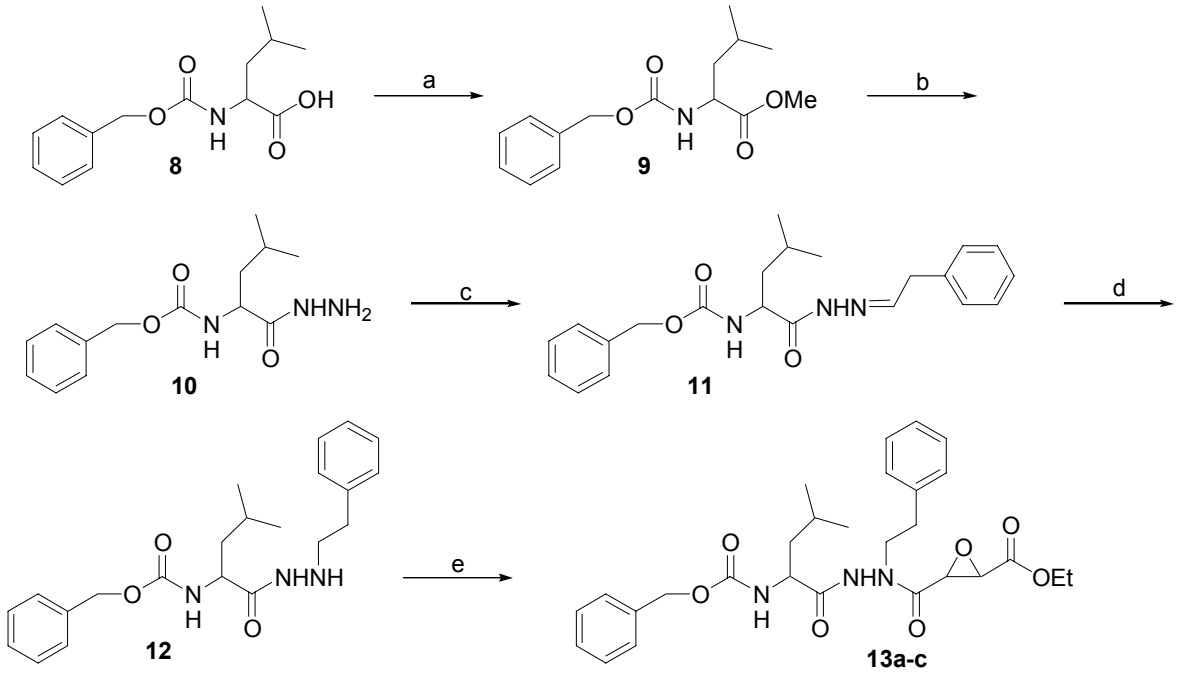

Figure 2.6. Synthesis of Aza-Peptide Epoxide Inhibitors for Calpains. Reagents and conditions: a) $SOCl_2$, MeOH. b) 10 eq NH_2NH_2, THF. c) phenylacetaldehyde, THF. d) $NaCNBH_3$, *p*-TsOH, THF. e) oxirane-2,3-dicarboxylic acid monoethyl ester, EDC, HOBT, DMF.

The synthesis of the aza-EP460 derivatives can be seen in Figure 2.7. Boc-hydrazine was condensed with isobutyraldehyde followed by reduction with $NaBH_3CN$ under acidic conditions to yield **15**. Carbonyldiimidazole was treated with *N*-(benzyloxycarbonyl)-butane-1,4-diamine, synthesized by method of Atwell and Denny,[45] followed by **15** to yield the urea **16**. The Boc protecting group was removed by treatment with 4 N HCl in EtOAc, followed by mixed anhydride coupling with ethyl (2*S*, 3*S*)-oxirane-2,3-dicarboxylate, which is synthesized by method of Mori.[44] In the final step the ethyl ester was hydrolyzed under basic conditions.

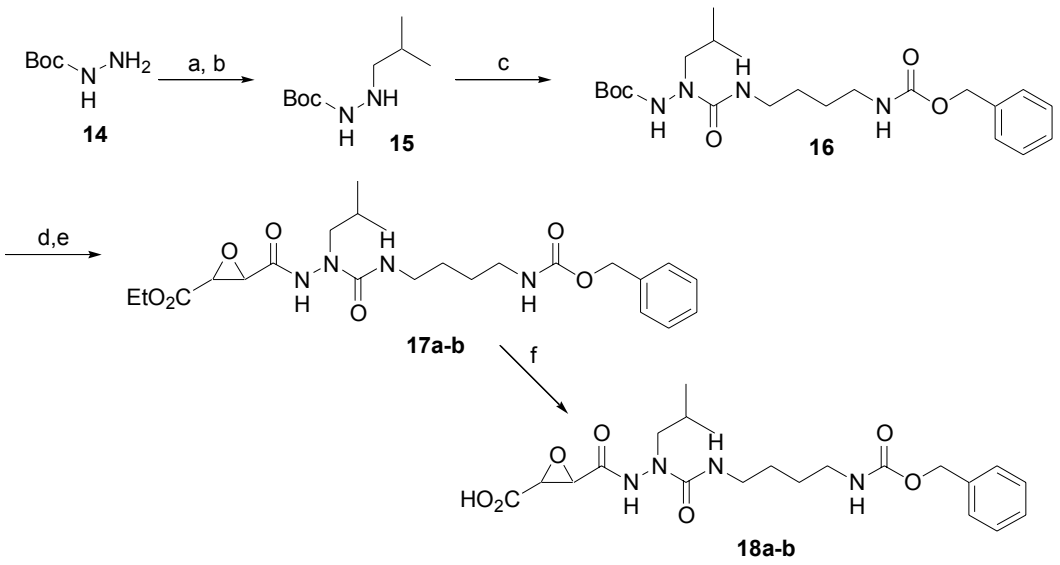

Figure 2.7. Synthesis of Aza-EP460 Inhibitors for Calpains. Reagents and conditions: a) isobutyraldehyde, EtOH, reflux. b) $NaBH_3CN$, *p*-TsOH, THF. c) CDI, NMM, $NH_2(CH_2)_4NH$-Cbz, CH_2Cl_2. d) 4N HCl in EtOAc. e) ethyl (2*S*,3*S*)-oxirane-2,3-dicarboxylate, IBCF, NMM, DMF, EtOAc. f) NaOH, EtOH.

Results and Discussion

The inhibitory results of the first design of aza-peptide epoxide compounds can be seen in Table 2.2. Clearly, these compounds are poor inhibitors of calpain, cathepsin B, and papain, with all inhibition rates being less than 10 $M^{-1}s^{-1}$. The epoxide stereochemistry preference seems to be 2*S*,3*S* > 2*R*,3*R* > *cis*, while the ALeu sequence is preferred over the AHph. It seems that the change in geometry afforded by the aza-residues is not tolerated by these clan CA proteases in this inhibitor design. This is

interesting given the fact that inhibitors of the same design with peptide sequences targeted towards clan CD proteases (caspases, gingipains, legumain) easily have inhibition rates in the millions.[43] These aza-peptide epoxide inhibitors designed for calpain demonstrate that this inhibitor design selectively inhibits clan CD proteases over the larger populated clan CA. While these inhibitors are not very potent and show little promise of being used in further calpain studies, this discovery demonstrates that the aza-epoxide warhead is a specific deactivator of clan CD enzymes.

Table 2.2. Inhibition of Clan CA Proteases by Aza-Peptide Epoxides.

			$k_{obs}/[I]$ ($M^{-1}s^{-1}$)		
No.	**Inhibitor**	**EP Stereo chemistry**	**Calpain I**	**Cathepsin B**	**Papain**
19a[a]	Z-Leu-ALeu-EP-COOEt	2*S*,3*S*	8.6	1.8	10
19b	Z-Leu-ALeu-EP-COOEt	2*R*,3*R*	1.4	NI	6.7
19c	Z-Leu-ALeu-EP-COOEt	*cis*	1.9	NI	0.4
13a	Z-Leu-AHph-EP-COOEt	2*S*,3*S*	2.3	0.7	5.7
13b	Z-Leu-AHph-EP-COOEt	2*R*,3*R*	2.1	NI	2.2
13c	Z-Leu-AHph-EP-COOEt	*cis*	1.1	NI	1.0

[a]Synthesized by Juliana Asgian

Inhibition data for calpain I, cathepsin B, and papain with the aza-EP460 analog inhibitors can be seen in Table 2.3. All of these compounds are significantly less potent than the parent EP460 compound, however the inhibition rates are 100-fold higher for this series of compounds compared with the previous design. The epoxide with the

(2*S*,3*S*) epoxide stereochemistry and the P1' carboxylic acid (**18a**) displayed the most potency. While these aza-EP460 compounds are modest inhibitors of calpain, cathepsin B, and papain, it seems that clan CA enzymes do not accept the change in geometry afforded by the aza amino acid.

Table 2.3. Inhibition of Clan CA Proteases by Aza-EP460 Analogs.

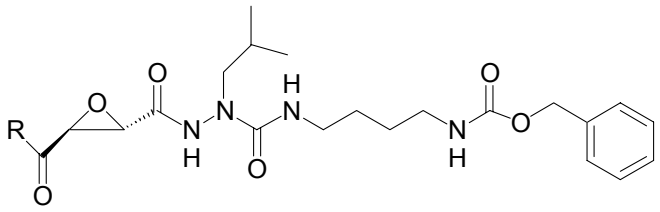

			$k_{obs}/[I]$ ($M^{-1}s^{-1}$)		
No.	**R**	**Stereochemistry**	**Calpain I**	**Cathepsin B**	**Papain**
18a	HO	2*S*,3*S*	1,450 ± 240	1,220 ± 390	1,000 ± 30
17a	EtO	2*S*,3*S*	NI	8.0	NI
18b	HO	2*R*,3*R*	NI	NI	NI
17b	EtO	2*R*,3*R*	NI	NI	NI

NI = no inhibition after 45 min. incubation

One of the major differences in the clan CA and CD active sites is that clan CA enzymes have a deeper, narrower active site cleft, while the active site of clan CD enzymes is more shallow and wide. The shallower, wider active site of the clan CD proteases seems to allow for the aza-peptide epoxides to bind productively, while the narrower active site of clan CA proteases prohibits productive binding. Hence, we have

discovered one of the few types of inhibitor warheads which discriminates between clans of cysteine proteases. This discovery strengthens the importance of the potent aza-peptide epoxide inhibitors that the Powers laboratory has produced for the caspases and other clan CD proteases.

New Epoxide Inhibitor Design

With the previous results in mind, the focus of the design was shifted away from the aza-peptide epoxide, to design non-aza epoxide inhibitors by modifying the "C-terminal" end of the inhibitor EP460. The goal of this design is not a new warhead for calpain inhibitors, as the previous work, but to determine the best group for the P3-P4 region of the EP460 inhibitor to create a more potent and selective inhibitor. Calpain has a stringent requirement for Leu or Val in the P2 position of substrates and inhibitors. As demonstrated by EP460, calpain seems to prefer a larger aromatic group in the P3/P4 region.[34] Therefore, we designed a series of inhibitors with various aromatics and various spacings to replace the benzyl group of EP460, as seen in Figure 2.8. The goal was to discover inhibitors with greater inhibitory potency towards calpain, while decreasing inhibitory potency towards other clan CA enzymes.

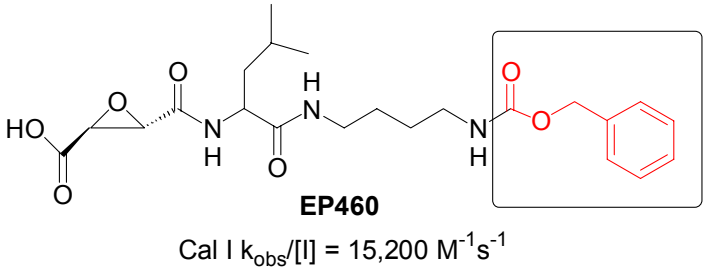

Figure 2.8. EP460 Inhibitor Structure with Proposed Modification Site.

Synthesis

The synthesis of the new EP460 analog compounds can be seen in Figure 2.9. Diaminobutane was selectively protected on one amine with the Boc protecting group to yield **20**. The aromatic side chains were added through reaction with various isocyanates, or through mixed anhydride peptide couplings to give **21a-i**. The Boc group was then removed with TFA, and Boc-leucine was coupled through mixed anhydride conditions to the resulting amine yielding **22a-i**. The Boc group was again removed with TFA, and the epoxysuccinate was introduced by mixed anhydride coupling giving **23a-i**. In the final step the ethyl ester was hydrolyzed under basic conditions to yield the final compounds **24a-i**.

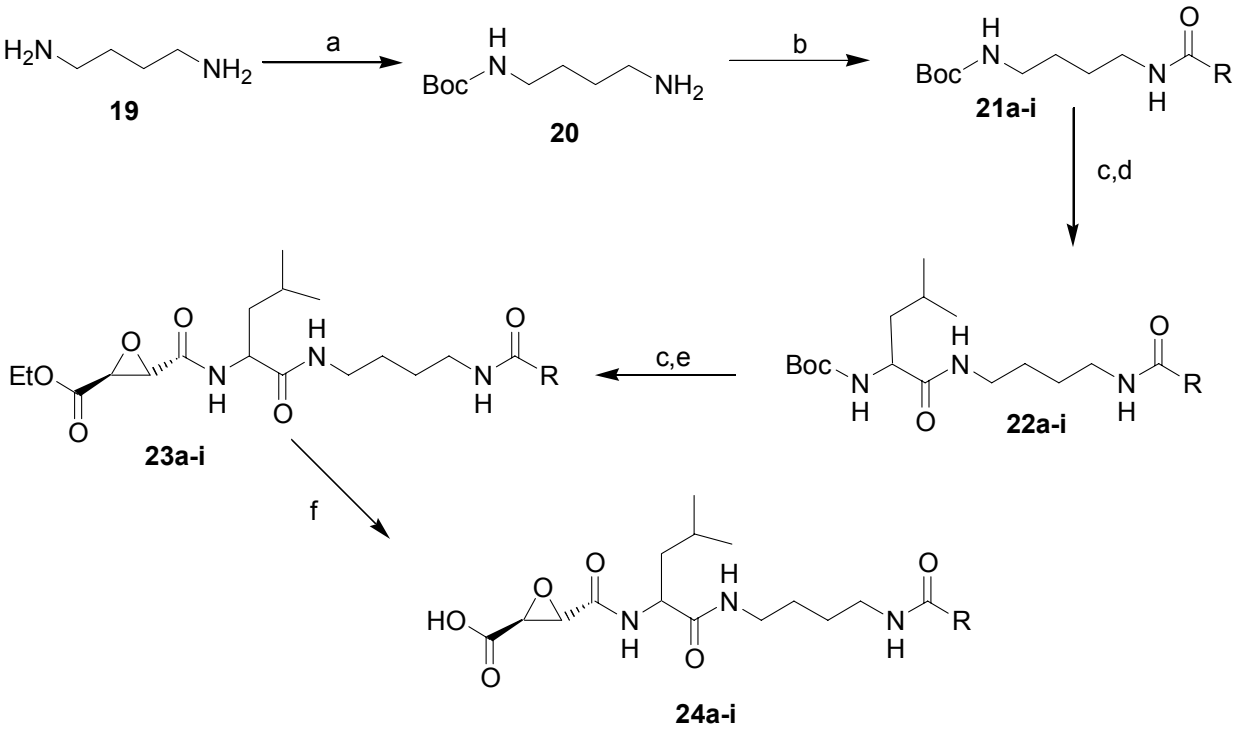

Figure 2.9. Synthesis of Epoxide Inhibitors Which Are Analogs of EP460. Reagents and conditions: a) $(Boc)_2O$, dioxane. b) R-N=C=O, CH_2Cl_2 or HOOC-R, IBCF, NMM. c) TFA, CH_2Cl_2. d) Boc-Leu-OH, IBCF, NMM, CH_2Cl_2. e) ethyl (2S,3S)-oxirane-2,3-dicarboxylate, IBCF, NMM, CH_2Cl_2. f) NaOH, EtOH.

Results and Discussion

The kinetic inhibition results can be seen in Table 2.4. Most of the inhibitors synthesized were in the same potency range with calpain I and II as EP460, with a few being more potent. The best inhibitors for the calpains incorporated the 1-naphthyl moiety (**24f**, **24h**). The benzyl urea compound (**24b**) and the phenoxyphenyl urea (**24i**) were also potent inhibitors. The EP460 analog containing the ethyl ester (**23a**) was a significantly less potent inhibitor with all of the enzymes, demonstrating the importance of the carboxylic acid for inhibitor binding. Generally, the best inhibitors for calpain I and calpain II were the same, however the inhibitor potency with calpain II was 2-fold greater than calpain I. It is worth noting that while some of the inhibitors demonstrated greater inhibitory potency with calpain than EP460, all of the new inhibitors are significantly less potent than EP460 with cathepsin B and papain. A few of the inhibitors (**24b**, **24c**, **24f**) are even more potent with calpain II than with cathepsin B, which has been a difficult property to attain in inhibitors. Since papain is not a human protease, selectivity over papain is inconsequential for our purposes of drug development. We have therefore succeeded in the discovery of epoxide inhibitors that are more potent and selective than EP460.

Table 2.4. Inhibition of Clan CA Proteases by EP460 Analog Inhibitors.

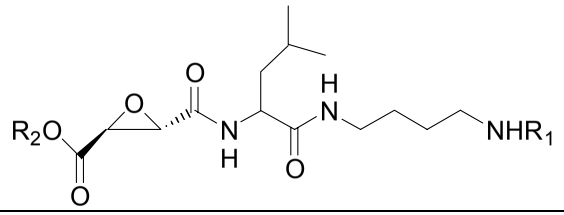

			$k_{obs}/[I]$ $(M^{-1}s^{-1})$				% Inhibition of Calpain in
No.	**R_1**	**R_2**	**Calpain I**	**Calpain II**	**Cathepsin B**	**Papain**	**PC12 Cells**
24a	CO_2-CH_2-C_6H_5 **EP460**	H	15,200 ± 5,600	43,300 ± 3,700	78,300 ± 1,150	834,000 ± 160,000	95 ± 1
23a	CO_2-CH_2-C_6H_5	Et	500	1,520 ± 440	120	510	90 ± 3
24b	CONH-CH_2-C_6H_5	H	18,400 ± 83	40,700 ± 7,300	32,400 ± 6,600	203,000 ± 96,000	42 ± 46
24c	CONH-C_6H_5	H	13,400 ± 880	41,200 ± 8,200	36,000 ± 7,000	308,000 ± 25,000	ND
24d	CONH-C_6H_4-4-(OCH_3)	H	11,500 ± 580	28,300 ± 5,800	30,000 ± 1,700	387,000 ± 3,400	73 ± 6
24e	$COCH_2$-(3-pyridyl)	H	3,080 ± 350	8,060 ± 1,700	19,500 ± 190	188,000 ± 21,000	ND
24f	$COCH_2O$-(1-naphthyl)	H	21,600 ± 91	46,500 ± 9,400	42,500 ± 6,000	232,000 ± 73,000	81 ± 5
24g	$COCH_2O$-(2-naphthyl)	H	12,400 ± 68	20,200 ± 160	17,600 ± 500	194,000 ± 54,000	ND
24h	CONH-(1-naphthyl)	H	20,000 ± 1,100	44,000 ± 9,200	45,100 ± 9,000	666,000 ± 300,000	70 ± 19
24i	CONH-C_6H_4-2-(OC_6H_5)	H	15,600 ± 1,300	39,500 ± 3,600	57,300 ± 7,400	651,000 ± 74,000	84 ± 6

ND = not determined

Calpain activation has been shown to be an important step in the pathology of several neurological diseases. Calpains, when activated, can degrade neurons and axons, causing symptoms of numbness, weakness, and even abnormalities of cognition. We collaborated with Dr. Jonathan Glass at Emory University in order to test our calpain inhibitors in a model of calpain-mediated neurodegeneration. This model uses rat pheochomocytoma (PC12) cells to test the ability of calpain inhibitors to penetrate cell membranes and inhibit intracellular calpain activity. PC12 cells are considered "neuron-like", and so are relevant to testing for efficacy in nervous system diseases. In this assay PC12 cells are treated with the chemotherapy drug paclitaxel, which creates an increase in intracellular calpain activity. Our calpain inhibitors were introduced into the cell culture media before treatment with paclitaxel in order to determine if these compounds could cross the cell membrane and inhibit intracellular calpain activity.

The results of these experiments are shown in Table 2.4 and reported as % inhibition of calpain relative to the amount of calpain activity with paclitaxel alone. Several of the epoxide inhibitors proved to be more potent calpain inhibitors than the α-ketoamide AK295, our benchmark calpain inhibitor. EP460 (**24a**) was the most potent inhibitor in this assay, along with the ethyl ester derivative **23a**. Although the **23a** was a much weaker inhibitor in the non cell based kinetic studies, the ethyl ester is hydrolyzed by esterases in cells, generating the more potent acid form **24a**. It is therefore reasonable that **23a** and **24a** have differing potencies in non-cell based assays, but inhibit similarly in cells. The methoxyphenyl and phenoxyphenyl inhibitors **24d** and **24i** were the most potent of the new inhibitors in this assay. It is interesting to note that **24d** and **24i** were not the most potent inhibitors in the non-cell based assays. These inhibitors may be

better able to cross the cell membrane to inhibit intracellular calpain activity. These experiments demonstrate that our epoxide inhibitors are able to cross cell membranes and efficiently inhibit calpain in cell culture, which is an important step toward their development as therapeutic agents.

Conclusion

The aza-peptide epoxide designs were unable to provide potent inhibitors for calpain and the other clan CA enzymes. This is a very important discovery given the potency of this design for the clan CD enzymes. These compounds proved that the aza-peptide epoxide warhead is specific for clan CD proteases, which is a rare characteristic of warheads. The difference in the active site cleft between these two clans of proteases is probably responsible for the different aza-peptide epoxide potencies.

We were successful in the development of new epoxide inhibitors for calpains I and II based on the inhibitor EP460. By varying the P3-P4 region of EP460 we were able to discover inhibitors that were more potent and selective for the calpains than EP460. The increased selectivity for the calpains over cathepsin B is the most significant discovery, given that specific calpain inhibitors have been elusive. These epoxide inhibitors were also able to inhibit calpain activity in a cellular assay, which demonstrates that they are bioavailable enough to cross cell membranes and reach the calpain where it is active.

Experimental

Enzyme Assays. Calpains I and II, cathepsin B, and papain inhibition rates were determined using the progress curve method. The calpains and cathepsin B activities were determined using the appropriate fluorogenic peptide 7-amino-4-methylcoumarin substrates (AMC, excitation λ = 360 nm, emission λ = 405 nm), while papain activity was determined using the appropriate *p*-nitroaniline absorbance substrate. The fluorescence and absorbance was detected with a Tecan Spectraflour Microplate Reader (Tecan US, Research Triangle Park, NC).

Calpains I and II. Calpains I and II were obtained from Calbiochem, (LaJolla, CA) and stored at –78 ^{o}C in a storage buffer of 50 mM Tris-HCl, 5 mM EDTA, 5 mM β-ME, 100 mM NaCl, 40% glycerol, pH 7.8 at a concentration of 1.14 mg/mL. The kinetic assay buffer is 50 mM HEPES, 10 mM cysteine, 5 mM $CaCl_2$, pH 7.5. The inhibitor dissolved in DMSO was diluted with kinetic assay buffer containing the substrate Suc-Leu-Tyr-AMC (final concentration [S] = 1.30 mM). At t = 0 s, the enzyme in storage buffer was added to the mixture (calpain I [E] = 0.117 μM, calpain II [E] = 0.117 μM, [I] = 0.42 μM to 84 μM). The reaction was monitored over 10 min. by following the change in fluorescence at 465 nm. Inhibition rates were performed in duplicate, and the error ranges are reported.

Cathepsin B. Cathepsin B was purchased from Athens Research Technologies (Athens, GA) in a solution of 20 mM NaAc, 1 mM EDTA, pH 5.0 at a concentration of 31.2 μM. A 100-fold dilution of the enzyme in the kinetic assay buffer 0.1 M potassium phosphate, 1.25 mM EDTA, 0.01% Brij, 1 mM DTT, pH 6.0 was activated for 1 hour at 0

^{o}C. The inhibitor dissolved in DMSO was diluted with kinetic assay buffer containing the substrate Z-Arg-Arg-AMC (final concentration [S] = 0.40 mM). At t = 0, the activated enzyme was added to the mixture ([E] = 5.23 nM, [I] = 0.42 μM to 0.84 μM). The reaction was monitored over 20 min. by following the change in fluorescence at 465 nm. Inhibition rates were performed in duplicate, and the error ranges are reported.

Papain. Papain was purchased from Sigma Chemical Co. (St. Louis, MO) as a purified powder and stored at –20 ^{o}C in a stock solution of the kinetic assay buffer 50 mM HEPES, 3 mM DTT, 2.5 mM EDTA, pH 7.5 at a concentration of 51.7 μM. For the assay a 100-fold dilution of the stock enzyme solution in kinetic assay buffer was allowed to activate at 0 ^{o}C for 30 min. The inhibitor dissolved in DMSO was diluted with assay buffer containing the substrate Z-Phe-Arg-pNA (final concentration [S] = 0.550 mM). At t = 0, the activated enzyme was added to the mixture (final [E] = 8.67 nM, [I] = 21 nM to 42 nM). The reaction was monitored over 20 min. by following the change in absorbance at 405 nm. Inhibition rates were performed in duplicate, and the error ranges are reported.

PC12 Cellular Assay with Paclitaxel. PC12 cells were cultured for 24 hours and then treated with 200 ng/mL paclitaxel (Sigma) and 50 μM inhibitor in DMSO for 24 hours. After washing with PBS, the cells were resuspended in 8 mL KRH (125 mM NaCl, 5 mM KCl, 1.2 mM $MgSO_4$, 1.2 mM KH_2PO_4, 2 mM $CaCl_2$, 6 mM glucose and 25 mM HEPES, pH 7.4) containing 50 μM inhibitor. To 2 mL of this solution was added 100 μL Suc-Leu-Leu-Val-Tyr-AMC to a final concentration of 45 μM. The cells were incubated at 37 ^{o}C for 15 minutes, and the reaction was terminated by the addition of 100 μL of 0.4 N HCl. The cells were sonicated for 10 seconds and centrifuged for 5 minutes. The supernatant (200 μL) was transferred to a 96 well plate and fluorescence measured at

excitation 355 nm and emission 460 nm. The experiment was duplicated 6 times per inhibitor, and the average percent inhibition and standard deviations were reported.

Materials and Methods. Amino acids and their analogs were purchased from Bachem Biosciences Inc. (King of Prussia, PA). Column chromatography was carried out on flash silica gel, 32-63 u, 60 Å, purchased from Sorbent Technologies (Norcross, GA). The ^{1}H NMR spectra were obtained using a Varian Mercury Vx 400 MHz spectrometer. Electrospray ionization (ESI), fast-atom bombardment (FAB) and high-resolution mass spectrometry were performed using Micromass Quattro LC and VG Analytical 70-SE instruments by Georgia Tech MS laboratory personnel.

Z-Leu-OMe. Z-Leu-OH (3.05 g, 11.3 mmol) was dissolved in methanol and cooled to -78 ^{o}C in a dry ice/acetone bath. Thionyl chloride (5.25 g, 34.0 mmol) was added dropwise to the solution, and the reaction was allowed to warm to room temperature and stir overnight. The reaction was concentrated to yield Z-Leu-OMe quantitatively without further purification.

Z-Leu-NH-NH$_2$. Z-Leu-OMe (3.00 g, 10.8 mmol) was dissolved in methanol (40 mL). Hydrazine (3.45 6g, 108 mmol) was added to the solution, and the reaction was stirred overnight. The reaction was concentrated under vacuum and crystallized in ether to yield Z-Leu-NH-NH$_2$ as a white solid quantitatively.

Z-Leu-NH-N=CHCH$_2$-C$_6$H$_5$. Z-Leu-NH-NH$_2$ (3.00 g, 10.8 mmol) was dissolved in dry THF (40 mL) with molecular sieves. Phenylacetaldehyde (1.42 6g, 11.9 mmol) was added dropwise to the solution, and the reaction was allowed to stir for 3 hrs. The molecular sieves were removed by filtration, the reaction concentrated, and the crude

product purified by column chromatography (5% MeOH in CH_2Cl_2) to yield Z-Leu-NH-N=$CHCH_2$-C_6H_5 (2.568 g, 62% yield).

Z-Leu-NH-NH-CH_2CH_2-C_6H_5. Z-Leu-NH-N=$CHCH_2$-C_6H_5 (0.666 g, 1.75 mmol) was dissolved in dry THF (50 mL). $NaBH_4$ (0.330 g, 8.74 mmol) was added to the solution, and the reaction was allowed to stir for 90 min. The reaction was concentrated and the residue dissolved in CH_2Cl_2 and washed with sat. NaCl. The organic layer was concentrated, and the residue crystallized from CH_2Cl_2/hexanes to yield a white solid. The solid was purified by column chromatography (1:2 EtOAc:CH_2Cl_2) to yield Z-Leu-NH-NH-CH_2CH_2-C_6H_5 (0.131 g, 19% yield). ^{1}H NMR ($CDCl_3$): 0.83-0.95 (d, 6H), 1.40-1.45 (m, 1H), 1.59-1.70 (m, 2H), 2.72-2.80 (t, 2H), 3.01-3.15 (m, 2H), 4.01-4.12 (m, 1H), 4.93-5.01 (s, 1H), 5.08-5.11 (s, 2H), 7.13-7.22 (s, 1H), 7.22-7.42 (m, 10H).

***cis*-3-(N^2-(*N*-Benzyloxycarbonylleucyl)-N^1-(2-phenethylhydrazinocarbonyl))oxirane-2-carboxylic acid ethyl ester (Z-Leu-AHph-*cis*-EP-COOEt)**. **General EDC/HOBT Coupling Method**. To a solution of *cis*-Ethyl-2,3-oxirane-dicarboxylate (180 mg, 1.125 mmol) in DMF (9 mL) was added HOBT (154 mg, 1.135 mmol). Z-Leu-NH-NH-CH_2CH_2-C_6H_5 (415 mg, 1.083 mmol) was added to the reaction followed by EDC (229 mg, 1.195 mmol) and the reaction was allowed to stir overnight. The reaction was concentrated *in vacuo*, and the residue was taken up in EtOAc and washed successively with 2% citric acid, sat. $NaHCO_3$, water, and sat. NaCl. The organic layer was concentrated and purified by column chromatography (2.5% MeOH, 25% EtOAc, 72.5% CH_2Cl_2) and recrystallized from EtOAc/hexanes to yield Z-Leu-AHph-*cis*-EP-COOEt (177 mg, 20%). ^{1}H NMR ($CDCl_3$): 0.85-0.96 (d, 6H, J = 6

Hz), 1.21-1.35 (t, 3H, J = 6 Hz), 1.48-1.53 (m, 1H), 1.60-1.71 (m, 1H), 2.78-2.88 (t, 2H, J = 7 Hz), 3.50-3.52 (d, 2H, J = 4 Hz), 3.58-3.68 (t, 2H, J = 6 Hz), 3.95-4.00 (s, 1H), 4.19-4.28 (q, 2H, J = 6 Hz), 5.08-5.17 (s, 2H), 7.28-7.40 (m, 10H), 8.20-8.24 (s, 1H), 8.32-8.39 (s, 1H). HRMS (FAB) Calcd. For $C_{28}H_{36}N_3O_7$: 526.25533. Observed *m/z* 526.25508.

(2*S*,3*S*)-3-(N^2-(*N*-Benzyloxycarbonylleucyl)-N^1-(2-phenethylhydrazinocarbonyl))oxirane-2-carboxylic acid ethyl ester (Z-Leu-AHph-(2*S*,3*S*)-EP-COOEt). (2*S*,3*S*)-Ethyl-2,3-oxirane-dicarboxylate (43 mg, 0.271 mmol) and Z-Leu-NH-NH-CH_2CH_2-C_6H_5 (100 mg, 0.261 mmol) were reacted following the general EDC/HOBT coupling method. The crude product was purified by column chromatography to yield Z-Leu-AHph-(2*S*,3*S*)-EP-COOEt (66 mg, 48% yield). ^{1}H NMR ($CDCl_3$): 0.82-0.96 (d, 6H, J = 9 Hz), 1.21-1.33 (t, 3H, J = 9 Hz), 1.41-1.50 (m, 1H), 1.50-1.63 (m, 2H), 2.75-2.82 (t, 2H, J = 6 Hz), 3.58-3.59 (s, 1H), 3.76-3.77 (s, 1H), 3.88-4.05 (m, 2H), 4.10-4.25 (q, 2H, J = 3 Hz), 4.89-4.96 (d, 1H, J = 8 Hz), 5.08-5.21 (s, 2H), 7.23-7.40 (m, 10H), 8.02-8.13 (s, 1H). HRMS (FAB) Calcd. For $C_{28}H_{36}N_3O_7$: 526.25533. Observed *m/z* 526.25164.

(2*R*,3*R*)-3-(N^2-(*N*-Benzyloxycarbonylleucyl)-N^1-(2-phenethylhydrazinocarbonyl))oxirane-2-carboxylic acid ethyl ester (Z-Leu-AHph-(2*R*,3*R*)-EP-COOEt). (2*R*,3*R*)-Ethyl-2,3-oxirane-dicarboxylate (43 mg, 0.271mmol) and Z-Leu-NH-NH-CH_2CH_2-C_6H_5 (100 mg, 0.261 mmol) were reacted following the general EDC/HOBT coupling method. The crude product was purified by column chromatography (1:2 EtOAc:CH_2Cl_2) to yield Z-Leu-AHph-(2*R*,3*R*)-EP-COOEt (88 mg, 64% yield). ^{1}H NMR ($CDCl_3$): 0.81-0.96 (d, 6H, J = 8 Hz), 1.20-1.31 (t, 3H, J = 8 Hz),

1.39-1.48 (m, 1H), 1.51-1.63 (m, 2H), 2.78-2.84 (t, 2H, J = 6 Hz), 3.42-3.55 (m, 2H), 3.58-3.59 (s, 1H), 3.80-3.81 (s, 1H), 3.93-4.08 (m, 1H), 4.12-4.29 (q, 2H, J = 3 Hz), 4.80-4.85 (s, 1H), 5.08-5.12 (s, 2H), 7.25-7.39 (m, 10H), 7.83-7.94 (s, 1H). HRMS (FAB) Calcd. For $C_{28}H_{36}N_3O_7$: 526.25533. Observed *m/z* 526.25386.

Z-Leu-NH-N=CHCH(CH$_3$)$_2$. Z-Leu-NH-NH$_2$ (3 g, 10.6 mmol) and isobutyraldehyde (0.85 g, 11.8 mmol) were reacted following the same procedure as Z-Leu-NH-N=CHCH$_2$-C$_6$H$_5$. The crude produce was purified by column chromatography (10% MeOH in CH_2Cl_2) to yield Z-Leu-NH-N=CHCH(CH$_3$)$_2$ (1.971 g, 54% yield).

Z-Leu-NH-NH-CH$_2$CH(CH$_3$)$_2$. Z-Leu-NH-N=CHCH(CH$_3$)$_2$ (1.971 g, 5.29 mmol) was reduced with $NaBH_4$ (1.12 g, 52.9 mmol) following the same procedure as Z-Leu-NH-NH-CH$_2$CH$_2$-C$_6$H$_5$. The crude product was purified by column chromatography (1:2 EtOAc:CH_2Cl_2) to yield Z-Leu-NH-NH-CH$_2$CH(CH$_3$)$_2$ (0.59 g, 30% yield). ^{1}H NMR ($CDCl_3$): 0.83-0.96 (d, 12H), 1.23-1.24 (m, 2H), 1.62-1.78 (m, 4H), 2.60-2.67 (d, 2H), 4.04-4.16 (s, 1H), 5.10-5.12 (s, 2H), 7.25-7.38 (m, 5H).

***cis*-3-(*N*^{2}-(*N*-Benzyloxycarbonylleucyl)-*N*^{1}-(isobutylhydrazinocarbonyl))oxirane-2-carboxylic acid ethyl ester (Z-Leu-ALeu-*cis*-EP-COOEt).** The *cis*-ethyl-2,3-oxirane-dicarboxylate (49 mg, 0.309 mmol) and Z-Leu-NH-NH-CH$_2$CH(CH$_3$)$_2$ (100 mg, 0.298 mmol) were reacted following the general EDC/HOBT coupling method. The crude product was purified by column chromatography (1:2 EtOAc:CH_2Cl_2) to yield Z-Leu-ALeu-*cis*-EP-COOEt (58 mg, 41% yield). ^{1}H NMR ($CDCl_3$): 0.78-0.93 (m, 12H), 1.20-1.34 (t, 3H, J = 6 Hz), 1.40-1.45 (m, 2H), 1.61-1.79 (m, 4H), 3.50-3.60 (m, 2H), 4.07-4.14 (q, 2H, J = 7 Hz), 5.03-5.16 (s,

2H), 7.26-7.40 (m, 5H). HRMS (FAB) Calcd. For $C_{24}H_{36}N_3O_7$: 478.25533. Observed *m/z* 478.25729.

(2*R*,3*R*)-3-(N^2-(*N*-Benzyloxycarbonylleucyl)-N^1-(isobutylhydrazinocarbonyl))oxirane-2-carboxylic acid ethyl ester (Z-Leu-ALeu-(2*R*,3*R*)-EP-COOEt). (2*R*,3*R*)-Ethyl-2,3-oxirane-dicarboxylate (49 mg, 0.309 mmol) and Z-Leu-NH-NH-$CH_2CH(CH_3)_2$ (100 mg, 0.298 mmol) were reacted following the general EDC/HOBT coupling method. The crude product was purified by column chromatography (2.5% MeOH, 25% EtOAc, 72.5% CH_2Cl_2) to yield Z-Leu-ALeu-(2*R*,3*R*)-EP-COOEt (73 mg, 51% yield). ^{1}H NMR ($CDCl_3$): 0.79-0.98 (m, 12H), 1.20-1.35 (t, 3H, *J* = 7 Hz), 1.45-1.53 (m, 4H), 1.62-1.78 (m, 2H), 3.07-3.20 (s, 1H), 3.59-3.60 (s, 1H), 3.86-3.87 (s, 1H), 4.03-4.16 (q, 2H, *J* = 6 Hz), 4.16-4.23 (t, 2H, *J* = 7 Hz), 5.00-5.09 (d, 1H, *J* = 7 Hz), 5.09-5.12 (s, 2H), 7.30-7.40 (m, 5H), 8.49-8.53 (s, 1H). HRMS (FAB) Calcd. For $C_{24}H_{36}N_3O_7$: 478.25533. Observed *m/z* 478.25508.

Z-NH-$(CH_2)_4$-NH_2. To a solution of 1,4-diaminobutane (3 g, 34.0 mmol) in water (10 mL) was added bromocresol green. Methane sulfonic acid (6.08 mL in 9.75 mL H_2O) was added to the solution until the blue to yellow color change occurred. The mixture was diluted with EtOH (20 mL) and alternate drops of benzyl chloroformate (4.27 mL in 6.55 mL dimethoxyethane) and potassium acetate (50% in H_2O) were added to the solution in order to maintain the emerald green color. The reaction was allowed to stir for 1 hr after the green color remained steady. The reaction was concentrated, taken up in water (65 mL), and the solid bis-Z-diaminobutane was isolated by filtration. The water layer was washed with benzene, and then adjusted to pH 10 with 40% NaOH. The water layer was then extracted with benzene, and the benzene layers washed with sat.

NaCl, dried over Na_2SO_4, and concentrated to yield Z-NH-$(CH_2)_4$-NH_2 (1.392 g, 21% yield).

Boc-NH-N=CH-CH$(CH_3)_2$. To a solution of *t*-butyl carbazate (5.00 g, 37.9 mmol) in EtOH (100 mL) was added isobutyraldehyde (3.00 g, 41.7 mmol), and the reaction was heated to reflux for 3 hrs. The reaction was concentrated and the residue crystallized in water (50 mL). The solid was filtered and dried *in vacuo* to yield Boc-NH-N=CH-$CH(CH_3)_2$ (6.74 g, 95% yield).

Boc-NH-NH-$CH_2CH(CH_3)_2$. Boc-NH-N=CH-$CH(CH_3)_2$ (5.69 g, 30.59 mmol) was dissolved in dry THF (80 mL) along with $NaBH_3CN$ (1.921 g, 30.59 mmol). A solution of *p*-TsOH in THF (5.819 g, 30.59 mmol in 30 mL) was added to the mixture dropwise over 40 min, and the reaction was allowed to stir for 3 hrs. The reaction was concentrated, and the residue taken up in EtOAc and washed with sat. $NaHCO_3$, sat. NaCl, and dried over Na_2SO_4. The EtOAc layer was concentrated to yield a white solid. The solid was taken up in 1 N NaOH (90 mL) and stirred for 1 hr. The solution was neutralized with 3N HCl and extracted with CH_2Cl_2. The CH_2Cl_2 layers were washed with sat. NaCl, dried over Na_2SO_4, and concentrated. The crude product was purified by column chromatography (1:4 EtOAc:CH_2Cl_2) to yield Boc-NH-NH-$CH_2CH(CH_3)_2$ (3.57 g, 62% yield). ^{1}H NMR ($CDCl_3$): 0.91-0.94 (d, 6H), 1.42-1.48 (s, 9H), 1.69-1.76 (p, 1H), 2.63-2.67 (d, 2H), 3.85-3.94 (s, 1H), 6.15-6.20 (s, 1H).

Boc-ALeu-NH-$(CH_2)_4$-NH-Z. Carbonyldiimidazole (0.517 g, 3.19 mmol) was dissolved in CH_2Cl_2 (25 mL) under argon. A solution of Z-NH-$(CH_2)_4$-NH_2 (0.75 g, 2.90 mmol) and NMM (0.293 g, 2.90 mmol) in CH_2Cl_2 (10 mL) was added to the flask, and the reaction was allowed to stir for 45 min. A solution of Boc-NH-NH-$CH_2CH(CH_3)_2$

(0.545 g, 2.90 mmol) and NMM (0.103 g, 1.02 mmol) in CH_2Cl_2 (3 mL) was added to the flask, and the reaction was allowed to stir overnight. The reaction was concentrated and the residue was purified by column chromatography (2:1 EtOAc:Hexanes) to yield Boc-ALeu-NH-$(CH_2)_4$-NH-Z (0.888 g, 70% yield). ^{1}H NMR ($CDCl_3$): 0.91-0.97 (d, 6H), 1.44-1.49 (s, 9H), 1.52-1.67 (m, 4H), 1.70-1.78 (p, 1H), 2.64-2.70 (d, 2H), 3.15-3.26 (m, 4H), 5.05-5.11 (s, 2H), 4.76-4.83 (s, 1H), 5.94-6.03 (s, 1H), 7.26-7.39 (m, 5H).

ALeu-NH-$(CH_2)_4$-NH-Z·TFA. Boc-ALeu-NH-$(CH_2)_4$-NH-Z (0.400 g, 0.917 mmol) was dissolved in CH_2Cl_2 (3 mL) and cooled in an icebath. TFA (1 mL/mmol reactant) was added to the flask, and the reaction was monitored by TLC until complete (6 hrs). The reaction was concentrated, and the residue was crystallized in ether/hexanes to yield ALeu-NH-$(CH_2)_4$-NH-Z·TFA (0.297 g, 72% yield).

EtO-(2*S*,3*S*)-EPS-ALeu-NH-$(CH_2)_4$-NH-Z. **General Mixed Anhydride Procedure**. (2*S*,3*S*)-Ethyl-2,3-oxirane dicarboxylate (114 mg, 0.71 mmol) was dissolved in CH_2Cl_2 (15 mL) and cooled to –20 ^{o}C in a dry ice/acetone bath. The base NMM (72 mg, 0.71 mmol) was added to the reaction, followed by isobutylchloroformate (97 mg, 0.71 mmol), and the reaction was allowed to stir for 20 min. ALeu-NH-$(CH_2)_4$-NH-Z·TFA (160 mg, 0.355 mmol) was dissolved in CH_2Cl_2 (2 mL) and added to the flask, followed by NMM (36 mg, 0.355 mmol). The reaction was allowed to stir for 1 hr in the cold, then at room temperature overnight. The reaction was concentrated, and the residue was purified by column chromatography (8% MeOH, 20% EtOAc, 72% CH_2Cl_2) to yield EtO-(2*S*,3*S*)-EPS-ALeu-NH-$(CH_2)_4$-NH-Z (36 mg, 21% yield). ^{1}H NMR ($CDCl_3$): 0.86-1.01 (m, 9H), 1.25-1.37 (m, 4H), 1.81-2.01 (p, 1H, J = 7 Hz), 3.58-3.64 (q, 2H, J = 6 Hz),

3.75-3.78 (d, 1H, J = 2 Hz), 3.79-3.82 (d, 1H, J = 2 Hz), 4.21-4.33 (m, 6H), 4.66-4.72 (s, 2H), 7.21-7.39 (m, 5H), 8.20-8.23 (s, 1H).

(2*S*,3*S*)-3-(N^2-(4-(Benzyloxycarbamoyl)butylcarbamoyl)-N^1-(3-methylbutyl)hydrazinocarbonyl)oxirane-2-carboxylic acid. (HO-(2*S*,3*S*)-EPS-ALeu-NH-$(CH_2)_4$-NH-Z). EtO-(2*S*,3*S*)-EPS-ALeu-NH-$(CH_2)_4$-NH-Z (49 mg, 0.102 mmol) was dissolved in EtOH (4 mL) and cooled in an ice bath. A solution of 1 N NaOH (175 µL) was added to the flask, and the reaction allowed to stir for 1 hr in the cold, then for 5 hrs at room temperature. The reaction was quenched with acetic acid and concentrated. The residue was dissolved in H_2O (20 mL) and washed with EtOAc. The water layer was cooled in an ice bath and the pH was adjusted to 3 with 3 N HCl. The water layer was extracted with EtOAc, and the organic layers were dried over Na_2SO_4 and concentrated. The residue was recrystallized from EtOAc/hexanes to yield HO-(2*S*,3*S*)-EPS-ALeu-NH-$(CH_2)_4$-NH-Z (12 mg, 26% yield). ^{1}H NMR (d_6-DMSO): 0.78-0.85 (d, 6H, J = 6 Hz), 1.32-1.40 (m, 4H), 1.61-1.69 (p, 1H, J = 3 Hz), 2.93-3.02 (m, 4H), 3.13-3.18 (d, 2H, J = 5 Hz), 4.95-4.98 (s, 1H), 6.90-6.94 (s, 1H), 7.18-7.27 (m, 5H). HRMS (FAB): Calcd for $C_{21}H_{31}N_4O_7$: 451.21927. Observed *m/z*: 451.22404.

EtO-(2*R*,3*R*)-EPS-ALeu-NH-$(CH_2)_4$-NH-Z. (2*R*,3*R*)-Ethyl-2,3-oxirane dicarboxylate (160 mg, 0.999 mmol) and ALeu-NH-$(CH_2)_4$-NH-Z·TFA (150 mg, 0.333 mmol) were coupled following the general mixed anhydride procedure. The crude product was purified by column chromatography (8% MeOH, 20% EtOAc, 72% CH_2Cl_2) to yield EtO-(2*R*,3*R*)-EPS-ALeu-NH-$(CH_2)_4$-NH-Z (57 mg, 36% yield). ^{1}H NMR ($CDCl_3$): 0.90-0.94 (d, 6H, J = 5 Hz), 1.50-1.57 (m, 4H), 1.78-1.85 (p, 1H, J = 5 Hz),

3.14-3.23 (m, 4H), 3.26-3.32 (d, 2H, J = 4 Hz), 3.38-3.42 (d, 2H, J = 4 Hz), 4.89-4.96 (s, 1H), 5.04-5.10 (s, 2H), 5.33-5.37 (s, 1H), 7.25-7.37 (m, 5H), 9.04-9.10 (s, 1H).

(2*R*,3*R*)-3-(N^2-(4-(Benzyloxycarbamoyl)butylcarbamoyl)-N^1-(3-methylbutyl)hydrazinocarbonyl)oxirane-2-carboxylic acid. (HO-(2*R*,3*R*)-EPS-ALeu-NH-$(CH_2)_4$-NH-Z). EtO-(2*R*,3*R*)-EPS-ALeu-NH-$(CH_2)_4$-NH-Z (49 mg, 0.102 mmol) was hydrolyzed with 1 N NaOH (200 μL) following the same procedure as HO-(2*S*,3*S*)-EPS-ALeu-NH-$(CH_2)_4$-NH-Z. The crude product was recrystallized from ether/hexanes to yield HO-(2*R*,3*R*)-EPS-ALeu-NH-$(CH_2)_4$-NH-Z (21 mg, 45% yield). ^{1}H NMR (d_6-DMSO): 0.78-0.85 (d, 6H, J = 6 Hz), 1.32-1.40 (m, 4H), 1.61-1.69 (p, 1H, J = 5 Hz), 2.93-3.02 (m, 4H), 3.13-3.18 (d, 2H, J = 5 Hz), 4.95-4.98 (s, 1H), 6.90-6.94 (s, 1H), 7.18-7.27 (m, 5H). HRMS (ESI): Calcd for $C_{21}H_{31}N_4O_7$: 451.21927. Observed *m/z*: 451.2231.

Boc-Leu-NH-$(CH_2)_4$-NH-Z. Boc-Leu-OH·H_2O (1.125 g, 4.5 mmol) was taken up in toluene and evaporated several times to remove the water. Boc-Leu-OH was coupled with NH_2-$(CH_2)_4$-NH-Z·HCl (1.163 g, 4.5 mmol) following the general mixed anhydride reaction. The crude product was purified by column chromatography (10% MeOH in CH_2Cl_2) to yield Boc-Leu-NH-$(CH_2)_4$-NH-Z (1.675 g, 85% yield). ^{1}H NMR ($CDCl_3$): 0.86-0.97 (dd, 6H), 1.38-1.45 (s, 9H), 1.48-1.55 (m, 4H), 1.65-1.71 (p, 1H), 3.10-3.32 (m, 4H), 3.95-4.10 (m, 1H), 4.79-4.96 (s, 1H), 5.05-5.13 (s, 2H), 6.18-6.30 (s, 1H), 7.23-7.40 (m, 5H).

Leu-NH-$(CH_2)_4$-NH-Z·HCl. Boc-Leu-NH-$(CH_2)_4$-NH-Z (1.675 g, 3.82 mmol) was dissolved in 4 N HCl/EtOAc in an ice bath and allowed to stir for 3 hrs. The reaction

was concentrated *in vacuo* and crystallized in ether/hexanes to yield Leu-NH-$(CH_2)_4$-NH-Z·HCl quantitatively.

EtO-(2*S*,3*S*)-EPS-Leu-NH$(CH_2)_4$NH-Z. (2*S*,3*S*)-Ethyl-2,3-oxirane dicarboxylate (212 mg, 1.20 mmol) and Leu-NH-$(CH_2)_4$-NH-Z·HCl (446 mg, 1.20 mmol) were coupled following the general mixed anhydride procedure. The crude product was purified by recrystallization in 1:3 EtOAc:hexanes to yield EtO-(2*S*,3*S*)-EPS-Leu-NH$(CH_2)_4$NH-Z (289 mg, 51% yield). ^{1}H NMR ($CDCl_3$): 0.86-0.95 (m, 9H), 1.22-1.34 (m, 4H), 1.46-1.57 (m, 2H), 1.58-1.67 (p, 1H, J = 5 Hz), 3.16-3.30 (m, 4H), 3.43-3.46 (d, 1H, J = 2 Hz), 3.66-3.70 (d, 1H, J = 2 Hz), 4.22-4.30 (q, 2H, J = 3 Hz), 4.32-4.41 (m, 1H), 4.84-4.93 (s, 1H), 5.07-5.11 (s, 2H), 6.23-6.35 (s, 1H), 6.51-6.60 (d, 1H, J = 8 Hz), 7.25-7.38 (m, 5H). HRMS (FAB): Calcd for $C_{24}H_{36}N_3O_7$: 478.25533. Observed *m/z*: 478.25560.

(2*S*,3*S*)-3-(1-(4-Benzyloxycarbonylaminobutylcarbamoyl)-3-methylbutylcarbamoyl)oxirane-2-carboxylic acid. (HO-(2*S*,3*S*)-EPS-Leu-NH$(CH_2)_4$NH-Z). EtO-(2*S*,3*S*)-EPS-Leu-NH$(CH_2)_4$NH-Z (66 mg, 0.138 mmol) was hydrolyzed with 1 N NaOH (151 μL) following the same procedure as HO-(2*S*,3*S*)-EPS-ALeu-NH-$(CH_2)_4$-NH-Z. The crude product was recrystallized in EtOAc/hexanes to yield HO-(2*S*,3*S*)-EPS-Leu-NH$(CH_2)_4$NH-Z (41 mg, 66% yield). ^{1}H NMR (d_6-DMSO): 0.78-0.89 (m, 6H), 1.20-1.28 (m, 4H), 1.32-1.38 (m, 2H), 1.39-1.48 (p, 1H, J = 3 Hz), 2.23-2.26 (m, 1H), 2.68-2.73 (m, 1H), 2.88-3.06 (m, 4H), 4.20-4.31 (m, 1H), 4.92-4.96 (s, 2H), 7.23-7.28 (m, 5H), 8.00-8.09 (s, 1H). HRMS (FAB): Calcd for $C_{22}H_{32}N_3O_7$: 450.22403. Observed *m/z*: 450.22510.

***N*-Boc-1,4-diaminobutane (Boc-NH-$(CH_2)_4$-NH_2)**. To a solution of diaminobutane (6 g, 68.3 mmol) in dioxane (30 mL) was added BOC-ON (2-(*tert*-butoxycarbonyloxyimino)-2-phenylacetonitrile) (1.923 g, 8.62 mmol) in dioxane (30 mL) over 2.5 hours. The reaction was stirred overnight, during which time a white precipitate formed. The dioxane was evaporated under reduced pressure, the residue was taken up in water (50 mL), and the solid *bis*-Boc-diaminobutane side product was removed by filtration. The water layer was extracted with CH_2Cl_2 (3 × 50 mL) and the combined CH_2Cl_2 layers were dried over Na_2SO_4 and concentrated to give N-Boc-1,4-diaminobutane, a clear oil, in quantitative yield. ^{1}H NMR ($CDCl_3$): 1.38-1.58 (m, 13H), 2.68-2.72 (t, 2H), 3.09-3.15 (d, 2H), 3.70 (s, 2H), 4.70 (s, 1H).

Boc-NH-$(CH_2)_4$-NH-CO-NH-$CH_2C_6H_5$. To a cooled solution of N-Boc-1,4-diaminobutane (400 mg, 2.13 mmol) in CH_2Cl_2 (7 mL) was added benzyl isocyanate (283 mg, 2.13 mmol) along with NMM (50 mg, 0.49 mmol). The reaction was allowed to stir at room temperature overnight, during which time a white precipitate formed. The solvent was evaporated *in vacuo* and the residue was purified by column chromatography to yield Boc-NH-$(CH_2)_4$-NH-CO-NH-$CH_2C_6H_5$ (496 mg,1.42 mmol, 67%) ^{1}H NMR ($CDCl_3$): 1.41 (s, 9H), 1.50-1.56 (m, 4H), 3.08-3.16 (m, 2H), 3.20-3.24 (m, 2H), 4.38-4.40 (d, 2H), 4.60 (s, 1H), 4.75 (s, 1H), 7.23-7.32 (m, 5H).

$NH_2(CH_2)_4$-NH-CO-NH-$CH_2C_6H_5$·TFA. To a cooled solution of Boc-NH-$(CH_2)_4$-NH-CO-NH-$CH_2C_6H_5$ (496 mg, 1.55 mmol) in CH_2Cl_2 (5 mL) was added TFA (1.5 mL) and the reaction was stirred for 2 hours on ice until reacted by TLC. The solvents were evaporated *in vacuo* and the residue was crystallized from ether/hexanes to yield $NH_2(CH_2)_4$-NH-CO-NH-$CH_2C_6H_5$ ·TFA (505 mg, 1.50 mmol, 97% yield).

Boc-Leu-NH-$(CH_2)_4$-NH CO-NH-$CH_2C_6H_5$. Boc-Leu-OH·H_2O (378 mg, 1.51 mmol) and $NH_2(CH_2)_4$-NH-CO-NH-$CH_2C_6H_5$·TFA (505 mg, 1.51 mmol) were reacting following the general mixed anhydride coupling procedure to yield Boc-Leu-NH-$(CH_2)_4$-NH-CO-NH-$CH_2C_6H_5$ (510 mg, 1.17 mmol, 78%). ^{1}H NMR ($CDCl_3$): 0.89-0.93 (t, 6H), 1.40-1.53 (m, 15H), 1.58-1.67 (m, 1H), 3.07-3.29 (m, 4H), 4.06-4.12 (m, 1H), 4.32-4.36 (d, 2H), 5.05-5.08 (d, 1H), 5.16-5.21 (m, 1H), 5.45 (s, 1H), 6.73 (s, 1H), 7.19-7.38 (m, 5H).

Leu-NH-$(CH_2)_4$-NH-CO-NH-$CH_2C_6H_5$·HCl. Leu-NH-$(CH_2)_4$-NH-CO-NH-$CH_2C_6H_5$·HCl was synthesized from Boc-Leu-NH-$(CH_2)_4$-NH CO-NH-$CH_2C_6H_5$ (510 mg, 1.17 mmol) by the same method as Leu-NH-$(CH_2)_4$-NH-*Z*·HCl. The crude product was crystallized from ether/hexanes to yield Leu-NH-$(CH_2)_4$-NH-CO-NH-$CH_2C_6H_5$·HCl quantitatively.

EtO-(2*S*,3*S*)-EPS-Leu-NH-$(CH_2)_4$-NH-CO-NH-$CH_2C_6H_5$. (2*S*,3*S*)-Ethyl-2,3-oxirane dicarboxylate (187 mg, 1.17 mmol) and Leu-NH-$(CH_2)_4$-NH-CO-NH-$CH_2C_6H_5$·HCl (433 mg, 1.17 mmol) were coupled following the general mixed anhydride coupling procedure. The crude product was purified by column chromatography (8% MeOH, 20% EtOAc, 72% CH_2Cl_2) to yield EtO-(2*S*,3*S*)-EPS-Leu-NH-$(CH_2)_4$-NH-CO-NH-$CH_2C_6H_5$ (157 mg, 0.33 mmol, 28% yield). ^{1}H NMR ($CDCl_3$): 0.90-0.95 (t, 6H), 1.30-1.34 (t, 3H), 1.47-1.55 (m, 4H), 1.58-1.63 (m, 1H), 1.66 (s, 2H), 3.16-3.22 (m, 4H), 3.45-3.46 (d, 1H), 3.65-3.66 (d, 1H), 4.22-4.30 (m, 2H), 4.34-4.42 (m, 3H), 4.82 (s, 1H), 5.06 (s, 1H), 6.64-6.72 (m, 1H), 7.20-7.33 (m, 5H).

(2*S*,3*S*)-3-(1-(4-(3-Benzylureido)butylcarbamoyl)-3-methylbutylcarbamoyl))oxirane-2-carboxylic acid. (HO-(2*S*,3*S*)-EPS-Leu-NH-

$(CH_2)_4$-NH-CO-NH-$CH_2C_6H_5$). EtO-(2*S*,3*S*)-EPS-Leu-NH-$(CH_2)_4$-NH-CO-NH-$CH_2C_6H_5$ (137 mg, 0.29 mmol) was hydrolyzed following the same procedure as HO-(2*S*,3*S*)-EPS-ALeu-NH-$(CH_2)_4$-NH-Z to yield HO-(2*S*,3*S*)-EPS-Leu-NH-$(CH_2)_4$-NH-CO-NH-$CH_2C_6H_5$ (73 mg, 0.16 mmol, 57% yield). ^{1}H NMR (d_6-DMSO): 0.82-0.90 (dd, 6H, *J* = 3, 8 Hz), 1.32-1.39 (m, 4H), 1.42-1.47 (m, 2H), 1.49-1.57 (m, 1H), 2.96-3.07 (m, 4H), 3.44-3.45 (d, 1H, *J* = 3 Hz), 3.64-3.65 (d, 1H, *J* = 3 Hz), 4.15-4.19 (d, 2H, *J* = 5 Hz), 4.26-4.32 (m, 1H), 5.87-5.92 (t, 1H, *J* = 6 Hz), 6.22-6.27 (t, 1H, *J* = 6 Hz), 7.16-7.30 (m, 5H), 8.06-8.09 (t, 1H, *J* = 5 Hz), 8.54-8.57 (d, 1H, *J* = 6 Hz). HRMS (ESI) Calcd. for $C_{22}H_{33}N_4O_6$: 449.24001. Observed *m/z* 449.2394.

Boc-NH-$(CH_2)_4$-NH-CO-NH-C_6H_5. Boc-NH-$(CH_2)_4$-NH_2 (400 mg, 2.13 mmol) and phenyl isocyanate (253 mg, 2.13 mmol) were reacted following the same procedure as Boc-NH-$(CH_2)_4$-NH-CO-NH-$CH_2C_6H_5$ to yield Boc-NH-$(CH_2)_4$-NH-CO-NH-C_6H_5 (466 mg, 1.51 mmol, 71% yield). ^{1}H NMR ($CDCl_3$): 1.41-1.47 (s, 9H), 1.49-1.56 (m, 4H), 3.10-3.18 (m, 2H), 3.23-3.30 (m, 2H), 4.62-4.69 (s, 1H), 5.13-5.23 (s, 1H), 6.60-6.68 (s, 1H), 7.28-7.39 (m, 5H).

NH_2-$(CH_2)_4$-NH-CO-NH-C_6H_5·TFA. Boc-NH-$(CH_2)_4$-NH-CO-NH-C_6H_5 (466 mg, 1.52 mmol) was deblocked following the same procedure as NH_2-$(CH_2)_4$-NH-CO-NH-$CH_2C_6H_5$·TFA to yield NH_2-$(CH_2)_4$-NH-CO-NH-C_6H_5·TFA quantitatively.

Boc-Leu-NH-$(CH_2)_4$-NH-CO-NH-C_6H_5. Boc-Leu-OH·H_2O (380 mg, 1.52 mmol) and NH_2-$(CH_2)_4$-NH-CO-NH-C_6H_5·TFA (488 mg, 1.52 mmol) were coupled following the general mixed anhydride coupling procedure to yield Boc-Leu-NH-$(CH_2)_4$-NH-CO-NH-C_6H_5 (370 mg, 0.88 mmol, 58% yield). ^{1}H NMR ($CDCl_3$): 0.91-0.97 (dd, 6H), 1.41-1.45 (s, 9H), 1.47-1.56 (m, 4H), 1.58-1.62 (m, 2H), 1.65-1.71 (p, 1H), 3.12-

3.40 (m, 4H), 4.05-4.14 (m, 1H), 4.93-5.02 (s, 1H), 5.27-5.32 (s, 1H), 6.52-6.58 (s, 1H), 6.98-7.06 (t, 2H), 7.26-7.30 (d, 1H), 7.33-7.39 (d, 2H).

Leu-NH-$(CH_2)_4$-NH-CO-NH-C_6H_5·TFA. Boc-Leu-NH-$(CH_2)_4$-NH-CO-NH-C_6H_5 (370 mg, 0.88 mmol) was deblocked following the same procedure as NH_2-$(CH_2)_4$-NH-CO-NH-$CH_2C_6H_5$·TFA to yield Leu-NH_2-$(CH_2)_4$-NH-CO-NH-C_6H_5·TFA quantitatively.

EtO-(2*S*,3*S*)-EPS-Leu-NH-$(CH_2)_4$-NH-CO-NH-C_6H_5. (2*S*,3*S*)-Ethyl-2,3-oxirane dicarboxylate (141 mg, 0.88 mmol) and Leu-NH_2-$(CH_2)_4$-NH-CO-NH-C_6H_5·TFA (382 mg, 0.88 mmol) were coupled following the general mixed anhydride coupling procedure. The crude product was purified by column chromatography (8% MeOH, 20% EtOAc, 72% CH_2Cl_2) to yield EtO-(2*S*,3*S*)-EPS-Leu-NH-$(CH_2)_4$-NH-CO-NH-C_6H_5 (61 mg, 0.132 mmol, 15% yield). ^{1}H NMR (d_6-DMSO): 0.78-0.90 (dd, 6H), 1.34-1.42 (m, 7H), 1.44-1.48 (m, 2H), 1.48-1.56 (p, 1H), 2.97-3.07 (m, 4H), 3.43-3.45 (d, 1H), 3.62-3.65 (d, 1H), 4.15-4.22 (m, 2H), 4.24-4.33 (m, 1H), 6.05-6.10 (t, 1H), 6.82-6.88 (t, 1H), 7.14-7.21 (t, 2H), 7.31-7.36 (d, 2H), 8.06-8.11 (t, 1H), 8.32-8.36 (s, 1H), 8.54-8.58 (d, 1H).

(2*S*,3*S*)-3-(1-(4-(3-Phenylureido)butylcarbamoyl)-3-methylbutylcarbamoyl)oxirane-2-carboxylic acid. (HO-(2*S*,3*S*)-EPS-Leu-NH-$(CH_2)_4$-NH-CO-NH-C_6H_5). EtO-(2*S*,3*S*)-EPS-Leu-NH-$(CH_2)_4$-NH-CO-NH-C_6H_5 (61 mg, 0.132 mmol) was deblocked following the same procedure as HO-(2*S*,3*S*)-EPS-ALeu-NH-$(CH_2)_4$-NH-Z to yield HO-(2*S*,3*S*)-EPS-Leu-NH-$(CH_2)_4$-NH-CO-NH-C_6H_5 (36 mg, 0.83 mmol, 63% yield). ^{1}H NMR (d_6-DMSO): 0.79-0.88 (dd, 6H, J = 5, 8 Hz), 1.34-1.40 (m, 4H), 1.41-1.46 (m, 2H), 1.48-1.56 (p, 1H, J = 5 Hz), 2.97-3.07 (m, 4H),

3.43-3.45 (d, 1H, *J* = 2 Hz), 3.62-3.65 (d, 1H, *J* = 2 Hz), 4.24-4.33 (m, 1H), 6.05-6.10 (t, 1H, *J* = 5 Hz), 6.82-6.88 (t, 1H, *J* = 6 Hz), 7.14-7.21 (t, 2H, *J* = 6 Hz), 7.31-7.36 (d, 2H, *J* = 7 Hz), 8.06-8.11 (t, 1H, *J* = 4 Hz), 8.32-8.36 (s, 1H), 8.54-8.58 (d, 1H, *J* = 6 Hz)**.** HRMS (ESI) Calcd. for $C_{21}H_{31}N_4O_6$: 435.223812. Observed *m/z* 435.2303.

Boc-NH-$(CH_2)_4$-NH-CO-NH-C_6H_4-4-(OCH_3). Boc-NH-$(CH_2)_4$-NH-Z (400 mg, 2.13 mmol) and 4-methoxyphenyl isocyanate (317 mg, 2.13 mmol) were reacted following the same procedure as Boc-NH-$(CH_2)_4$-NH-CO-NH-$CH_2C_6H_5$ to yield Boc-NH-$(CH_2)_4$-NH-CO-NH-C_6H_4-4-(OCH_3) (556 mg, 1.65 mmol, 77% yield). ^{1}H NMR ($CDCl_3$): 1.44 (s, 9H), 1.47-1.52 (m, 4H), 3.08-3.15 (d, 2H), 3.19-3.25 (s, 3H), 4.66 (s, 1H), 5.00 (s, 1H), 6.51 (s, 1H), 6.82-6.86 (d, 2H), 7.17-7.21 (d, 2H).

NH_2-$(CH_2)_4$-NH-CO-NH-C_6H_4-4-(OCH_3)·TFA. Boc-NH-$(CH_2)_4$-NH-CO-NH-C_6H_4-4-(OCH_3) (556 mg, 1.65 mmol) was deblocked following the same procedure as $NH_2(CH_2)_4$-NH-CO-NH-$CH_2C_6H_5$ ·TFA to yield NH_2-$(CH_2)_4$-NH-CO-NH-C_6H_4-4-(OCH_3)·TFA quantitatively.

Boc-Leu-NH-$(CH_2)_4$-NH-CO-NH-C_6H_4-4-(OCH_3). Boc-Leu-OH·H_2O (413 mg, 1.65 mmol) and NH_2-$(CH_2)_4$-NH-CO-NH-C_6H_4-4-(OCH_3)·TFA (579 mg, 1.65 mmol) were coupled following the general mixed anhydride coupling procedure to yield Boc-Leu-NH-$(CH_2)_4$-NH-CO-NH-C_6H_4-4-(OCH_3) (576 mg, 1.28 mmol, 77% yield). ^{1}H NMR ($CDCl_3$): 0.92-0.96 (m, 6H), 1.43 (s, 9H), 1.48-1.50 (m, 4H), 1.61-1.71 (m, 3H), 3.15-3.38 (m, 4H), 3.79 (s, 3H), 4.06-4.13 (m, 1H), 4.98 (s, 1H), 5.05 (s, 1H), 6.55 (s, 1H), 6.67 (s, 1H), 6.76-6.80 (d, 2H), 7.20-7.24 (d, 2H).

Leu-NH-$(CH_2)_4$-NH-CO-NH-C_6H_4-4-(OCH_3)·HCl. Boc-Leu-NH-$(CH_2)_4$-NH-CO-NH-C_6H_4-4-(OCH_3) (576 mg, 1.28 mmol) was deblocked following the same method

as Leu-NH-$(CH_2)_4$-NH-Z·HCl. The crude product was crystallized from ether/hexanes to yield Leu-NH-$(CH_2)_4$-NH-CO-NH-C_6H_4-4-(OCH_3)·HCl quantitatively.

EtO-(2*S*,3*S*)-EPS-Leu-NH-$(CH_2)_4$-NH-CO-NH-C_6H_4-4-(OCH_3). (2*S*,3*S*)-Ethyl-2,3-oxirane dicarboxylate (205 mg, 1.28 mmol) and Leu-NH-$(CH_2)_4$-NH-CO-NH-C_6H_4-4-(OCH_3)·HCl (495 mg, 1.28 mmol) were coupled following the general mixed anhydride coupling procedure. The crude product was purified by column chromatography (8% MeOH, 20% EtOAc, 72% CH_2Cl_2) to yield EtO-(2*S*,3*S*)-EPS-Leu-NH-$(CH_2)_4$-NH-CO-NH-C_6H_4-4-(OCH_3) (106 mg, 0.22 mmol, 17% yield). ^{1}H NMR ($CDCl_3$): 0.92-0.95 (t, 6H), 1.31-1.34 (t, 3H), 1.51-1.61 (m, 6H), 1.63-1.69 (m, 1H), 3.21-3.37 (m, 4H), 3.46-3.47 (d, 1H), 3.69-3.70 (d, 1H), 3.80 (s, 3H), 4.22-4.30 (m, 2H), 4.39-4.44 (m, 1H), 4.81-4.85 (t, 1H), 6.32 (s, 1H), 6.65-6.68 (d, 1H), 6.85-6.88 (d, 2H), 7.18-7.21 (d, 2H).

(2*S*,3*S*)-3-(1-(4-(3-(4-methoxyphenyl)ureido)butylcarbamoyl)-3-methylbutylcarbamoyl)oxirane-2-carboxylic acid. (HO-(2*S*,3*S*)-EPS-Leu-NH-$(CH_2)_4$-NH-CO-NH-C_6H_4-4-(OCH_3)). EtO-(2*S*,3*S*)-EPS-Leu-NH-$(CH_2)_4$-NH-CO-NH-C_6H_4-4-(OCH_3) (84 mg, 0.17 mmol) was hydrolyzed following the same procedure as HO-(2*S*,3*S*)-EPS-ALeu-NH-$(CH_2)_4$-NH-Z to yield HO-(2*S*,3*S*)-EPS-Leu-NH-$(CH_2)_4$-NH-CO-NH-C_6H_4-4-(OCH_3) (76 mg, 0.16 mmol, 96% yield). ^{1}H NMR (d_6-DMSO): 0.82-0.88 (dd, 6H, J = 5, 9 Hz), 1.36-1.41 (m, 4H), 1.43-1.48 (m, 2H), 1.50-1.57 (m, 1H), 3.00-3.07 (m, 4H), 3.44-3.45 (d, 1H, J = 2 Hz), 3.64-3.65 (d, 1H, J = 2 Hz), 3.67 (s, 3H), 4.26-4.32 (m, 1H), 5.98 (s, 1H), 6.76-6.79 (d, 2H, J = 6 Hz), 7.23-7.26 (d, 2H, J = 6 Hz), 8.08 (s, 1H), 8.14 (s, 1H), 8.54-8.56 (s, 1H). HRMS (ESI) Calcd. for $C_{22}H_{33}N_4O_7$: 465.234925. Observed *m/z* 465.2269.

Boc-NH-$(CH_2)_4$-NH-CO-(3-pyridyl). Boc-NH-$(CH_2)_4$-NH_2 (400 mg, 2.13 mmol) and isonicotinic acid (262 mg, 2.13 mmol) were coupled following the general mixed anhydride coupling procedure. The crude product was purified by column chromatography (8% MeOH, 20% EtOAc, 72% CH_2Cl_2) to yield Boc-NH-$(CH_2)_4$-NH-CO-(3-pyridyl) (210 mg, 0.716 mmol, 33% yield). ^{1}H NMR ($CDCl_3$): 1.42-1.47 (s, 9H), 1.59-1.71 (m, 4H), 3.13-3.22 (q, 2H), 3.48-3.56 (q, 2H), 4.63-4.70 (s, 1H), 6.92-6.99 (s, 1H),), 7.33-7.43 (m, 1H), 8.16-8.25 (d of d, 1H), 8.61-8.74 (m, 1H).

NH_2-$(CH_2)_4$-NH-CO-(3-pyridyl)·HCl. Boc-NH-$(CH_2)_4$-NH-CO-(3-pyridyl) (210 mg, 0.716 mmol) was deblocked by the same method as Leu-NH-$(CH_2)_4$-NH-Z·HCl. The crude product was crystallized from ether/hexanes to yield NH_2-$(CH_2)_4$-NH-CO-(3-pyridyl)·HCl quantitatively.

Boc-Leu-NH-$(CH_2)_4$-NH-CO-(3-pyridyl). Boc-Leu-OH·H_2O (195 mg, 0.78 mmol) and NH_2-$(CH_2)_4$-NH-CO-(3-pyridyl)·HCl (178 mg, 0.78 mmol) were coupled following the general mixed anhydride coupling procedure to yield Boc-Leu-NH-$(CH_2)_4$-NH-CO-(3-pyridyl) (200 mg, 0.49 mmol, 63% yield). ^{1}H NMR ($CDCl_3$): 0.89-0.98 (dd, 6H), 1.40-1.45 (s, 9H), 1.57-1.76 (m, 7H), 3.21-3.39 (m, 2H), 3.45-3.56 (m, 2H), 4.05-4.12 (m, 1H), 4.86-4.96 (s, 1H), 6.45-6.55 (s, 1H), 7.02-7.10 (s, 1H), 7.33-7.40 (m, 1H), 8.15-8.23 (d of d, 1H), 8.66-8.72 (m, 1H), 9.09-9.15 (s, 1H).

Leu-NH-$(CH_2)_4$-NH-CO-(3-pyridyl)·TFA. Boc-Leu-NH_2-$(CH_2)_4$-NH-CO-(3-pyridyl) (261 mg, 0.643 mmol) was deblocked following the same procedure as NH_2-$(CH_2)_4$-NH-CO-NH-$CH_2C_6H_5$·TFA to yield Leu-NH-$(CH_2)_4$-NH-CO-(3-pyridyl)·TFA quantitatively.

EtO-(2*S*,3*S*)-EPS-Leu-NH-$(CH_2)_4$-NH-CO-(3-pyridyl). (2*S*,3*S*)-Ethyl-2,3-oxirane dicarboxylate (103 mg, 0.643 mmol) and Leu-NH-$(CH_2)_4$-NH-CO-(3-pyridyl)·TFA (270 mg, 0.643 mmol) were coupled following the general mixed anhydride coupling procedure. The crude product was purified by column chromatography (8% MeOH, 20% EtOAc, 72% CH_2Cl_2) to yield EtO-(2*S*,3*S*)-EPS-Leu-NH-$(CH_2)_4$-NH-CO-(3-pyridyl) (86 mg, 0.19 mmol, 30% yield). ^{1}H NMR ($CDCl_3$): 0.87-0.95 (dd, 6H), 1.14-1.17 (t, 3H), 1.47-1.60 (m, 7H), 3.27-3.41 (m, 2H), 3.46-3.47 (d, 1H), 3.49-3.55 (q, 2H), 3.67-3.68 (d, 1H), 4.21-4.31 (m, 2H), 4.36-4.42 (m, 1H), 6.42-6.50 (s, 1H), 6.57-6.63 (s, 1H), 6.79-6.85 (s, 1H), 7.37-7.41 (d of d, 1H), 8.14-8.19 (d of t, 1H), 8.69-8.73 (d of d, 1H), 9.02-9.04 (d, 1H).

(2*S*,3*S*)-3-(1-(4-(3-pyridylcarbamoyl)butylcarbamoyl)-3-methylbutylcarbamoyl)oxirane-2-carboxylic acid. (HO-(2*S*,3*S*)-EPS-Leu-NH-$(CH_2)_4$-NH-CO-(3-pyridyl)). EtO-(2*S*,3*S*)-EPS-Leu-NH-$(CH_2)_4$-NH-CO-(3-pyridyl) (71 mg, 0.158 mmol) was hydrolyzed following the same procedure as HO-(2*S*,3*S*)-EPS-ALeu-NH-$(CH_2)_4$-NH-Z to yield HO-(2*S*,3*S*)-EPS-Leu-NH-$(CH_2)_4$-NH-CO-(3-pyridyl) (12 mg , 0.029 mmol, 18% yield). ^{1}H NMR (d_6-DMSO): 0.77-0.88 (dd, 6H, J = 5, 9 Hz), 1.37-1.58 (m, 7H), 2.97-3.10 (m, 4H), 3.42-3.45 (d, 1H, J = 2 Hz), 3.62-3.65 (d, 1H, J = 2 Hz), 4.24-4.30 (m, 1H), 7.45-7.50 (q, 1H, J = 5 Hz), 8.06-8.11 (m, 1H), 8.13-8.19 (dt, 1H, J = 2, 6 Hz), 8.53-8.59 (d, 1H, J = 7 Hz), 8.62-8.65 (m, 1H), 8.66-8.70 (d, 1H, J = 5 Hz), 8.95-8.98 (s, 1H). HRMS (ESI): Calcd for $C_{20}H_{29}N_4O_6$: 421.208161. Observed *m/z*: 421.2102.

Boc-NH-$(CH_2)_4$-NH-CO-CH_2-O-(1-naphthyl). Boc-NH-$(CH_2)_4$-NH_2 (1.02 g, 5.45 mmol) and 1-naphthoxyacetic acid (1.00 g, 4.95 mmol) were coupled following the

general mixed anhydride coupling procedure. The crude product was purified by column chromatography (8% MeOH, 20% EtOAc, 72% CH_2Cl_2) to yield Boc-NH-$(CH_2)_4$-NH-CO-CH_2-O-(1-naphthyl) (1.15 g, 3.09 mmol, 62% yield). ^{1}H NMR ($CDCl_3$): 1.44 (s, 9H), 1.46-1.54 (m, 2H), 1.56-1.63 (m, 2H), 3.09-3.15 (q, 2H), 3.37-3.42 (q, 2H), 4.55 (s, 1H), 4.70 (s, 2H), 6.66 (s, 1H), 6.78-6.81 (d, 1H), 7.38-7.42 (t, 1H), 7.50-7.55 (m, 3H), 7.82-7.86 (m, 1H), 8.18-8.22 (m, 1H).

NH_2-$(CH_2)_4$-NH-CO-CH_2-O-(1-naphthyl)·HCl. Boc-NH-$(CH_2)_4$-NH-CO-CH_2-O-(1-naphthyl) (1.15 g, 3.09 mmol) was deblocked following the same procedure as Leu-NH-$(CH_2)_4$-NH-Z·HCl. The crude product was crystallized from ether/hexanes to yield NH_2-$(CH_2)_4$-NH-CO-CH_2-O-(1-naphthyl)·HCl (841 mg, 3.04 mmol, 98% yield).

Boc-Leu-NH-$(CH_2)_4$-NH-CO-CH_2-O-(1-naphthyl). Boc-Leu-OH·H_2O (760 mg, 3.04 mmol) and NH_2-$(CH_2)_4$-NH-CO-CH_2-O-(1-naphthyl)·HCl (841mg, 3.04 mmol) were coupled following the general mixed anhydride coupling procedure. The crude product was purified by column chromatography (8% MeOH, 20% EtOAc, 72% CH_2Cl_2) to yield Boc-Leu-NH-$(CH_2)_4$-NH-CO-CH_2-O-(1-naphthyl) (288 mg, 0.59 mmol, 20% yield). ^{1}H NMR ($CDCl_3$): 0.91-0.99 (m, 6H), 1.42 (s, 9H), 1.51-1.62 (m, 7H), 3.21-3.31 (m, 2H), 3.38-3.43 (m, 2H), 4.20 (s, 1H), 4.72 (s, 2H), 4.83 (s, 1H), 6.22 (s, 1H), 6.73 (s, 1H), 6.79-6.83 (d, 1H), 7.38-7.42 (t, 1H), 7.49-7.56 (m, 3H), 7.82-7.87 (m, 1H), 8.18-8.24 (m, 1H).

Leu-NH-$(CH_2)_4$-NH-CO-CH_2-O-(1-naphthyl)·HCl. Boc-Leu-NH-$(CH_2)_4$-NH-CO-CH_2-O-(1-naphthyl) (288 mg, 0.59 mmol) was deblocked by the same method as Leu-NH-$(CH_2)_4$-NH-Z·HCl. The crude product was crystallized from ether/hexanes to

yield Leu-NH-$(CH_2)_4$-NH-CO-CH_2-O-(1-naphthyl)·HCl (229 mg, 0.53 mmol, 92% yield).

EtO-(2*S*,3*S*)-EPS-Leu-NH-$(CH_2)_4$-NH-CO-CH_2-O-(1-naphthyl). (2*S*,3*S*)-Ethyl-2,3-oxirane dicarboxylate (96 mg, 0.54 mmol) and Leu-NH-$(CH_2)_4$-NH-CO-CH_2-O-(1-naphthyl)·HCl (229 mg, 0.54 mmol) were coupled following the general mixed anhydride coupling procedure. The crude product was purified by column chromatography (8% MeOH, 20% EtOAc, 72% CH_2Cl_2) to yield EtO-(2*S*,3*S*)-EPS-Leu-NH-$(CH_2)_4$-NH-CO-CH_2-O-(1-naphthyl) (129 mg, 0.24 mmol, 45% yield). ^{1}H NMR ($CDCl_3$): 0.87-0.95 (m, 6H), 1.29-1.33 (t, 3H), 1.47-1.66 (m, 7H), 3.23-3.29 (m, 2H), 3.37-3.40 (m, 2H), 3.42-3.43 (d, 2H), 3.66-3.67 (d, 1H), 4.20-4.29 (m, 2H), 4.31-4.37 (m, 1H), 4.71 (s, 2H), 6.21 (s, 1H), 6.46-6.49 (d, 1H), 6.80-6.82 (d, 1H), 7.35-7.39 (t, 1H), 7.47-7.54 (m, 3H), 7.80-7.85 (m, 1H), 8.16-8.22 (m, 1H).

(2*S*,3*S*)-3-(1-(4-(2-(1-naphthaloxy)acetylamino)butylcarbamoyl)-3-methylbutylcarbamoyl)oxirane-2-carboxylic acid. (HO-(2*S*,3*S*)-EPS-Leu-NH-$(CH_2)_4$-NH-CO-CH_2-O-(1-naphthyl)). EtO-(2*S*,3*S*)-EPS-Leu-NH-$(CH_2)_4$-NH-CO-CH_2-O-(1-naphthyl) (115 mg, 0.22 mmol) was hydrolyzed with 1 N NaOH (294 µL) following the same method as HO-(2*S*,3*S*)-EPS-ALeu-NH-$(CH_2)_4$-NH-Z to yield HO-(2*S*,3*S*)-EPS-Leu-NH-$(CH_2)_4$-NH-CO-CH_2-O-(1-naphthyl) (87 mg, 0.17 mmol, 80% yield). ^{1}H NMR ($CDCl_3$): 0.91-0.97 (t, 6H, J = 5 Hz), 1.48-1.69 (m, 7H), 3.19-3.33 (m, 2H), 3.37-3.42 (q, 2H, J = 5 Hz), 3.60 (s, 2H), 4.46-4.53 (m, 1H), 4.72 (s, 2H), 6.76 (s, 1H), 6.79-6.84 (d, 1H, J = 5 Hz), 7.37-7.41 (t, 1H, J = 6 Hz), 7.49-7.53 (m, 3H), 7.81-7.87 (m, 1H), 8.16-8.21 (m, 1H). HRMS (ESI) Calcd. for $C_{26}H_{34}N_3O_7$: 500.239676. Observed *m/z* 500.2324.

Boc-NH-$(CH_2)_4$-NH-CO-CH_2-O-(2-naphthyl). Boc-NH-$(CH_2)_4$-NH_2 (1.02 g, 5.45 mmol) and 2-naphthoxyacetic acid (1.00 g, 4.95 mmol) were coupled following the general mixed anhydride coupling procedure. The crude product was purified by column chromatography (8% MeOH, 20% EtOAc, 72% CH_2Cl_2) to yield Boc-NH-$(CH_2)_4$-NH-CO-CH_2-O-(2-naphthyl) (1.32g, 3.54 mmol, 71% yield) ^{1}H NMR ($CDCl_3$): 1.45 (s, 9H), 1.46-1.53 (m, 2H), 1.55-1.62 (m, 2H), 3.07-3.12 (q, 2H), 3.37-3.42 (q, 2H), 4.55 (s, 1H), 4.70 (s, 2H), 6.19-6.24 (t, 1H), 6.50-6.55 (d, 1H), 6.72-6.79 (s, 1H), 7.11-7.23 (m, 1H), 7.35-7.41 (t, 1H), 7.44-7.50 (t, 1H), 7.70-7.81 (m, 4H).

NH_2-$(CH_2)_4$-NH-CO-CH_2-O-(2-naphthyl)·HCl. Boc-NH-$(CH_2)_4$-NH-CO-CH_2-O-(2-naphthyl) (1.15 g, 3.09 mmol) was deblocked following the same procedure as Leu-NH-$(CH_2)_4$-NH-Z·HCl. The crude product was crystallized from ether/hexanes to yield NH_2-$(CH_2)_4$-NH-CO-CH_2-O-(2-naphthyl)·HCl quantitatively.

Boc-Leu-NH-$(CH_2)_4$-NH-CO-CH_2-O-(2-naphthyl). Boc-Leu-OH·H_2O (768 mg, 3.07 mmol) and NH_2-$(CH_2)_4$-NH-CO-CH_2-O-(2-naphthyl)·HCl (850mg, 3.07 mmol) were coupled following the general mixed anhydride coupling procedure. The crude product was purified by column chromatography (8% MeOH, 20% EtOAc, 72% CH_2Cl_2) to yield Boc-Leu-NH-$(CH_2)_4$-NH-CO-CH_2-O-(2-naphthyl) (328 mg, 0.67 mmol, 23% yield). ^{1}H NMR ($CDCl_3$): 0.87-0.99 (m, 6H), 1.45 (s, 9H), 1.51-1.63 (m, 7H), 3.20-3.31 (m, 2H), 3.38-3.43 (m, 2H), 4.18 (s, 1H), 4.68 (s, 2H), 4.85 (s, 1H), 6.19-6.24 (t, 1H), 6.50-6.55 (d, 1H), 6.72-6.79 (s, 1H), 7.13-7.24 (m, 1H), 7.35-7.41 (t, 1H), 7.44-7.50 (t, 1H), 7.70-7.81 (m, 4H).

Leu-NH-$(CH_2)_4$-NH-CO-CH_2-O-(2-naphthyl)·HCl. Boc-Leu-NH-$(CH_2)_4$-NH-CO-CH_2-O-(2-naphthyl) (328 mg, 0.67 mmol) was deblocked by the same method as

Leu-NH-$(CH_2)_4$-NH-Z·HCl. The crude product was crystallized from ether/hexanes to yield Leu-NH-$(CH_2)_4$-NH-CO-CH_2-O-(2-naphthyl)·HCl (240 mg, 0.55 mmol, 96% yield).

EtO-(2*S*,3*S*)-EPS-Leu-NH-$(CH_2)_4$-NH-CO-CH_2-O-(2-naphthyl). (2*S*,3*S*)-Ethyl-2,3-oxirane dicarboxylate (98 mg, 0.55 mmol) and Leu-NH-$(CH_2)_4$-NH-CO-CH_2-O-(2-naphthyl)·HCl (240 mg, 0.55 mmol) were coupled following the general mixed anhydride coupling procedure. The crude product was purified by column chromatography (8% MeOH, 20% EtOAc, 72% CH_2Cl_2) to yield EtO-(2*S*,3*S*)-EPS-Leu-NH-$(CH_2)_4$-NH-CO-CH_2-O-(2-naphthyl) (46 mg, 0.087 mmol, 16% yield). ^{1}H NMR ($CDCl_3$): 0.90-0.97 (dd, 6H), 1.29-1.33 (t, 3H), 1.48-1.70 (m, 7H), 3.21-3.30 (m, 2H), 3.36-3.42 (m, 2H), 3.45-3.46 (d, 1H), 3.68-3.69 (d, 1H), 4.22-4.30 (q, 2H), 4.32-4.39 (m, 1H), 4.62-4.64 (s, 2H), 6.19-6.24 (t, 1H), 6.50-6.55 (d, 1H), 6.72-6.79 (s, 1H), 7.11-7.23 (m, 1H), 7.35-7.41 (t, 1H), 7.44-7.50 (t, 1H), 7.70-7.81 (m, 4H). HRMS (FAB): Calcd for $C_{28}H_{38}N_3O_7$: 528.270976. Observed *m/z*: 528.262.

(2*S*,3*S*)-3-(1-(4-(2-(2-naphthaloxy)acetylamino)butylcarbamoyl)-3-methylbutylcarbamoyl)oxirane-2-carboxylic acid. (HO-(2*S*,3*S*)-EPS-Leu-NH-$(CH_2)_4$-NH-CO-CH_2-O-(2-naphthyl)). EtO-(2*S*,3*S*)-EPS-Leu-NH-$(CH_2)_4$-NH-CO-CH_2-O-(2-naphthyl) (46 mg, 0.087 mmol) was hydrolyzed with 1 N NaOH (117 µL) following the same method as HO-(2*S*,3*S*)-EPS-ALeu-NH-$(CH_2)_4$-NH-Z to yield HO-(2*S*,3*S*)-EPS-Leu-NH-$(CH_2)_4$-NH-CO-CH_2-O-(2-naphthyl) (29 mg, 0.058 mmol, 67% yield). ^{1}H NMR (d6-DMSO): 0.79-0.89 (dd, 6H, J = 5, 8 Hz), 1.32-1.48 (m, 4H), 1.48-1.58 (m, 1H), 2.93-3.06 (m, 4H), 3.10-3.17 (m, 2H), 3.43-3.45 (d, 1H, J = 2 Hz), 3.63-3.65 (d, 1H, J = 2 Hz), 4.25-4.32 (m, 1H), 4.53-4.56 (s, 2H), 7.20-7.27 (m, 2H), 7.31-

7.36 (t, 1H, J = 7 Hz), 7.41-7.46 (t, 1H, J = 7 Hz), 7.73-7.77 (d, 1H, J = 6 Hz), 7.79-7.85 (t, 2H, J = 6 Hz), 8.04-8.08 (t, 1H, J = 5 Hz), 8.11-8.16 (t, 1H, J = 5 Hz), 8.54-8.57 (d, 1H, J = 6 Hz). HRMS (ESI) Calcd. for $C_{26}H_{34}N_3O_7$: 500.239127. Observed *m/z* 500.2422.

Boc-NH-$(CH_2)_4$-NH-CO-NH-(1-naphthyl). Boc-NH-$(CH_2)_4$-NH_2 (400 mg, 2.13 mmol) and 1-naphthyl isocyanate (360 mg, 2.13 mmol) were reacted following the same method as Boc-NH-$(CH_2)_4$-NH-CO-NH-$CH_2C_5H_6$ to yield Boc-NH-$(CH_2)_4$-NH-CO-NH-(1-naphthyl) (510 mg, 1.42 mmol, 67% yield). ^{1}H NMR ($CDCl_3$): 1.43 (s, 9H), 1.46-1.48 (m, 4H), 3.08-3.12 (m, 2H), 3.21-3.27 (d, 2H), 4.56 (s, 1H), 4.87 (s, 1H), 6.48 (s, 1H), 7.45-7.49 (t, 1H), 7.52-7.59 (m, 3H), 7.74-7.78 (d, 1H), 7.85-7.89 (m, 1H), 8.03-8.07 (m, 1H).

NH_2-$(CH_2)_4$-NH-CO-NH-(1-naphthyl)·TFA. Boc-NH-$(CH_2)_4$-NH-CO-NH-(1-naphthyl) (510 mg, 1.42 mmol) was deblocked following the same method as NH_2-$(CH_2)_4$-NH-CO-NH-$CH_2C_5H_6$·TFA to yield NH_2-$(CH_2)_4$-NH-CO-NH-(1-naphthyl)·TFA quantitatively.

Boc-Leu-NH-$(CH_2)_4$-NH CO-NH-(1-naphthyl). Boc-Leu-OH·H_2O (355 mg, 1.42 mmol) and NH_2-$(CH_2)_4$-NH-CO-NH-(1-naphthyl)·TFA (527 mg, 1.42 mmol) were coupled following the general mixed anhydride coupling procedure to yield Boc-Leu-NH-$(CH_2)_4$-NH-CO-NH-(1-naphthyl) (419 mg, 0.891 mmol, 63% yield). ^{1}H NMR ($CDCl_3$): 0.90-0.93 (t, 6H), 1.41 (s, 9H), 1.46-1.52 (m, 4H), 1.59-1.60 (m, 3H), 3.13-3.33 (m, 4H), 4.07-4.15 (m, 1H), 4.92-4.98 (d, 1H), 5.21 (s, 1H), 6.54-6.58 (t, 1H), 7.00 (s, 1H), 7.43-7.51 (m, 3H), 7.67-7.70 (d, 2H), 7.83-7.88 (m, 1H), 8.04-8.08 (m, 1H).

Leu-NH-$(CH_2)_4$-NH-CO-NH-(1-naphthyl)·HCl. Boc-Leu-NH-$(CH_2)_4$-NH-CO-NH-(1-naphthyl) (419 mg, 0.89 mmol) was deblocked by the same method as Leu-NH-$(CH_2)_4$-NH-Z·HCl. The crude product was crystallized from ether/hexanes to yield Leu-NH-$(CH_2)_4$-NH-CO-NH-(1-naphthyl)·HCl quantitatively.

EtO-(2*S*,3*S*)-EPS-Leu-NH-$(CH_2)_4$-NH-CO-NH-(1-naphthyl). (2*S*,3*S*)-Ethyl-2,3-oxirane dicarboxylate (142 mg, 0.89 mmol) and Leu-NH-$(CH_2)_4$-NH-CO-NH-(1-naphthyl)·HCl (362 mg, 0.89 mmol) were coupled following the general mixed anhydride coupling procedure. The crude product was purified by column chromatography (8% MeOH, 20% EtOAc, 72% CH_2Cl_2) to yield EtO-(2*S*,3*S*)-EPS-Leu-NH-$(CH_2)_4$-NH-CO-NH-(1-naphthyl) (92 mg, 0.18 mmol, 21% yield). ^{1}H NMR ($CDCl_3$): 0.87-0.99 (m, 6H), 1.29-1.33 (t, 3H), 1.48-1.55 (m, 6H), 1.64-1.71 (p, 1H), 3.21-3.23 (m, 4H), 3.45-3.46 (d, 1H), 3.69-3.70 (d, 1H), 4.21-4.29 (m, 2H), 4.39-4.40 (m, 1H), 4.82-4.86 (t, 1H), 6.57-6.68 (m, 2H), 7.46-7.51 (q, 1H), 7.52-7.57 (m, 2H), 7.75-7.78 (d, 1H), 7.87-7.92 (m, 1H), 8.03-8.07 (d, 1H).

(2*S*,3*S*)-3-(1-(4-(3-(2-naphthyl)ureido)butylcarbamoyl)-3-methylbutylcarbamoyl)oxirane-2-carboxylic acid. (HO-(2*S*,3*S*)-EPS-Leu-NH-$(CH_2)_4$-NH-CO-NH-(1-naphthyl)). EtO-(2*S*,3*S*)-EPS-Leu-NH-$(CH_2)_4$-NH-CO-NH-(1-naphthyl) (92 mg, 0.18 mmol) was hydrolyzed following the same procedure as HO-(2*S*,3*S*)-EPS-ALeu-NH-$(CH_2)_4$-NH-Z to yield HO-(2*S*,3*S*)-EPS-Leu-NH-$(CH_2)_4$-NH-CO-NH-(1-naphthyl) (58 mg, 0.12 mmol, 67% yield). ^{1}H NMR (d_6-DMSO): 0.82-0.88 (m, 6H), 1.43-1.49 (m, 6H), 1.51-1.57 (m, 1H), 3.03-3.15 (m, 4H), 3.45-3.46 (d, 1H, J = 2 Hz), 3.64-3.65 (d, 1H, J = 2 Hz), 4.27-4.34 (m, 1H), 6.58 (s, 1H), 7.38-7.42 (t, 1H, J = 6 Hz), 7.47-7.53 (m, 2H), 7.84-7.87 (d, 1H, J = 6 Hz), 7.96-7.98 (d, 1H, J = 6 Hz), 8.02-

8.06 (d, 1H, J = 6 Hz), 8.08-8.13 (m, 1H), 8.44 (s, 1H), 8.54-8.58 (d, 1H, J = 6 Hz). HRMS (ESI) Calcd. for $C_{25}H_{33}N_4O_6$: 485.24001. Observed *m/z* 485.2388.

Boc-NH-$(CH_2)_4$-NH-CO-NH-C_6H_4-2-(OC_6H_5). Boc-NH-$(CH_2)_4$-NH_2 (400 mg, 2.13 mmol) and 2-phenoxyphenyl isocyanate (493 mg, 2.13 mmol) were reacted following the same procedure as Boc-NH-$(CH_2)_4$-NH-CO-NH-$CH_2C_5H_6$ to yield Boc-NH-$(CH_2)_4$-NH-CO-NH-C_6H_4-2-(OC_6H_5) (850 mg, 2.13 mmol, 100% yield). ^{1}H NMR ($CDCl_3$): 1.39-1.44 (s, 9H), 1.50-1.56 (m, 4H), 3.06-3.16 (m, 2H), 3.22-3.30 (m, 2H), 4.55-4.62 (s, 1H), 5.06-5.14 (s, 1H), 6.85-6.87 (d, 2H), 6.89-6.94 (t, 1H), 6.95-7.00 (d, 2H), 7.05-7.14 (m, 2H), 7.28-7.35 (m, 2H), 8.11-8.19 (m, 1H).

NH_2-$(CH_2)_4$-NH-CO-NH-C_6H_4-2-(OC_6H_5)·TFA. Boc-NH-$(CH_2)_4$-NH-CO-NH-C_6H_4-2-(OC_6H_5) (850 mg, 2.13 mmol) was deblocked following the same procedure as $NH_2(CH_2)_4$-NH-CO-NH-$CH_2C_6H_5$·TFA to yield NH_2-$(CH_2)_4$-NH-CO-NH-C_6H_4-2-(OC_6H_5)·TFA quantitatively.

Boc-Leu-NH-$(CH_2)_4$-NH-CO-NH-C_6H_4-2-(OC_6H_5). Boc-Leu-OH·H_2O (560 mg, 2.24 mmol) and NH_2-$(CH_2)_4$-NH-CO-NH-C_6H_4-2-(OC_6H_5)·TFA (392 mg, 2.13 mmol) were coupled following the general mixed anhydride coupling procedure to yield Boc-Leu-NH-$(CH_2)_4$-NH-CO-NH-C_6H_4-2-(OC_6H_5) (529 mg, 1.03 mmol, 46% yield). ^{1}H NMR ($CDCl_3$): 0.84-0.89 (dd, 6H), 1.34-1.38 (s, 9H), 1.41-1.62 (m, 7H), 2.92-3.38 (m, 4H), 4.07-4.15 (d, 1H), 4.95-5.01 (d, 1H), 5.71-5.79 (s, 1H), 6.71-6.77 (s, 1H), 6.78-6.82 (d, 1H), 6.85-6.90 (t, 1H), 6.96-7.09 (m, 2H), 7.27-7.33 (t, 2H), 7.44-7.49 (s, 1H), 8.26-8.32 (d, 1H).

Leu-NH-$(CH_2)_4$-NH-CO-NH-C_6H_4-2-(OC_6H_5)·TFA. Boc-Leu-NH-$(CH_2)_4$-NH-CO-NH-C_6H_4-2-(OC_6H_5) (529 mg, 1.03 mmol) was deblocked following the same

procedure as $NH_2(CH_2)_4$-NH-CO-NH-$CH_2C_6H_5$·TFA to yield Leu-NH-$(CH_2)_4$-NH-CO-NH-C_6H_4-2-(OC_6H_5)·TFA (505 mg, 0.96 mmol, 93% yield).

EtO-(2*S*,3*S*)-EPS-Leu-NH-$(CH_2)_4$-NH-CO-NH-C_6H_4-2-(OC_6H_5). (2*S*,3*S*)-Ethyl-2,3-oxirane dicarboxylate (154 mg, 0.96 mmol) and Leu-NH-$(CH_2)_4$-NH-CO-NH-C_6H_4-2-(OC_6H_5)·TFA (505 mg, 0.96 mmol) were coupled following the general mixed anhydride coupling procedure. The crude product was purified by column chromatography (8% MeOH, 20% EtOAc, 72% CH_2Cl_2) to yield EtO-(2*S*,3*S*)-EPS-Leu-NH_2-$(CH_2)_4$-NH-CO-NH-C_6H_4-2-(OC_6H_5) (136 mg, 0.24 mmol, 26% yield). ^{1}H NMR ($CDCl_3$): 0.86-0.95 (dd, 6H), 1.28-1.33 (t, 3H), 1.45-1.66 (m, 7H), 3.10-3.37 (m, 4H), 3.40-3.42 (d, 1H), 3.63-3.65 (d, 1H), 4.19-4.29 (q, 2H), 4.33-4.40 (m, 1H), 5.21-5.25 (t, 1H), 6.48-6.54 (t, 1H), 6.60-6.64 (d, 1H), 6.78-6.84 (d, 1H), 6.88-6.93 (t, 1H), 6.94-6.99 (d, 2H), 7.04-7.13 (m, 3H), 7.27-7.34 (t, 2H), 8.14-8.19 (d, 1H).

(2*S*,3*S*)-3-(1-(4-(3-(2-phenoxyphenyl)ureido)butylcarbamoyl)-3-methylbutylcarbamoyl)oxirane-2-carboxylic acid. (HO-(2*S*,3*S*)-EPS-Leu-NH-$(CH_2)_4$-NH-CO-NH-C_6H_4-2-(OC_6H_5)). EtO-(2*S*,3*S*)-EPS-Leu-NH-$(CH_2)_4$-NH-CO-NH-C_6H_4-2-(OC_6H_5) (125 mg, 0.225 mmol) was hydrolyzed following the same procedure as HO-(2*S*,3*S*)-EPS-ALeu-NH-$(CH_2)_4$-NH-Z to yield HO-(2*S*,3*S*)-EPS-Leu-NH-$(CH_2)_4$-NH-CO-NH-C_6H_4-2-(OC_6H_5) (118 mg, 0.226 mmol, 100%). ^{1}H NMR (d_6-DMSO): 0.78-0.88 (dd, 6H, J = 5, 9 Hz), 1.31-1.38 (m, 4H), 1.39-1.45 (m, 2H), 1.47-1.55 (p, 1H, J = 4 Hz), 2.93-3.08 (m, 4H), 3.42-3.44 (d, 1H, J = 2 Hz), 3.61-3.64 (d, 1H, J = 2 Hz), 4.24-4.32 (m, 1H), 6.74-6.88 (m, 3H), 6.93-6.98 (d, 1H, J = 5 Hz), 6.99-7.05 (t, 1H, J = 5 Hz), 7.08-7.12 (t, 1H, J = 5 Hz), 7.32-7.40 (t, 2H, J = 6 Hz), 8.03-8.10 (m, 2H), 8.19-8.24 (d,

1H, J = 6 Hz), 8.51-8.56 (d, 1H, J = 6 Hz). HRMS (ESI) Calcd. for $C_{27}H_{35}N_4O_7$: 527.250026. Observed *m/z* 527.2542.

CHAPTER THREE

SOLID-PHASE SYNTHESIS OF AZA-PEPTIDE MICHAEL ACCEPTOR INHIBITORS OF CASPASES

Introduction

Caspases. The term "caspase" originates from ***c***ysteinyl ***asp***artate specific prote***ase***. Caspase-1, or ICE (interleukin-1β converting enzyme), was the first member of the caspase family identified.[46] ICE is responsible for the proteolytic maturation of proIL-1β to its pro-inflammatory, active form.[47] ICE represented a new class of cysteine proteases based on general structural organization and the absolute requirement for a P1 Asp residue. Subsequent caspases were discovered and linked to ICE through the homology of ICE with the protein CED-3, which was known to be involved for cell death in *C. elegans*.[48]

There are 14 mammalian caspases identified to date, of which 11 are human enzymes.[49] The caspases can be divided into three groups. Group I caspases (1, 4, 5, 13) are mediators of inflammation, and known as cytokine activators. Groups II and III are both involved in apoptosis, but differ in their role in the apoptosis cascade and general substrate specificity. Group II caspases (3, 6, 7) are known as executioner caspases, and are effectors of cell death. Group III caspases (2, 8, 9, 10) are initiator caspases, and are

upstream of Group II caspases in the apoptosis cascade. Studies have shown that initiator caspase-8 is an activator of caspases -3 and -7,[50] while initiator caspase-9 is an activator of caspase-3.[51]

Caspases exist as inactive zymogens in cells.[52] Group II initiator caspases are activated through the extrinsic pathway, including binding of adaptor molecules through their N-terminal prodomain. The adaptor molecules are recruited by ligand-mediated trimerization at the cell surface. The executioner caspases are then activated through proteolytic cleavage of their zymogen prodomain. Two intrinsic pathways of apoptosis activation exist, in which cellular stress leads to caspase-9 activation mediated by cytochrome *c*, or caspase-12 activation (Figure 3.1).

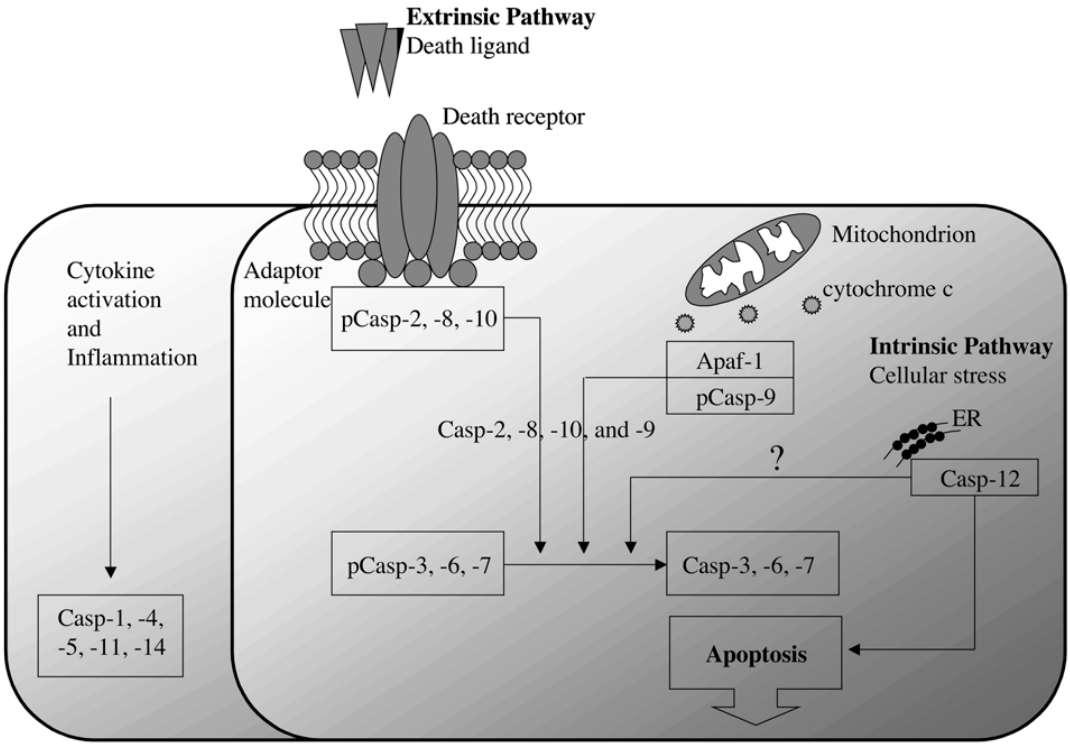

Figure 3.1. Known Apoptotic Pathways Involving Caspases.[52]

Caspase Specificity. Other than the serine protease Granzyme B, the caspases are the only proteases that are specific for a P1 Asp residue in substrates and inhibitors. All caspases display a strict and rigid requirement for a P1 Asp residue. The caspases recognize a tetrapeptide sequence in protein substrates which spans the S4-S1 region of the active site. The S4 subsite is the most diverse among caspases and provides for the most differentiation between caspases. Group I caspases have larger, more hydrophobic S4 pockets and prefer a P4 Trp residue. Group II caspases have smaller, more hydrophilic S4 subsites and are highly selective for a P4 Asp residue. Group III caspases have a wider P4 tolerance, but prefer branched, aliphatic side chains such as Val, Leu, or Ile. The S3 pocket of caspases is highly conserved, and contains a conserved Arg residue that has an ionic interaction with a P3 Glu, the preferred residue at this position in caspases. In the S2 subsite, Group I caspases prefer a His residue, Group II caspases prefer small aliphatic side chains, and Group III can accommodate a larger variety of side chains. The three-dimensional structure of protein substrates is also a key factor in determining whether the presence of the appropriate peptide sequence makes it eligible for caspase proteolysis.[53] Table 3.1 displayed the preferred sequences of the caspases.

Table 3.1. Sequence Specificity of Caspases.

Group	Caspase	Sequence Specificity
Group I	Caspase-1	Trp-Glu-His-Asp
Cytokine Activators	Caspase-4	Trp-Glu-His-Asp
	Caspase-5	Trp-Glu-His-Asp
	Caspase-13	not determined
Group II	Caspase-3	Asp-Glu-X-Asp
Executioner Caspases	Caspase-6	Leu, Val, Ile-Glu-X-Asp
	Caspase-7	Asp-Glu-X-Asp
Group III	Caspase-2	Asp-Glu-X-Asp
Initiator Caspases	Caspase-8	Val, Leu, Ile-Glu-X-Asp
	Caspase-9	Val, Leu, Ile-Glu-X-Asp
	Caspase-10	Val, Leu, Ile-Glu-X-Asp

X = any amino acid

Little is known about substrate and inhibitor specificity on the prime side of the caspase active site. Crystal structures of caspases suggest that the prime side interactions could help to differentiate between the caspases in substrates and inhibitors.

Caspase Structure. Caspases are composed of three domains, including the large subunit, the small subunit, and the N-terminal prodomain.[53] Both the large and small subunits contribute residues that form the active site binding cleft, however the major determinants for substrate specificity between caspases (the S4 subsite) are found in the small subunit.

The crystal structure of caspases -1,[54] -3,[55,56] -7,[57] -8,[58] and -9[59] have been solved alone and/or with inhibitors bound. Models of the active sites of the other caspases have been proposed based on sequence homology with the known caspase structures.[60] The general caspase-substrate interactions can be seen in Figure 3.2, with caspase-1 numbering. A Cys285 and His237 form the conserved catalytic dyad in the active site. Two Arg residues and a Gln residue in the S1 pocked interact with the P1 Asp side chain. Ser339 and Arg341 make hydrogen bonding contacts with the substrate backbone. The conserved Gly238 and Cys285 backbone form an "oxyanion hole" which stabilized the tetrahedral intermediate of substrate hydrolysis.

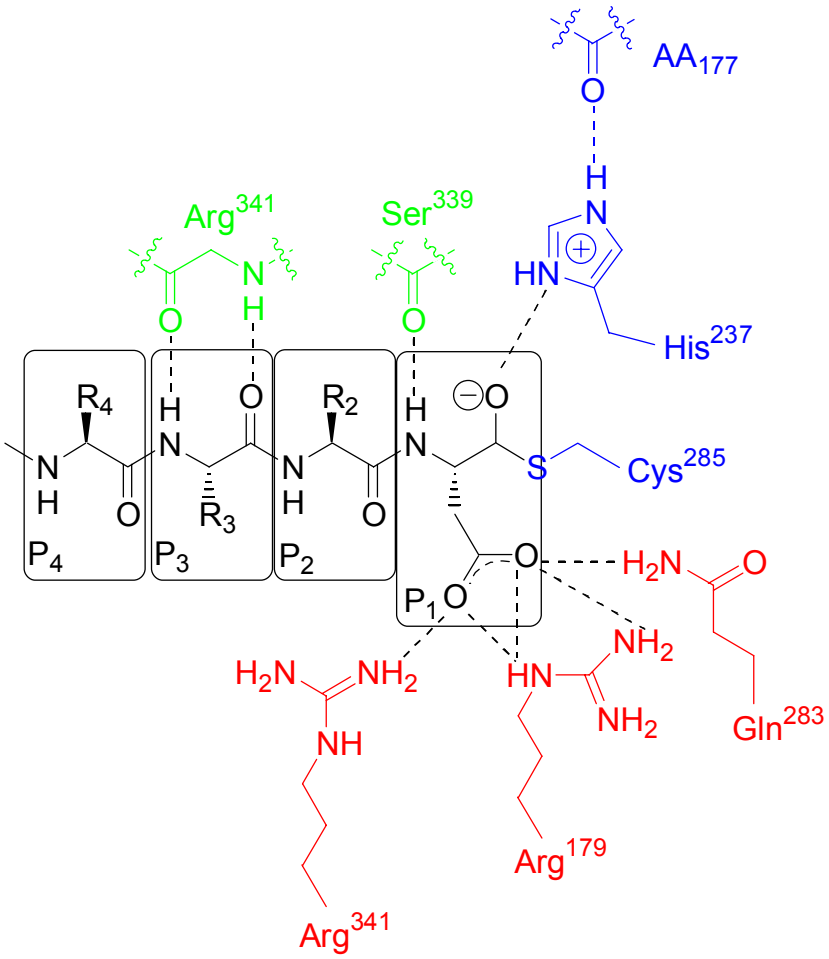

Figure 3.2. General Caspase Substrate Binding. (caspase-1 numbering)[53]

Caspases in Diseases. Caspases are major players in any disease or condition that involves excessive levels of apoptosis. Caspase involvement has been shown in myocardial infarction,[61] stroke,[62] traumatic brain injury,[63] spinal cord injury,[64] sepsis,[65] liver failure,[66] Alzheimers disease,[67] Parkinsons disease,[68] and Huntington's disease.[69] Group I caspases are involved in inflammatory conditions, such as rheumatoid arthritis.[70] Caspases are the main targets of drug design to stop excessive apoptosis. Hence, caspase inhibitors have great therapeutic potential for a wide variety of diseases.

Caspase Inhibitors. Caspase inhibitors generally have involved a tetrapeptide sequence (based on substrate specificity) along with a warhead that interacts with the active site cysteine residue. Several of these inhibitors have been used extensively to elucidate the roles of caspases in cellular systems. These inhibitors include peptide aldehydes (Ac-DEVD-H, Ac-YVAD-H) and peptide halomethylketones (Z-VAD-CH_2F, Ac-DEVD-CH_2Cl, Ac-DEVD-CH_2F, Z-IETD-CH_2F, Z-LEHD-CH_2F, Ac-YVAD-CH_2Cl).[17]

One of the problems with these inhibitors is that they are not as specific for caspases as originally thought.[71] For instance, many of these inhibitors contain a P2 Val residue, which is a preference of the clan CA enzyme calpain. It has been demonstrated that these "caspase-specific" inhibitors also inhibit calpain.[72] Given that calpain is also a major player in neurodegenerative diseases and conditions, the use of these inhibitors to elucidate caspase roles should be questioned.

Another problem with these inhibitors is that they are not able to absolutely differentiate between caspases. Even with their tetrapeptide specificity sequences, a

specific inhibitor does not exist for many of the caspases. Inhibitors that are specific for a particular caspase would be important in the elucidation of caspase roles.

Table 3.2. Nonselectivity of caspase inhibitors.

Caspases	**Ac-DEVD-CHO (K_I, nM)[73]**	**Z-VAD-FMK (k, $M^{-1}s^{-1}$)[74]**
Caspase-1	18	280,000
Caspase-4	132	5500
Caspase-5	205	130,000
Caspase-3	0.23	16,000
Caspase-6	31	7,100
Caspase-7	1.6	18,000
Caspase-2	1710	290
Caspase-8	0.92	280,000
Caspase-9	60	180,000
Caspase-10	12	nd

nd = not determined

Caspase Inhibitors As Therapeutic Agents. The peptidic nature of many caspase inhibitors gives them poor pharmacokinetic properties, therefore rendering them poor drug candidates. The peptide portion of these inhibitors gives them poor membrane permeability as well as makes them susceptible to metabolic elimination. One area of research is the development of peptidomimetics to replace the tetrapeptide portion of caspase inhibitors.[14]

Inhibitor Design

The Powers laboratory has been successful in the design of aza-peptide epoxide and Michael acceptor inhibitors for caspases, with rates of inhibition in the millions.[43,75] The aza-peptide epoxide and Michael acceptor design included extending the inhibitor in the P1' direction in order to discover inhibitors that are selective between the caspases. We have been successful in utilizing the S1' subsite as a specificity determinant. In an extension of these series of inhibitors, we designed a series of aza-peptide Michael acceptor inhibitors that would explore the S3' subsite and could be synthesized by solid phase synthetic methods.

Aza-peptide Michael acceptor inhibitors. The aza-peptide epoxide design was described previously in reference to calpain inhibitors. The aza-peptide Michael acceptor design is an extension of the epoxide design, where a double bond is substituted for the epoxide moiety (Figure 3.3).

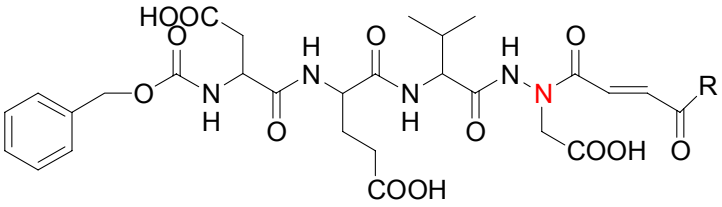

Z-Asp-Glu-Val-AAsp-CH=CH-CO-R

Figure 3.3. Aza-Peptide Michael Acceptor Inhibitors for Caspases.

Similar to the aza-peptide epoxide inhibitors, the protease cysteine thiol in the active site attacks one of the double bond carbons in a Michael acceptor reaction. The cysteine residue is alkylated by the inhibitor and the enzyme is permanently inactivated. Examples of a few Michael acceptor inhibitors discovered in the Powers laboratory can be seen in Table 3.3.

Table 3.3. Representative Aza-Peptide Michael Acceptor Inhibitors for Caspases.

		$k_{obs}/[I]$ ($M^{-1}s^{-1}$)		
No	**Inhibitor**	**Caspase 3**	**Caspase 6**	**Caspase 8**
1	Z-DEVaD-CH=CH-COOEt	2,130,000	35,600	273,000
2	Z-DEVaD-CH=CH-CON(CH_3)Bzl	2,640,000	9,500	90,300
3	Z-LETaD-CH=CH-COOEt	5,560	18,700	237,000
4	Z-LETaD-CH=CH-CON(CH_3)Bzl	6,000	10,800	169,000

New Aza-Peptide Michael Acceptor inhibitors: Scanning the P3' Subsites of Caspases. The new aza-peptide Michael acceptor inhibitor design serves two purposes. The first objective is to develop solid phase synthesis methods to speed the synthesis and increase the yields of aza-peptide Michael acceptors. The second objective is to explore the specificity of the P3' region of caspases, which has so far not been investigated.

The solution phase synthesis of aza-peptide epoxide and Michael acceptor inhibitors is slow and tedious, involving many peptide bond formation steps. Purification of the inhibitors is difficult and final inhibitor yields are low. Given the many peptide bonds in these caspase inhibitors, they are good candidates for solid phase peptide synthetic methods. Using the Wang resin and standard Fmoc amino acid coupling procedures, these inhibitors could be synthesized easily from the C-terminal end. In order to incorporate the aza-peptide Michael acceptor moiety into solid phase synthesis, a Fmoc unit containing the inhibitor warhead must be designed and synthesized. The unit chosen can be seen in Figure 3.4. Fmoc-AAsp(O-*t*Bu)CH=CH-COOH combines the AAsp residue and the double bond warhead, and can be easily synthesized in three steps. For ease of synthesis, we chose to investigate Michael acceptor inhibitors first, however the epoxide inhibitors could be synthesized by the same method.

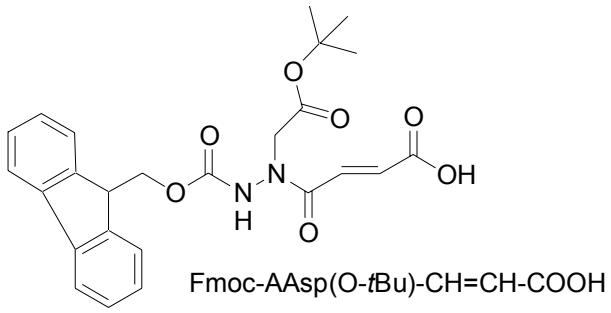

Figure 3.4. Fmoc Aza-Peptide Michael Acceptor Unit for Solid Phase Inhibitor Synthesis.

We chose three tetrapeptide sequences for the non-prime side of the Michael acceptors based on preferred substrate sequences. The Z-Asp-Glu-Val-AAsp sequence was chosen for caspases-3 and -7. The sequence Z-Leu-Glu-Thr-AAsp was chosen for caspase-8. The sequence Z-Ile-Glu-Thr-AAsp was chosen for caspase-6.

Five representative amino acids were chosen for the P3' position of the inhibitors. Ala was chosen as a small aliphatic residue, Phe was chosen as an aromatic, Leu was chosen as a hydrophobic aliphatic residue, Glu was chosen for its negatively charged side chain, and Lys was chosen for its positively charged side chain. A Gly residue was placed in the P2' position as a spacer between the double bond and the P3' residues. Combining the 3 tetrapeptide sequences with the five P3' residue gives a library of 15 aza-peptide Michael acceptor inhibitors (Figure 3.5).

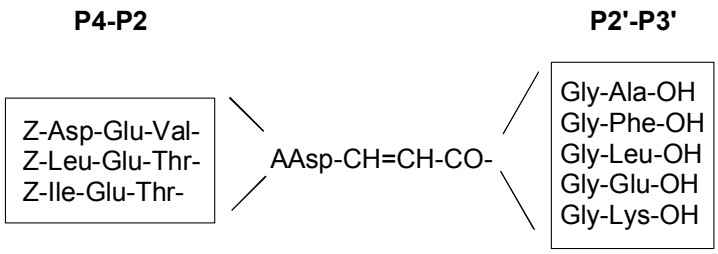

Figure 3.5. Aza-Peptide Michael Acceptor Inhibitor Design.

Synthesis

The synthesis of the Fmoc-AAsp(O-*t*bu)-CH=CH-COOH unit can be seen in Figure 3.6. Fmoc chloroformate is treated with hydrazine to yield Fmoc-hydrazine **6**, which is reacted with *t*-butylbromoacetate to incorporate the blocked Asp side chain (**7**). The hydrazide is then coupled by the mixed anhydride method with fumaric acid, which is present in excess to prevent bis coupling. This unit is now ready to be incorporated into solid phase synthesis.

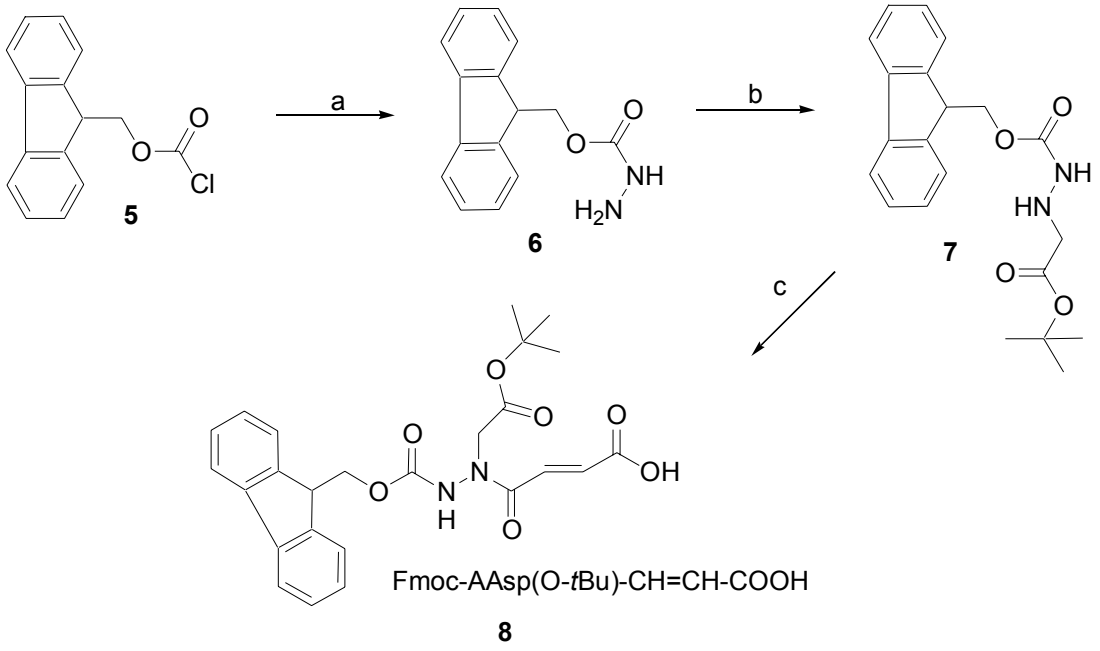

Figure 3.6. Synthesis of Fmoc Aza-Peptide Michael Acceptor Unit for Solid Phase Inhibitor Synthesis. Reagents and conditions: a) NH_2NH_2, ether. b) *t*-butylbromoacetate, NMM, DMF. c) 2eq fumaric acid, IBCF, NMM, CH_2Cl_2.

Solid phase synthesis of the aza-peptide Michael acceptor inhibitors proceeds from the C-terminal end using the Wang resin, which leaves a C-terminal carboxylic acid upon cleavage from the resin. For each P3' amino acid, the three non-prime sequences can be synthesized in parallel through the addition of the AAsp precursor. At this point, a third of the resin is divided out and carried forward to the Z-Asp-Glu-Val-AAsp sequence. The rest of the resin is carried on to the Z-Leu-Glu-Thr-AAsp and Z-Ile-Glu-Thr-AAsp sequences, and is split in half for the final amino acid couplings. The amino acid couplings are carried out with diisopropylcarbonyldiimidazole (DIC) and HOBT, and the Fmoc group is removed with 20% piperidine in DMF. Final inhibitor cleavage from the resin and deblocking of the *t*-butyl side chains occurs through treatment with a TFA solution. The Kaiser test for free amines is performed between each coupling and Fmoc deblocking step to confirm the completeness of reaction. The general solid phase synthesis method can be seen in Figure 3.7.

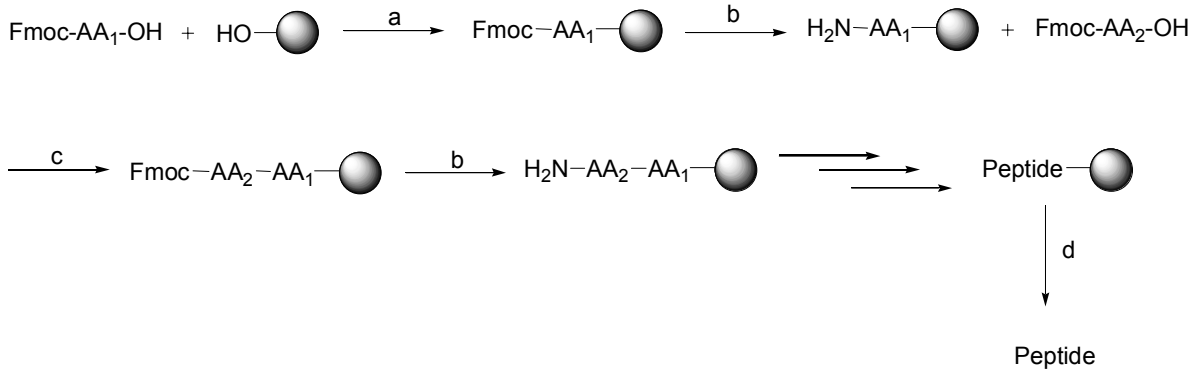

Figure 3.7. General Solid Phase Synthesis Method with the Wang Resin. Reagents and conditions: a) DIPCDI, DMAP, DMF. B) 20% piperidine in DMF. C) DIC, HOBT, DMF. D) 95% TFA, 2.5% TIPS, 2.5% H_2O.

Results and Discussion

The inhibition rate constants of the aza-peptide Michael acceptor inhibitors can be seen in Table 3.4.

Table 3.4. Inhibition of Caspases by Aza-Peptide Michael Acceptor P3' Inhibitors.

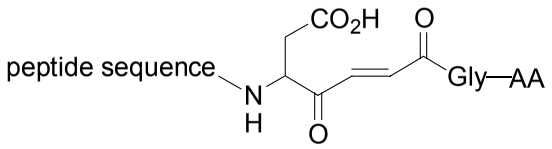

			$k_{obs}/[I]$ ($M^{-1}s^{-1}$)			
No.	**Peptide Sequence**	**AA**	**Casp 3**	**Casp 6**	**Casp 7**	**Casp 8**
9	Z-Asp-Glu-Val	Phe	5,690 ± 140	NI	861 ± 15	114 ± 7.8
10		Ala	4,550 ± 81	12 ± 1.3	717 ± 7.6	132 ± 2.2
11		Leu	25,800 ± 460	114 ± 7.1	2,220 ± 87	219 ± 44
12		Glu	18,400 ± 2,800	20.3 ± 2.1	1,870 ± 57	219 ± 9.2
13		Lys	21,500 ± 935	92.3 ± 6.4	2,860 ± 215	363 ± 3.5
14	Z-Leu-Glu-Thr	Phe	127 ± 4.2	54 ± 10	NI	1,800 ± 33
15		Ala	NI	28 ± 1.0	NI	1,050 ± 22
16		Leu	161 ± 7.8	235 ± 33	NI	3,680 ± 200
17		Glu	5,350 ± 80	79.9 ± 3.5	928 ± 240	797 ± 164
18		Lys	90.1 ± 1.4	40.6 ± 6.4	NI	865 ± 155
19	Z-Ile-Glu-Thr	Phe	434 ± 41	707 ± 0	58 ± 1.5	534 ± 67
20		Ala	NI	122 ± 32	NI	215 ± 14
21		Leu	363 ± 32	4,050 ± 164	38.9 ± 0	1,540 ± 800
22		Glu	181 ± 5.7	1,530 ± 8.5	NI	1,440 ± 26
23		Lys	87.1 ± 2.1	404 ± 62	NI	241 ± 68

NI = No inhibition after 30 min. incubation. Caspase assays were performed in the buffer 20 mM Pipes, 0.1% CHAPS, 10% sucrose, 100 mM NaCl, 1 mM EDTA, 10 mM DTT, pH 7.2, with final inhibitor concentrations in the range of 2.5 μM to 0.25 mM

The inhibition rates for this new series of aza-peptide Michael acceptor inhibitors are lower than the best of the previously discovered inhibitors. There could be several explanations for this phenomenon. First, the S3' pocket of caspases could be solvent exposed and not prone to binding amino acid side chains. Second, the P3' side chain could be binding in a way that is unproductive to inhibition. A third issue is the choice of the Wang resin that produces a C-terminal carboxylic acid. It is possible that a C-terminal amide, which mimics a continuing peptide chain, could be a better fit for the S3' site.

Despite the lower inhibition rates, conclusions can still be drawn from the inhibition results. As expected, caspases -3 and -7 prefer the Asp-Glu-Val-AAsp sequence, caspase-6 prefers the Ile-Glu-Thr-AAsp sequence, and caspase-8 prefers the Leu-Glu-Thr-AAsp slightly over the Ile-Glu-Thr-AAsp sequence. These results correlate well to the known P4 to P1 preferences of caspases. Interestingly, all of the caspases, with the exception of caspase-7, prefer a P3' Leu residue in the inhibitor of their preferred sequence.

Caspase-3: The caspase-3 P3' preference is Leu > Glu ~ Lys > Phe ~ Ala.

Caspase-6: The caspase-6 P3' preference is Leu > Glu > Phe > Lys > Ala.

Caspase-7: The caspase-7 P3' preference is Lys > Leu > Glu > Phe ~ Ala.

Caspase-8: The caspase-8 P3' preference is Leu > Glu > Phe > Ala ~ Lys.

Selectivity of Aza-Peptide Michael Acceptor Inhibitors Among Caspases.

Caspase-3 and -7. Because caspases-3 and -7 both prefer the sequence Z-Asp-Glu-Val-AAsp, differentiating between the two enzymes can be difficult. Inhibitor **11** with a P3' Leu residue is the most specific for caspase-3 over -7 (12:1). None of the inhibitors in the series were more potent for caspase-7 than -3.

Caspase-6 and -8. Because the sequence preferences of caspases -6 and -8 are so similar (P4 Ile vs. Leu), selectivity between the two enzymes can be difficult. There were no inhibitors in the series that are very selective for caspase -6 over -8, with the most selective being inhibitor **21** with a P3' Leu (2.6:1). This is a result of the fact that caspase-8 is reasonably inhibited by the caspase-6 sequence Z-Ile-Glu-Thr-AAsp. Several of the inhibitors were selective for caspase-8 over caspase-6, including inhibitor **16** with a P3' Leu (16:1), inhibitor **15** with a P3' Ala (37:1), and inhibitor **14** with a P3' Phe (33:1).

Stability of the Aza-Peptide Michael Acceptor Inhibitors. We have previously observed that some of the Michael acceptor inhibitors react with the thiol DTT required for cysteine protease activity in kinetic assays. Stability of the inhibitors to thiol reaction is dependant on the P' substituents of the inhibitor. These Michael acceptor inhibitors with P' dipeptides showed no instability over the time course of the kinetic experiments, and lost no inhibitory activity after incubation in buffer containing DTT (6 hrs).

Conclusion

We were successful in the solid phase synthesis of aza-peptide Michael acceptor inhibitors. Caspases -3, -6, -7, and -8 all preferred a Leu residue in the P3' position, suggesting that this region of caspases may be conserved. We were able to achieve modest selectivity between some of the caspases. One future experiment would be to perform the solid phase synthesis on the Rink resin, which leaves a C-terminal amide, to see if inhibitor potency is increased. An aza-peptide epoxide unit could also be synthesized in order to make aza-peptide epoxide inhibitors for caspases. Aza-peptide epoxide and Michael acceptor inhibitors for other clan CD enzymes (gingipains, clostripain, legumain) could also be synthesized by solid phase.

Experimental

Enzyme Assays. Caspases -3, -6, -7, and -8 were obtained from the laboratory of Guy Salvesen (Burnham Institute, La Jolla, CA) and stored at -78 ^{o}C prior to use. The fluorogenic substrate Ac-DEVD-AMC (AMC, excitation λ = 360 nm, emission λ = 405 nm) was purchased from Bachem Biosciences Inc. (King of Prussia, PA). Caspase inhibition rates were determined by the progress curve method. The fluorescence was detected with a Tecan Spectraflour Microplate Reader (Tecan US, Research Triangle

Park, NC). Enzyme-substrate K_M values, used to correct for substrate competition, were determined in the laboratory of Guy Salvesen.

Caspase-3. Caspase-3 was diluted to 2 nM in the assay buffer 20 mM Pipes, 0.1% CHAPS, 10% sucrose, 100 mM NaCl, 1 mM EDTA, 10 mM DTT, pH 7.2, and was activated for 10 min. at 37 ^{o}C. The inhibitor in DMSO was diluted with assay buffer containing the substrate Ac-DEVD-AMC (final concentration 0.10 mM, K_M = 9.7 μM). At t = 0 s, the enzyme was added to the mixture (final [E] = 1.0 nM, [I] = 2.5 μM to 0.25 mM). The reaction was monitored over 15 min by following the change in fluorescence at 465 nm. Inhibition rates were performed in duplicate and the error ranges are reported.

Caspase-6. Caspase-6 was diluted to 20 nM in the assay buffer 20 mM Pipes, 0.1% CHAPS, 10% sucrose, 100 mM NaCl, 1 mM EDTA, 10 mM DTT, pH 7.2, and was activated for 10 min at 37 ^{o}C. The inhibitor in DMSO was diluted with assay buffer containing the substrate Ac-DEVD-AMC (final concentration 0.10 mM, K_M = 246 μM). At t = 0 s, the enzyme was added to the mixture (final [E] = 10.0 nM, [I] = 7.8 μM to 0.25 mM). The reaction was monitored over 15 min by following the change in fluorescence at 465 nm. Inhibition rates were performed in duplicate and the error ranges are reported.

Caspase-7. Caspase-7 was diluted to 2 nM in the assay buffer 20 mM Pipes, 0.1% CHAPS, 10% sucrose, 100 mM NaCl, 1 mM EDTA, 10 mM DTT, pH 7.2, and was activated for 10 min at 37 ^{o}C. The inhibitor in DMSO was diluted with assay buffer containing the substrate Ac-DEVD-AMC (final concentration 0.10 mM, K_M = 23 μM). At t = 0 s, the enzyme was added to the mixture (final [E] = 1.0 nM, [I] = 12.5 μM to 0.25 mM). The reaction was monitored over 15 min by following the change in

fluorescence at 465 nm. Inhibition rates were determined in duplicate and the error ranges are reported.

Caspase-8. Caspase-8 was diluted to 100 nM in the assay buffer 20 mM Pipes, 0.1% CHAPS, 10% sucrose, 100 mM NaCl, 1 mM EDTA, 10 mM DTT, pH 7.2, and was activated for 10 min at 37 ^{o}C. The inhibitor in DMSO was diluted with assay buffer containing the substrate Ac-DEVD-AMC (final concentration 0.10 mM, K_M = 6.79 μM). At t = 0 s, the enzyme was added to the mixture (final [E] = 50.0 nM, [I] = 25 μM to 0.25 mM). The reaction was monitored over 15 min by following the change in fluorescence at 465 nm. Inhibition rates were performed in duplicate and the error ranges are reported.

Materials and Methods. Z-amino acid derivatives were purchased from Bachem Biosciences Inc. (King of Prussia, PA). The Wang resin (100-200 mesh) and Fmoc-protected amino acids were purchased from Calbiochem-Novabiochem (San Diego, CA).

Fmoc-NH-NH$_2$. Fmoc-chloroformate (1 g, 3.86 mmol) was dissolved in ether (20 mL) and cooled to 0 ^{o}C. Hydrazine (0.39 g, 12.2 mmol) was mixed with ether (20 mL) and added to the reaction. A white precipitate formed immediately, and the reaction was allowed to stir for 4 hrs. The reaction was concentrated under reduced pressure and the solid residue taken up in water, filtered, and dried *in vacuo* to yield Fmoc-NH-NH$_2$ (828 mg, 84% yield). ^{1}H NMR (d$_6$-acetone): 2.01-2.10 (m, 2H), 4.22-4.30 (t, 1H), 4.35-4.42 (d, 2H), 7.29-7.46 (dt, 4H), 7.70-7.78 (d, 2H), 7.85-7.89 (d, 2H), 8.88-8.98 (s, 1H).

Fmoc-NH-NH-CH$_2$-COO-*t*-Bu. Fmoc-NH-NH$_2$ (880 mg, 3.46 mmol) was dissolved in DMF (10 mL) and cooled to -20 ^{o}C. NMM (349 mg, 3.46 mmol) was added

to the reaction, followed by *t*-butyl bromoacetate (877 mg, 4.50 mmol). The reaction was allowed to stir in the cold for 30 min, then at room temperature overnight. The reaction was concentrated under reduced pressure, and the crude product was purified by column chromatography (8% MeOH, 20% EtOAc, 73% CH_2Cl_2) to yield Fmoc-NH-NH-CH_2-COO-*t*-Bu (556 mg, 44% yield). ^{1}H NMR (d_6-acetone): 1.38-1.47 (s, 9H), 3.43-3.54 (d, 2H), 4.18-4.27 (t, 1H), 4.30-4.37 (d, 2H), 4.49-4.57 (m, 1H), 7.27-7.45 (dt, 4H), 7.64-7.74 (d, 2H), 7.81-7.89 (d, 2H), 7.90-7.99 (s, 1H).

Fmoc-AAsp(O-*t*Bu)-CH=CH-COOH. Fumaric acid (275 mg, 2.37 mmol) was coupled to Fmoc-NH-NH-CH_2-COO-*t*-butyl (459 mg, 1.19 mg) following the general mixed anhydride procedure. The crude product was purified by column chromatography (8% MeOH, 20% EtOAc, 73% CH_2Cl_2) and recrystallized from ether/hexanes to yield Fmoc-AAsp(O-*t*Bu)-CH=CH-COOH (247 mg, 45% yield). ^{1}H NMR (d_6-acetone): 0.93-0.99 (s, 9H), 3.46-3.51 (d, 2H), 3.79-3.85 (t, 1H), 3.92-4.00 (s, 1H), 6.23-6.26 (d, 2H), 6.72-6.79 (d, 1H), 6.83-6.91 (t, 2H), 6.93-7.00 (t, 2H), 7.20-7.29 (s, 2H), 7.40-7.46 (d, 2H), 10.10-10.20 (s, 1H). HRMS (ESI) Calcd 466. Observed *m/z* $[M+ H]^+$ 467.3.

General Methods for Solid Phase Peptide Synthesis. Synthesis of the aza-peptide Michael acceptor inhibitors was carried out manually on the Wang resin in a 12 mL Bio-spin chromatography column. Fmoc-amino acids were used with *t*-butyl-protected side chains (Asp, Glu, Thr, Lys). The Fmoc-AAsp(O-*t*Bu)-CH=CH-COOH was synthesized as described above prior to incorporation into the solid phase synthesis.

Loading of the Resin with the First Amino Acid Residue. The resin (300 mg, 0.267 mmol, 0.89 mmol reactive sites/g) was allowed to swell in DMF for 30 min. The

Fmoc-AA-OH (10 eq to resin, 2.67 mmol) was dissolved in CH_2Cl_2 with a few drops of DMF and cooled in an ice bath. Diisopropylcarbodiimide (DIC) (73.7 mg, 0.534 mmol, 2 eq to resin) and DMAP (3 mg, 0.0267 mmol, 0.1 eq to resin) were added to the Fmoc-AA-OH solution and the reaction stirred for 20 min. The CH_2Cl_2 was evaporated *in vacuo* and the residue dissolved in minimal DMF. This solution was added to the resin and allowed to react for 2 hrs to overnight. The resin was then drained and washed with DMF (5 mL) and CH_2Cl_2 (5 mL). A second cycle was performed to ensure completion of reaction.

Fmoc Cleavage. Fmoc is cleaved from the N-terminal amino acid attached to the resin by the addition of 20% piperidine in DMF to the resin. The solution (2 mL) was added and drained in 3-three minute cycles. The resin was then washed with DMF (5 mL) and CH_2Cl_2 (5 mL).

Coupling Additional Amino Acid Residues to the Growing Chain. Fmoc-AA-OH (2 eq to resin, 0.534 mmol) was dissolved in CH_2Cl_2 with a few drops of DMF and cooled in an ice bath. Diisopropylcarbodiimide (DIC) (74 mg, 0.534 mmol, 2 eq to resin) and HOBT (73 mg, 0.534 mmol, 2 eq to resin) were added to the Fmoc-AA-OH solution and the reaction stirred for 20 min. The CH_2Cl_2 was evaporated *in vacuo* and the residue dissolved in minimal DMF. This solution was added to the resin and allowed to react for 2 hrs to overnight. The resin was then drained and washed with DMF (5 mL) and CH_2Cl_2 (5 mL) . A second coupling cycle was performed to ensure completion of reaction.

The Kaiser Test. The Kaiser test determines the presence or absence of free amines. It is performed after every amino acid coupling and Fmoc cleavage step to confirm completion of the reaction. A few beads of resin are sampled and washed with

EtOH. The beads were treated with two drops of a ninhydrin solution (0.5 g ninhydrin in 10mL EtOH), two drops of a phenol solution (8 g in 2 mL EtOH), and two drops of 1 mM KCN (aq.) in pyridine. The mixture was heated to 120 ^{o}C for 5 min. A dark blue solution indicates the presence of a free amine, which is expected after a Fmoc-deblocking step. A yellow/brown solution indicates the absence of free amines, which is expected after an amino acid coupling step.

Cleavage of Inhibitor from Resin and Deprotection of *t*-Butyl Protecting Groups. The resin was washed with EtOH and dried under reduced pressure. A cocktail of 95% TFA, 2.5% H_2O, and 2.5% TIS was added to the resin and allowed to react for 2 hrs. The resin was filtered and washed with the TFA solution, and the combined TFA solutions were concentrated *in vacuo*. The residue was recrystallized with ether/hexanes to yield the inhibitors as white powders.

***N*^{2}-(*N*-Benzyloxycarbonylaspartylglutamylvalyl)-*N*^{1}-carboxymethyl-*N*^{1}-*trans*-(3-(1-carboxyethylcarbamoyl)methylcarbamoylacryloyl)hydrazine (Z-Asp-Glu-Val-AAsp-*trans*-CH=CH-CO-Gly-Ala-OH).** Yield 113 mg, 53%. ^{1}H NMR (d_6-DMSO): 0.82-0.97 (dd, 6H, *J* = 5, 9 Hz), 1.19-1.28 (d, 3H, *J* = 5 Hz), 1.68-1.83 (m, 2H), 2.17-2.27 (m, 2H), 2.51-2.58 (m, 1H), 2.60-2.68 (m, 2H), 3.79-3.89 (d, 2H, *J* = 5 Hz), 4.13-4.23 (m, 4H), 4.29-4.40 (m, 2H), 4.97-5.04 (s, 2H), 7.25-7.38 (m, 5H), 7.52-7.62 (dd, 2H, *J* = 3, 6 Hz), 8.10-8.16 (m, 1H), 8.23-8.32 (m, 2H), 8.65-8.80 (m, 1H), 8.92-8.98 (s, 1H). HRMS (ESI) Calcd 793.27679. Observed *m/z* $[M - 2H]^-$ 790.9.

***N*^{2}-(*N*-Benzyloxycarbonylleucylglutamylthreonyl)-*N*^{1}-carboxymethyl-*N*^{1}-*trans*-(3-(1-carboxyethylcarbamoyl)methylcarbamoylacryloyl)hydrazine (Z-Leu-Glu-Thr-AAsp-*trans*-CH=CH-CO-Gly-Ala-OH).** Yield 52 mg, 49 %. ^{1}H NMR (d_6-

DMSO): 0.77-0.90 (dd, 6H, *J* = 4, 8 Hz), 0.99-1.07 (d, 3H, *J* = 3 Hz), 1.20-1.27 (d, 3H, *J* = 6 Hz), 1.53-1.62 (m, 2H), 1.82-1.91 (m, 1H), 2.18-2.26 (m, 2H), 2.28-2.32 (m, 2H), 3.66-3.75 (m, 2H), 3.78-3.82 (d, 2H, *J* = 6 Hz), 4.13-4.22 (q, 1H, *J* = 6 Hz), 4.31-4.38 (m, 4H), 4.96-5.01 (s, 2H), 7.25-7.34 (m, 5H), 7.38-7.44 (m, 2H), 7.90-7.99 (m, 1H), 8.01-8.04 (s, 1H), 8.09-8.16 (m, 1H), 8.22-8.31 (m, 1H), 8.53-8.57 (m, 1H). HRMS (ESI) Calcd 793.31321. Observed *m/z* $[M+ H - 44\ CO_2]^+$ 751.5.

***N^2*-(*N*-Benzyloxycarbonylisoleucylglutamylthreonyl)-*N^1*-carboxymethyl-*N^1*-*trans*-(3-(1-carboxyethylcarbamoyl)methylcarbamoylacryloyl)hydrazine (Z-Ile-Glu-Thr-AAsp-*trans*-CH=CH-CO-Gly-Ala-OH).** Yield 60 mg, 57%. ^{1}H NMR (d_6-DMSO): 0.73-0.91 (m, 6H), 1.00-1.08 (m, 3H), 1.11-1.14 (m, 2H), 1.21-1.27 (d, 3H, *J* = 6 Hz), 1.60-1.76 (m, 2H), 1.84-1.90 (m, 2H), 2.21-2.29 (s, 1H), 2.50-2.53 (m, 1H), 3.68-3.76 (m, 2H), 3.82-3.91 (m, 2H), 4.14-4.22 (m, 4H), 4.34-4.40 (m, 1H), 4.97-5.01 (s, 2H), 7.25-7.32 (m, 2H), 7.32-7.37 (m, 5H), 8.02-8.06 (s, 1H), 8.09-8.18 (m, 2H), 8.23-8.28 (m, 2H). HRMS (ESI) Calcd 793.31321. Observed *m/z* $[M + H - 44\ CO_2]^+$ 751.4.

***N^2*-(*N*-Benzyloxycarbonylaspartylglutamylvalyl)-*N^1*-carboxymethyl-*N^1*-*trans*-(3-(1-carboxy-2-phenylethylcarbamoyl)methylcarbamoylacryloyl)hydrazine (Z-Asp-Glu-Val-AAsp-*trans*-CH=CH-CO-Gly-Phe-OH).** Yield 39 mg, 56 %. ^{1}H NMR (d_6-DMSO): 0.80-0.93 (m, 6H), 1.83-1.94 (m, 2H), 2.18-2.27 (m, 2H), 2.58-2.62 (m, 1H), 2.64-2.68 (m, 2H), 3.82-3.92 (m, 2H), 4.14-4.23 (m, 2H), 4.30-3.33 (m, 4H), 4.98-5.04 (s, 4H), 7.25-7.42 (m, 10H), 7.52-7.63 (dd, 2H, *J* = 5, 8 Hz), 7.90-7.94 (s, 2H), 8.00-8.03 (s, 1H), 8.10-8.15 (d, 2H, *J* = 6 Hz). HRMS (ESI) Calcd 869.30811. Observed *m/z* $[M + H]^+$ 870.3.

***N*^{2}-(*N*-Benzyloxycarbonylleucylglutamylthreonyl)-*N*^{1}-carboxymethyl-*N*^{1}-*trans*-(3-(1-carboxy-2-phenylethylcarbamoyl)methylcarbamoylacryloyl)hydrazine (Z-Leu-Glu-Thr-AAsp-*trans*-CH=CH-CO-Gly-Phe-OH).** Yield 24 mg, 34%. ^{1}H NMR (d_6-DMSO): 0.78-0.91 (m, 6H), 0.94-0.97 (d, 3H, J = 3 Hz), 1.52-1.64 (m, 2H), 1.67-1.76 (m, 2H), 2.18-2.26 (m, 2H), 2.28-2.31 (m, 2H), 3.64-3.70 (m, 2H), 3.97-4.05 (m, 2H), 4.10-4.18 (m, 1H), 4.32-4.43 (m, 4H), 4.96-5.02 (s, 4H), 7.28-7.35 (m, 10H), 7.38-7.44 (dd, 2H, J = 1, 6 Hz), 7.98-8.23 (m, 5H). HRMS (ESI) Calcd 869.34453. Observed *m/z* $[M - H]^-$ 868.1

***N*^{2}-(*N*-Benzyloxycarbonylisoleucylglutamylthreonyl)-*N*^{1}-carboxymethyl-*N*^{1}-*trans*-(3-(1-carboxy-2-phenylethylcarbamoyl)methylcarbamoylacryloyl)hydrazine (Z-Ile-Glu-Thr-AAsp-*trans*-CH=CH-CO-Gly-Phe-OH).** Yield 19 mg, 27%. ^{1}H NMR (d_6-DMSO): 0.71-0.81 (m, H), 0.82-0.91 (m, 2H), 0.99-1.06 (m, 3H), 1.59-1.72 (m, 2H), 2.15-2.25 (m, 2H), 2.50-2.55 (m, 1H), 3.81-3.89 (m, 2H), 4.08-4.16 (m, 2H), 4.17-4.20 (m, 1H), 4.32-4.44 (m, 4H), 4.96-5.02 (m, 4), 7.16-7.24 (m, 2H), 7.30-7.36 (m, 10H), 7.75-7.81 (m, 1H), 7.99-8.10 (m, 3H), 8.15-8.17 (m, 1H). HRMS (ESI) Calcd 869.34453. Observed *m/z* $[M - H]^-$ 868.3

***N*^{2}-(*N*-Benzyloxycarbonylaspartylglutamylvalyl)-*N*^{1}-carboxymethyl-*N*^{1}-*trans*-(3-(1-carboxy-3-methylbutylcarbamoyl)methylcarbamoylacryloyl)hydrazine (Z-Asp-Glu-Val-AAsp-*trans*-CH=CH-CO-Gly-Leu-OH).** Yield 24.71 mg, 33%. ^{1}H NMR (d_6-DMSO): 0.76-0.91 (dd, 12H, J = 5, 8 Hz), 1.53-1.66 (m, 2H), 1.69-1.76 (p, 1H, J = 4 Hz), 1.86-1.97 (m, 2H), 2.17-2.28 (m, 2H), 2.58-2.62 (p, 1H, J = 3 Hz), 2.62-2.66 (d, 2H, J = 3 Hz), 3.78-3.87 (m, 2H), 4.12-4.19 (s, 2H), 4.29-4.39 (m, 4H), 4.98-5.02 (s,

2H), 7.26-7.35 (m, 5H), 7.59-7.64 (d, 2H, *J* = 6 Hz), 7.89-8.21 (m, 5H). HRMS (ESI) Calcd 835.32377. Observed *m/z* $[M - 2]^-$ 833.3.

N^2-(*N*-Benzyloxycarbonylleucylglutamylthreonyl)-N^1-carboxymethyl-N^1-*trans*-(3-(1-carboxy-3-methylbutylcarbamoyl)methylcarbamoylacryloyl)hydrazine (Z-Leu-Glu-Thr-AAsp-*trans*-CH=CH-CO-Gly-Leu-OH). Yield 29.69 mg, 40 %. ^{1}H NMR (d_6-DMSO): 0.76-0.93 (dd, 12H, *J* = 5, 8 Hz), 0.93-0.98 (d, 3H, *J* = 4 Hz), 1.52-1.62 (m, 4H), 1.83-1.95 (p, 2H, *J* = 3 Hz), 2.16-2.28 (m, 4H), 2.39-2.45 (m, 2H), 3.67-3.74 (s, 2H), 3.76-3.86 (m, 2H), 4.18-4.22 (m, 1H), 4.27-4.40 (m, 4H), 4.94-5.07 (s, 2H), 7.23-7.37 (m, 5H), 7.29-7.46 (d, 2H, *J* = 6 Hz), 7.68-7.75 (s, 1H), 7.81-7.86 (d, 1H, *J* = 6 Hz), 7.98-9.13 (m, 3H), 8.24-8.31 (s, 1H), 8.61-8.68 (d, 1H, *J* = 6 Hz), 12.10-12-60 (m, 3H). HRMS (ESI) Calcd 835.36019. Observed *m/z* $[M - H]^-$ 834.2.

N^2-(*N*-Benzyloxycarbonylisoleucylglutamylthreonyl)-N^1-carboxymethyl-N^1-*trans*-(3-(1-carboxy-3-methylbutylcarbamoyl)methylcarbamoylacryloyl)hydrazine (Z-Ile-Glu-Thr-AAsp-*trans*-CH=CH-CO-Gly-Leu-OH). Yield 21.35 mg, 29%. ^{1}H NMR (d_6-DMSO): 0.72-0.89 (dd, 12H, *J* = 5, 8 Hz), 0.97-1.16 (m, 5H), 1.33-1.50 (m, 2H), 1.53-1.62 (m, 2H), 1.67-1.74 (m, 2H), 1.84-1.92 (p, 1H, *J* = 3 Hz), 2.18-2.28 (s, 1H), 2.50-2.55 (q, 1H, *J* = 3 Hz), 3.78-3.87 (m, 2H), 4.18-4.23 (m, 1H), 4.28-4.39 (m, 4H), 4.94-5.02 (s, 2H), 7.26-7.37 (m, 7H), 7.98-8.15 (m, 5H). HRMS (ESI) Calcd 835.36019. Observed *m/z* $[M - H]^-$ 834.0.

N^2-(*N*-Benzyloxycarbonylaspartylglutamylvalyl)-N^1-carboxymethyl-N^1-*trans*-(3-(1-carboxy-3-carboxypropylcarbamoyl)methylcarbamoylacryloyl)hydrazine (Z-Asp-Glu-Val-AAsp-*trans*-CH=CH-CO-Gly-Glu-OH). Yield 10.72 mg, 14%. ^{1}H NMR (d_6-DMSO): 0.80-0.89 (dd, 6H, *J* = 2, 6 Hz), 1.96-2.08 (m, 4H), 2.16-2.29 (m, 4H),

2.39-2.43 (m, 1H), 2.56-2.62 (m, 2H), 3.72-3.78 (d, 2H, J = 6 Hz), 4.13-4.21 (m, 2H), 4.27-4.40 (m, 4H), 4.98-5.02 (s, 2H), 7.24-7.36 (m, 5H), 7.51-7.64 (dd, 2H, J = 6, 8 Hz), 7.89-7.95 (d, 2H, J = 5 Hz), 8.01-8.05 (s, 1H), 8.08-8.12 (d, 1H, J = 6 Hz), 8.16-8.22 (m, 1H). HRMS (ESI) Calcd 851.28225. Observed *m/z* $[M - H]^-$ 850.3.

N^2-(*N*-Benzyloxycarbonylleucylglutamylthreonyl)-N^1-carboxymethyl-N^1-*trans*-(3-(1-carboxy-3-carboxypropylcarbamoyl)methylcarbamoylacryloyl)hydrazine (Z-Leu-Glu-Thr-AAsp-*trans*-CH=CH-CO-Gly-Glu-OH). Yield 4.45 mg, 6 %. ^{1}H NMR (d6-DMSO): 0.78-0.90 (dd, 6H, J = 5, 8 Hz), 0.99-1.04 (m, 3H), 1.69-1.80 (m, 2H), 1.84-1.96 (m, 2H), 2.16-2.29 (m, 4H), 3.71-3.79 (m, 2H), 3.96-4.06 (m, 2H), 4.12-4.24 (m, 1H), 4.21-4.38 (m, 4H), 4.96-5.02 (s, 2H), 7.24-7.36 (m, 5H), 7.40-7.46 (m, 2H), 7.90-7.95 (m, 2H), 8.01-8.05 (m, 2H). HRMS (ESI) Calcd 851.31867. Observed *m/z* $[M - H]^-$ 850.2.

N^2-(*N*-Benzyloxycarbonylisoleucylglutamylthreonyl)-N^1-carboxymethyl-N^1-*trans*-(3-(1-carboxy-3-carboxypropylcarbamoyl)methylcarbamoylacryloyl)hydrazine (Z-Ile-Glu-Thr-AAsp-*trans*-CH=CH-CO-Gly-Glu-OH). Yield 6.80 mg, 9 %. ^{1}H NMR (d_6-DMSO): 0.73-0.88 (m, 6H), 0.99-1.06 (m, 3H), 1.65-1.79 (m, 4H), 1.85-1.98 (m, 4H), 2.27-2.31 (s, 1H), 2.61-2.65 (m, 1H), 3.69-3.78 (m, 2H), 4.11-4.25 (m, 4H), 4.31-4.39 (m, 1H), 4.98-5.02 (s, 2H), 7.25-7.30 (m, 2H), 7.31-7.38 (m, 5H), 7.91-7.94 (s, 1H), 8.00-8.10 (m, 2H), 8.16-8.22 (m, 1H). HRMS (ESI) Calcd 851.31067. Observed *m/z* $[M + H]^+$ 852.2.

N^2-(*N*-Benzyloxycarbonylaspartylglutamylvalyl)-N^1-carboxymethyl-N^1-*trans*-(3-(1-carboxy-5-aminopentylcarbamoyl)methylcarbamoylacryloyl)hydrazine (Z-Asp-Glu-Val-AAsp-*trans*-CH=CH-CO-Gly-Lys-OH). Yield 45.56 mg, 53%. ^{1}H

NMR (d_6-DMSO): 0.82-0.91 (d, 6H, J = 5 Hz), 1.27-1.36 (m, 2H), 1.45-1.52 (m, 2H), 1.65-1.72 (m, 2H), 2.17-2.27 (m, 2H), 2.52-2.62 (p, 1H, J = 3 Hz), 2.62-2.69 (m, 2H), 3.64-3.99 (m, 6H), 4.11-4.20 (m, 2H), 4.28-4.39 (m, 4H), 4.99-5.02 (s, 2H), 7.26-7.37 (m, 7H), 7.56-7.68 (m, 3H), 7.90-7.94 (s, 2H), 8.18-8.28 (m, 2H), 12.10-12.50 (m, 4H). HRMS (ESI) Calcd 964.32735. Observed *m/z* $[M + H - 114\ TFA]^+$ 851.5.

N^2-(*N*-Benzyloxycarbonylleucylglutamylthreonyl)-N^1-carboxymethyl-N^1-*trans*-(3-(1-carboxy-5-aminopentylcarbamoyl)methylcarbamoylacryloyl)hydrazine (Z-Leu-Glu-Thr-AAsp-*trans*-CH=CH-CO-Gly-Lys-OH). Yield 30.32 mg, 36%. ^{1}H NMR (d_6-DMSO): 0.79-0.90 (dd, 6H, J = 3, 6 Hz), 0.98-1.06 (m, 3H), 1.26-1.33 (m, 2H), 1.53-1.62 (m, 2H), 1.65-1.75 (m, 2H), 1.80-1.89 (p, 1H, J = 6 Hz), 2.21-2.31 (m, 2H), 2.51-2.55 (m, 2H), 2.69-2.79 (m, 4H), 3.77-3.84 (m, 2H), 3.84-3.90 (m, 2H), 3.98-4.08 (m, 1H), 4.12-4.22 (m, 4H), 4.96-5.01 (s, 2H), 7.26-7.35 (m, 5H), 7.38-7.44 (d, 2H, J = 5 Hz), 7.56-7.67 (m, 3H), 7.91-7.93 (s, 1H), 8.03-8.11 (m, 1H), 8.16-8.28 (m, 3H). HRMS (ESI) Calcd 964.36373. Observed *m/z* $[M + H - 114\ TFA]^+$ 852.0.

N^2-(*N*-Benzyloxycarbonylisoleucylglutamylthreonyl)-N^1-carboxymethyl-N^1-*trans*-(3-(1-carboxy-5-aminopentylcarbamoyl)methylcarbamoylacryloyl)hydrazine (Z-Ile-Glu-Thr-AAsp-*trans*-CH=CH-CO-Gly-Lys-OH). Yield 27.59 mg, 32%. ^{1}H NMR (d_6-DMSO): 0.72-0.90 (m, 6H), 0.93-0.98 (m, 2H), 1.00-1.07 (t, 3H, J = 6 Hz), 1.26-1.34 (m, 2H), 1.43-1.55 (m, 2H), 1.64-1.75 (m, 2H), 1.79-1.90 (m, 2H), 2.21-2.30 (s,1H), 2.48-2.56 (m, 1H), 2.68-2.78 (m, 2H), 3.76-3.82 (d, 2H, J = 6 Hz), 3.82-3.92 (m, 4H), 4.20-4.23 (m, 1H), 4.96-5.02 (s, 2H), 7.24-7.30 (m, 2H), 7.30-7.36 (m, 5H), 7.57-7.68 (m, 3H), 7.99-8.11 (m, 2H), 8.18-8.27 (m, 2H). HRMS (ESI) Calcd 964.36373. Observed *m/z* $[M - H - 114\ TFA]^-$ 850.5.

CHAPTER FOUR

AZA-PEPTIDE EPOXIDES AND MICHEAL ACCEPTORS AS INHIBITORS OF GINGIPAINS R AND K AND CLOSTRIPAIN

Introduction

Gingipains. Gingipains R and K are cysteine proteases isolated from the bacterium *Porphyromonas gingivalis*. *P. gingivalis* is a Gram-negative, anaerobic, nonmotile short rod bacteria which has been determined to be a major player in periodontal disease. Periodontitis is an inflammatory process induced by bacteria, which results in the destruction of connective tissue and bone that support the teeth. *P. gingivalis* expresses as many as eight virulence factors including Gingipains R and K, and other proteases and co-factors. Gingipains are responsible for 85% of the proteolytic activity present in *P. gingivalis*.[76]

Gingipains R and K are two important virulence factors in the progression of periodontitis. Gingipain R contributes to the bacterial adhesion to the host tissue through processing of fimbrilin, a cell surface protein.[77] Gingipains R and K cleave and inactivate interleukin-1β, interleukin-6, interleukin-8, and TNFα, which enables the bacteria to evade the host immune response.[78,79] Gingipain R activates Factor X, which leads to blood coagulation and sepsis, and explains the link between periodontitis and coronary disease.[80] Gingipain R is responsible for the type I collagenase activity present

in *P. gingivalis.*[81] The gingipains lyse erythrocytes and iron-binding proteins, which provides amino acids and iron as nutrition for the bacterium.[82,83]

Gingipains R and K are most active in the presence of reducing agents and above pH 8, which are the conditions of the periodontal pocket during advanced colonization of *P. gingivalis.*[84] The gingipains are excreted in a soluble form into bacterial culture media, as well as associated with bacterial cell membranes and vesicles.[85]

Gingipain Specificity. Gingipain R cleaves specifically after a P1 arginine residue. There are two forms of gingipain R known as HRgpA and RgpB.[15] These two forms have nearly identical catalytic domains. A few amino acid substitutions in the catalytic domain account for the small differences in their specificity. HRgpA contains additional hemagglutinin/adhesion domains, which seem to play a small role in substrate binding. Gingipain R is capable of autolysis in its propeptide form. The presence of glycyl-glycine is shown in increase gingipain R activity, which is not seen in any other enzyme.[86] Gingipain R has a preference for hydrophobic amino acids in the P2 and P3 positions.

Gingipain K (Kgp) cleaves specifically after a P1 lysine residue. The enzyme accepts a wide variety of amino acids in the P2 position, excluding lysine and arginine. Gingipain K will not cleave after a lysine at the N-terminus of a peptide. Unlike gingipain R, gingipain K is inhibited by the addition of glycyl- glycine.[84] Gingipain K is not auto-proteolytic, but is processed and activated by gingipain R.

Gingipain Structure. The crystal structure of Gingipain R (RgpB, pdb 1cvr) demonstrates a similar fold to caspases-1 and -3, representative clan CD cysteine proteases.[76] The deep S1 pocket formed by Val242 and Thr209 harbors the Asp163,

which binds the arginine guanidino group and accounts for the stringent P1 specificity. The guanidinium nitrogens are both close enough to the Met288 S to participate in hydrogen bonding. In gingipain K, this Met288 is replaced by a Tyr, which explains gingipain K's preference for a lysine ammonium. This is a key difference between gingipains R and K. The backbone amide nitrogens of Gly212 and Cys244 form the oxyanion hole of RgpB which stabilizes the intermediate formed from the attack of Cys244. A calcium ion is bound just below the S1 pocket, stabilizing this binding site. The structure of gingipain K has not yet been solved.

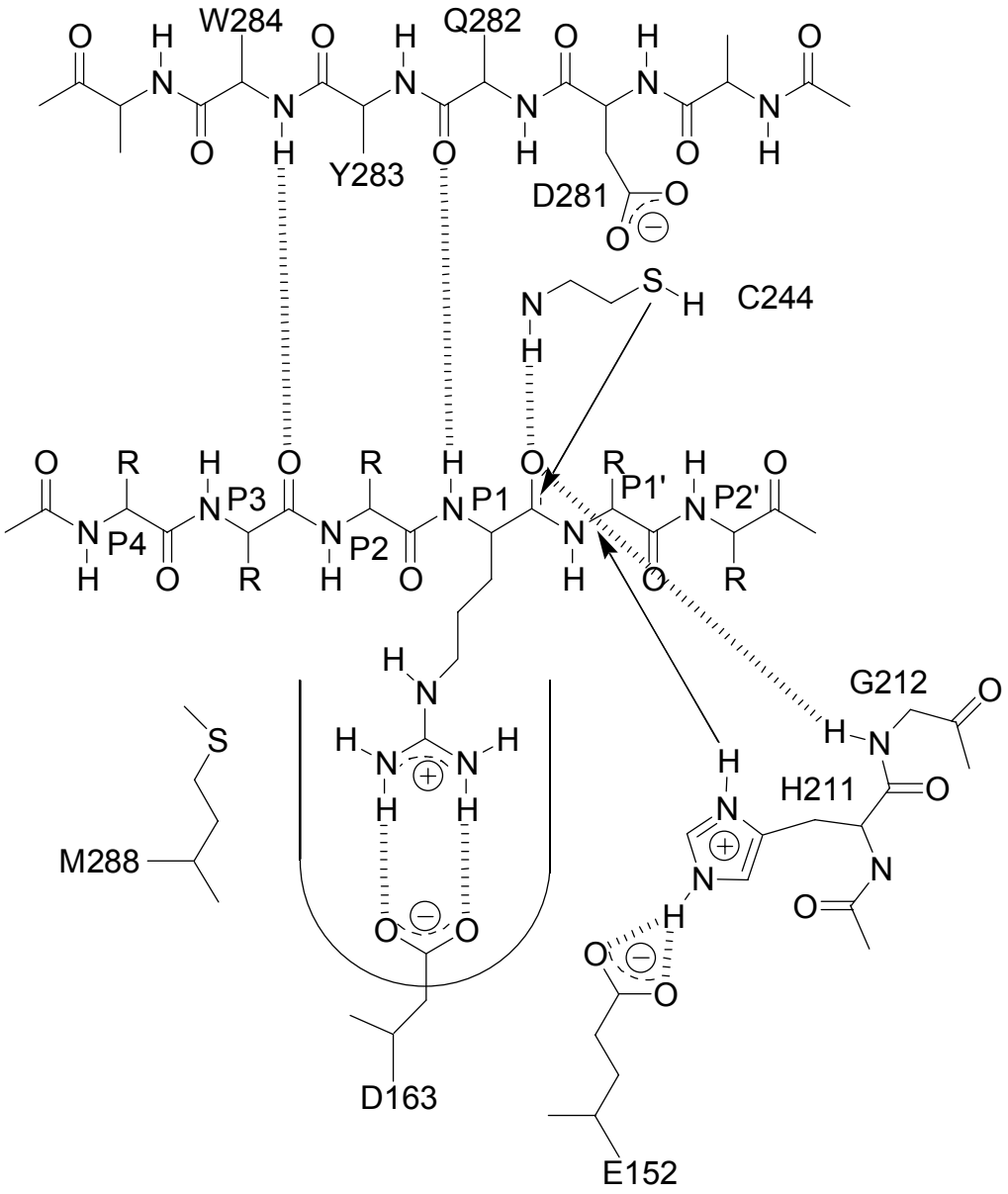

Figure 4.1. Substrate Binding Mode of Gingipain R.[76]

Gingipain Inhibitors. There are few inhibitors of the gingipains, with almost no inhibitors specifically designed for the enzymes. The epoxide inhibitor E64, a natural product inhibitor of cysteine proteases, is a modest inhibitor of gingipain R, while gingipain K is not inhibited.[84] Halomethylketones and aldehydes with P1 Lys and P1 Arg have been shown to be inhibitors of gingipains K and R, respectively.[76] A natural product non-covalent inhibitor of gingipain R has been reported with a K_I in the nanomolar range.[87]

Clostripain. *Clostridium hystoliticum* is a Gram-positive bacterium involved in gas gangrene syndrome.[88] The presence of a proteinase in the culture filtrate of *Clostridium hystolyticum* was first detected in the 1930's, and the enzyme was isolated and characterized as clostripain in 1948.[88] Clostripain has strict substrate specificity, cleaving only after Arg or Lys residues. It further prefers Arg over Lys, and has been shown to cleave only after Arg when Arg and Lys are both present in a substrate peptide.[89] This preference has been attributed to higher K_M and lower k_{cat} values of Lys peptide substrates.[89] This preference for Arg over Lys is much less pronounced in inhibitors than substrates.[90] Clostripain will also readily cleave the Arg-Pro bond, which is difficult for trypsin, a serine protease with similar specificity.

Clostripain Inhibitors. A number of inhibitors containing P1 Arg and Lys along with various reversible and irreversible warheads have been proven potent inactivators of clostripain.[90] These include aldehydes, chloromethylketones, aziridinyl peptides, and sulfonium methyl ketones. Similar to the gingipains, few inhibitors have been designed specifically for clostripain.

Inhibitor Design

Given the success of aza-peptide epoxide and Michael acceptor inhibitors for caspases, we turned our attention to extending this design to other clan CD enzymes, including the gingipains and clostripain. This design involves a P1 ALys and AArg residue followed by the epoxide or Michael acceptor warhead as seen in Figure 4.2. A Leu P2 residue was chosen along with a phenypropyl N-capping group for ease of synthesis, since the gingipains are tolerant of many amino acids at these positions. A series of AOrn inhibitors were synthesized as precursors of the AArg inhibitors, and were also tested for inhibitory potency. Varying functional groups are synthesized in the P1' position of the inhibitors in order to discover the most potent inhibitor. These inhibitors were synthesized and characterized by Zhao Zhao Li (unpublished), and the synthesis will not be discussed here.

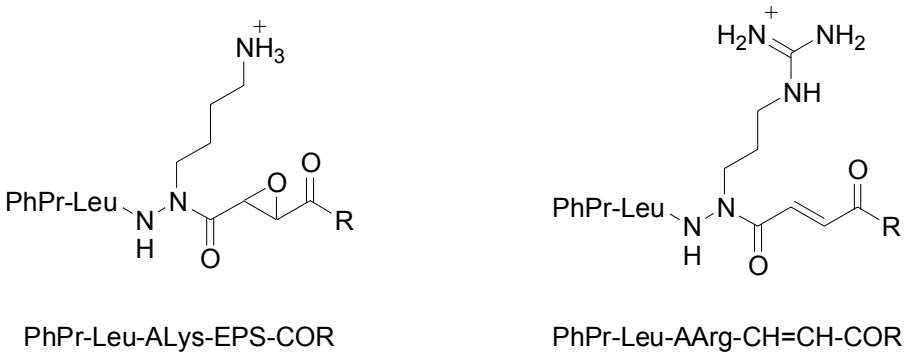

PhPr-Leu-ALys-EPS-COR PhPr-Leu-AArg-CH=CH-COR

Figure 4.2. Aza-Peptide Epoxide and Michael Acceptor Inhibitor Design for Gingipains and Clostripain.

Results and Discussion

The series of inhibitors synthesized for the gingipains and clostripain can be seen in Table 4.1 along with their inhibitory potency. The aza-peptide epoxide and Michael acceptor design provided extremely potent inhibitors for all three proteases.

Table 4.1. Inhibition of Gingipains K and R and Clostripain by Aza-Peptide Epoxide and Michael Acceptor Inhibitors.

No.	Sequence	Inhibitor	k_{obs} ($M^{-1}s^{-1}$) Gingipain K (KGP)[a]	Gingipain R (RGPB)[b]	Clostripain[c]
		Epoxides			
1	PhPr-Leu-ALys-	EP-CO_2Et	1,970,000 ± 17,000	156 ± 3.5	13,500 ± 6,000
2		EP-CONHEt	3,550,000 ± 267,000	156 ± 21	26,600 ± 3,600
3		EP-CON(N-butyl)$_2$	13,500 ± 1,100	3.79 ± 0.1	2,350 ± 160
4		EP-CONH-$CH_2C_6H_5$	6,210,000 ± 640,000	272 ± 22	24,700 ± 5,500
5		EP-CONH$(CH_2)_2$-C_6H_5	462,000 ± 151,000	118 ± 4.2	12,200 ± 370
6		EP-CON$(CH_2C_6H_5)_2$	452,000 ± 63,000	104 ± 16	24,300 ± 3,500
		Michael Acceptors			
7		CH=CH-CO_2Et	3,280,000 ± 652,000	289 ± 15	40,750 ± 7,600
8		CH=CH-CO_2-$CH_2C_6H_5$	2,510,000 ± 405,000	632 ± 23	20,500 ± 12,000
9		CH=CH-CONH-$CH_2C_6H_5$	236,000 ± 14,000	20 ± 6.4	1,050 ± 67
10		CH=CH-CON(CH_3)-$CH_2C_6H_5$	1,360,000 ± 230,000	79 ± 27	6,000 ± 730
11		CH=CH-CON$(CH_2C_6H_5)_2$	2,130,000 ± 643,000	65 ± 11	20,000 ± 11,000
12		CH=CH-CON$(CH_2C_6H_5)$-(*p*-$CH_2C_6H_4F$)	801,000 ± 32,000	75 ± 2.1	13,800 ± 5,200
13		CH=CH-CON$(CH_3)CH_2$-(1-naphthyl)	975,000 ± 161,000	576 ± 19	639 ± 126
14		CH=CH-CON(benzyl)-(CH_2-2-naphthyl)	811,000 ± 150,000	98 ± 15	17,500 ± 780
15		CH=CH-CON(CH_2-1-naphthyl)$_2$	1,890,000 ± 1,400	214 ± 1.4	2,250 ± 40
16		CH=CH-CO-*N*-(tetrahydroquinoline)	252,000 ± 16,000	73 ± 7.1	326 ± 120
		Epoxides			
17	PhPr-Leu-AArg-	EP-CO_2Et	5,200 ± 870	199,000 ± 12,000	85,400 ± 6,400
18		EP-CONH-$CH_2C_6H_5$	2,620 ± 83	146,000 ± 3,800	86,900 ± 14,700
19		EP-CON$(CH_2C_6H_5)_2$	1,170	20,400 ± 1,900	189,000 ± 38,000
		Michael Acceptors			
20		CH=CH-CO_2Et	1,580 ± 47	1,490,000 ± 6,500	69,600 ± 1,500
21		CH=CH-CONH-$CH_2C_6H_5$	538	555,000 ± 40,000	287,000 ± 47,000
22		CH=CH-CON$(CH_2C_6H_5)_2$	380	804,000 ± 108,000	474,000 ± 150,000

Table 4.1. Continued.

No.	Sequence	Inhibitor	Gingipain K (KGP)[a]	Gingipain R (RGPB)[b]	Clostripain[c]
		Epoxides			
23	PhPr-Leu-AOrn-	EP-CO_2Et	190,000 ± 99,000	64.5 ± 2.1	304 ± 140
24		EP-CONH-$CH_2C_6H_5$	939,000 ± 326,000	174 ± 12	476 ± 155
25		EP-CON($CH_2C_6H_5$)$_2$	51,700 ± 9,300	34.0 ± 2.8	1,080 ± 146
		Michael Acceptors			
26		CH=CH-CO_2Et	927,000 ± 59,000	32.0 ± 2.1	788 ± 169
27		CH=CH-CONH-$CH_2C_6H_5$	24,700 ± 3,700	70.5 ± 16	NI
28		CH=CH-CON($CH_2C_6H_5$)$_2$	61,600 ± 15,000	24.0 ± 1.4	541 ± 34

a)Inhibition rates for gingipain K were determined using the incubation method. The buffer was 20 mM Bis-Tris, 150 mM NaCl, 5 mM $CaCl_2$, 0.02% NaN_3, at pH 8.0. The final inhibitor concentrations ranged from 3.78 nM to 4.6 µM. b)Inhibition rates for gingipain R were determined using the incubation method. The buffer was 0.2 M Tris/HCl, 0.1 M NaCl, 5 mM $CaCl_2$, 2 mM DTT at pH 7.5. The final inhibitor concentrations ranged from 46.3 nM to 0.46 mM. c)Inhibition rates for clostripain were determined by the progress curve method. The buffer was 20 mM Tris/HCl, 10 mM $CaCl_2$, 0.005% Brij, 2 mM DTT at pH 7.6. The final inhibitor concentrations were 0.105 µM to 0.105 mM.

Gingipain K. The ALys inhibitors were the most potent inhibitors for gingipain K, as was expected given the enzyme's preference for a P1 Lys. The ALys epoxides and Michael acceptors were about equipotent, with differences in potency depending more on the P1' substituent than the type of warhead. The most potent inhibitor in the series was the epoxide benzyl amide (**4**) with a rate constant of k_{obs} = 6,210,000 $M^{-1}s^{-1}$, one of the highest rates of inhibition ever measured in the Powers laboratory. The epoxide dibutyl amide **3** showed drastically lower potency than the other inhibitors, with the dibutyl amide probably disrupting the productive binding of the epoxide warhead to the enzyme. The series of inhibitors includes both P1' monosubstituted amides and disubstituted amides. Generally, gingipain K seemed to tolerate the disubstituted amides in Michael acceptor inhibitors better than in epoxides. With the epoxide inhibitors the mono-substituted amides display higher potency (**4** vs. **6** or **3**), whereas in the Michael acceptor inhibitors some of the disubstituted inhibitors are more potent (**9** vs. **10** or **11**). There is possibly more flexibility in the binding of the Michael acceptors, which allows the two P1' substituents in the di-substituted amides to bind appropriately without sacrificing the binding of the double bond. The fact the Michael acceptors have two faces that are susceptible to thiol attack compared to one for epoxides could also explain this phenomenon, as demonstrated in Figure 4.3. If the larger, disubstituted P1' substituent binds in such a way that the double bond or epoxide warhead is turned in the active site, the double bond is still be able to inhibit through attack of the thiol on the other face, whereas the epoxide could not. The tetrahydroquinoline inhibitor (**16**) is not as potent as other Michael acceptor disubstituted amides, most likely because of the rigidity of the ring system. These inhibitors demonstrate that the S1' site of gingipain K can

accommodate large aromatic groups, as can be seen in the Michael acceptor dinaphthyl inhibitor (**15**). While some of the ALys inhibitors are more potent than others with gingipain K, all of the inhibitors are truly excellent inhibitors of gingipain K.

The gingipain K inhibitors are more effective inactivators of gingipain K than the gingipain R inhibitors for gingipain R. In a recent paper, Bialas et al[91] described the difference in the S3 subsites of gingipains K and R, stating that the gingipain K S3 site is deeper and could bind to bulky aromatics better than gingipain R. It is possible that the phenylpropyl N-capping group on our inhibitors is engaging with the S3 subsite of gingipain K, leading to generally higher rates of inhibition.

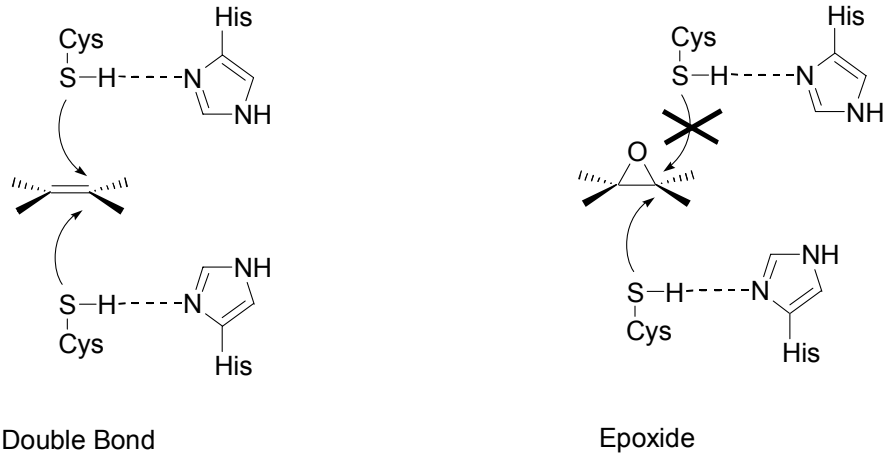

Double Bond Epoxide

Figure 4.3. Faces of possible thiol attack for double bonds and epoxides.

The AOrn inhibitors are similar to the ALys inhibitors, however the AOrn has one less methylene group in the side chain. With the shortened side chain, these inhibitors are still good inactivators of gingipain K, although they are less potent than the ALys series. The AOrn epoxide benzyl amide (**24**) is the best inhibitor of this series with gingipain K, which is consistent with the results of the ALys series. The Michael acceptor P1' preference is different than seen in the ALys series, with the P1'ethyl ester (**26**) having the greatest potency. The shorter AOrn side chain could pull the inhibitor farther into the S1 pocket in order to make contact with the deeply situated Glu, orienting the inhibitors such that larger P1' substituents are unable to bind as productively as in the ALys inhibitors.

As expected, the AArg inhibitors are only modest inhibitors of gingipain K. Generally, the epoxides are better inhibitors than the Michael acceptors in this series, and smaller P1' groups are better tolerated by the enzyme.

Gingipain R. As expected, the AArg inhibitors are the most potent inhibitors we found for gingipain R. While the rates of inhibition are not as high as the ALys with gingipain K, the AArg inhibitors are still excellent with gingipain R. Unlike gingipain K, the Michael acceptor inhibitors are generally better than the epoxides, and the choice of warhead has a greater effect on potency than the choice of P1' substituent. The ethyl ester P1' group is the best fit in both the epoxide and Michael acceptor inhibitors. Because of this, it appears that the S1' pocket of gingipain R is less accommodating of larger substituents than gingipain K.

The ALys and AOrn compounds proved to be much poorer inhibitors of gingipain R, with the ALys inhibitors being slightly more potent than the AOrn. The best of the ALys inhibitors all are Michael acceptors (**8**, **13**, **15**).

Clostripain. The AArg inhibitors are the most potent with clostripain, as is expected from clostripain specificity. Again, the potency of the AArg inhibitors with clostripain is lower than the ALys inhibitors with gingipain K. For the AArg series, the disubstituted aromatic amides are the best P1' substituent and the Michael acceptor warhead is more potent than the epoxide.

The ALys inhibitors are fair inhibitors of clostripain, but less potent than the AArg inhibitors. Of the three enzymes, clostripain shows the least specificity between AArg and ALys P1 residues.

The AOrn inhibitors are only weak inhibitors of clostripain.

Specificity. A representative number of these inhibitors were tested with caspases -3, -6, -7, and -8, and all showed no inhibition. The inhibitors tested were **2**, **4**, **8**, **11**, **15**, **20**, **23**, and **24**. Therefore, these inhibitors are specific to the gingipains and clostripain over other clan CD proteases. The caspases are potently inhibited by aza-peptide epoxides and Michael acceptors with a P1 AAsp, so this demonstrates that the P1 position is a major controller of inhibitor specificity.

Conclusion

In aza-peptide epoxides and Michael acceptors we have found an extremely potent class of inhibitors for the gingipains and clostripain. Of the three enzymes, gingipain K is the most susceptible to inhibition by this class of compounds. This class of compounds is also highly specific, both between the three proteases investigated and over other clan CD enzymes. Comparing Michael acceptor inhibitors with epoxide inhibitors containing the same P1' moiety has led to the insight that the Michael acceptors with larger P1' groups could be better inhibitors than comparable epoxides because of the two possible faces of attack. We found that the inhibitor potency is tunable depending on the P1' substituent present in the inhibitor. Given their potency and specificity, these inhibitors could be useful tools in the research and treatment of the bacterial infections involving the gingipains and clostripain.

Experimental

Enzyme Assays. Gingipains R and K were assayed with the inhibitors using the incubation method, while clostripain was assayed using the progress curve method. All enzyme activities were determined using the appropriate fluorogenic peptide 7-amino-4-methylcoumarin substrates (AMC, excitation λ = 360 nm, emission λ = 405 nm). The fluorescence was detected with a Tecan Spectraflour Microplate Reader (Tecan US, Research Triangle Park, NC).

Gingipain R. Gingipain R was obtained from the lab of Jan Potempa (University of Georgia, Athens, GA) and is stored in a buffer of 20 mM Bis-Tris, 150 mM NaCl, 5 mM $CaCl_2$, 0.02% NaN_3, pH 7.5, at a concentration of 1 mg/mL. The kinetic assay buffer is 0.2 M Tris/HCl, 0.1 M NaCl, 5 mM $CaCl_2$, 2 mM DTT, pH 7.5. The enzyme was activated in the kinetic assay buffer for 1 hr at 0 ^{o}C prior to use. Inhibitor in DMSO (25 μL) was diluted with the kinetic assay buffer (244 μL), and the inhibition reaction was initiated with the addition of enzyme (1 μL) at t = 0 s ([E] = 74.07 nM, [I] = 46.3 nM to 0.46 mM). Aliquots (25 μL) of this incubation solution were removed at intervals and diluted into a solution containing kinetic assay buffer (100 μL), and the substrate Z-Phe-Arg-AMC (26.7 μM) in DMSO (5 μL). Enzyme activity was monitored by following the change in fluorescence at 465 nm. Inhibition rates were determined in duplicate, and the error ranges were calculated.

Gingipain K. Gingipain K was obtained from the lab of Jan Potempa (University of Georgia, Athens, GA) and is stored in a buffer of 20 mM Bis-Tris, 150 mM NaCl, 5 mM $CaCl_2$, 0.02% NaN_3, pH 8.0 at a concentration of 3 μM. The kinetic assay buffer is 0.2 M Tris/HCl, 0.1 M NaCl, 5 mM $CaCl_2$, 2 mM DTT, pH 8.0. The enzyme was activated in the kinetic assay buffer for 1 hr at 0 ^{o}C prior to use. Inhibitor in DMSO was diluted with kinetic assay buffer, and the inhibition reaction was initiated with the addition of enzyme at t = 0 s ([E] = 5.43 nM). Aliquots of this incubation solution were taken and diluted into a solution containing kinetic assay buffer, and the substrate Suc-Ala-Phe-Lys-AMC·TFA (35 μM) with a small amount of DMSO to dissolve. Enzyme activity was monitored by following the change in fluorescence at 465 nm.

Clostripain. Clostripain was purchased from Worthington Biochemicals (Athens, GA) as a solid. The enzyme was activated in the kinetic assay buffer 20 mM Tris/HCl, 10 mM $CaCl_2$, 0.005% Brij, 2 mM DTT, pH 7.6 for 1 hr at 0 ^{o}C. The reaction was initiated by the addition of enzyme (25 nM final concentration) to a solution of kinetic assay buffer, inhibitor, and the substrate Z-Phe-Arg-AMC (0.273 mM, K_M = 91.6 μM) and the fluorescence was monitored at 465 nm over 10 min.

REFERENCES

(1) Puente, X. S.; Sanchez, L. M.; Gutierrez-Fernandez, A.; Velasco, G.; Lopez-Otin, C. A genomic view of the complexity of mammalian proteolytic systems. *Biochem. Soc. Trans.* **2005***, 33*, 331-334.

(2) Rawlings, N. D.; Barrett, A. J. Evolutionary families of peptidases. *Biochem. J.* **1993***, 290*, 205-218.

(3) Rawlings, N. D.; Barrett, A. J. Families of cysteine peptidases. *Methods Enzymol.* **1994***, 244*, 461-486.

(4) Schechter, I.; Berger, A. On the size of the active site in proteases. I. Papain. *Biochem. Biophys. Res. Commun.* **1967***, 27*, 157-162.

(5) Kamphius, I. G.; Kalk, K. H.; Swarte, M. B.; Drenth, J. Structure of papain refined at 1.65 Å resolution. *J. Mol. Biol.* **1984***, 1791*, 233-256.

(6) Ray, S. K.; Banik, N. L. Calpain and its involvement in the pathophysiology of CNS injuries and diseases: Therapeutic potential of calpain inhibitors for prevention of neurodegeneration. *Curr. Drug Targets- CNS Neurol. Dis.* **2003***, 2*, 173-189.

(7) Strobl, S.; Fernandez-Catalan, C.; Braun, M.; Huber, R.; Masumoto, H.; Nakagawa, K.; Irie, H.; Sorimachi, H.; Bourenkow, G.; Bartunik, H.; Suzuki, K.; Bode, W. The crystal structure of calcium-free human *m*-calpain suggests an electrostatic switch mechanism for activation by calcium. *Proc Natl Acad Sci U S A* **2000***, 97*, 588-592.

(8) Moldoveanu, T.; Hosfield, C. M.; Lim, D.; Elce, J. S.; Jia, Z.; Davies, P. L. A Ca^{2+} switch aligns the active site of calpain. *Cell* **2002***, 108*, 649-660.

(9) Donkor, I. O. A survey of calpain inhibitors. *Curr. Med. Chem.* **2000***, 7*, 1171-1188.

(10) Iqbal, M.; Messina, P. A.; Freed, B.; Das, M.; Chatterjee, S.; Tripathy, R.; Tao, M.; Josef, K. A.; Dembofsky, B.; Dunn, D.; Griffith, E.; Siman, R.; Senadhi, S. E.; Biazzo, W.; Bozyczko-Coyne, D.; Meyer, S. L.; Ator, M. A.; Bihovsky, R. Subsite requirements for peptide aldehyde inhibitors of human calpain I. *Bioorg. Med. Chem. Lett.* **1997***, 7*, 539-544.

(11) Yamamoto, A.; Tomoo, K.; Matsugi, K.; Hara, T.; In, Y.; Murata, M.; Kitamura, K.; Ishida, T. Structrural basis for development of cathepsin B-specific noncovalent-type inhibitor: crystal structure of cathepsin B-E64c complex. *Biochimica et Biophysica Acta* **2002***, 1597*, 244-251.

(12) Schaschke, N.; Assfalg-Machleidt, I.; Machleidt, W.; Turk, D.; Mororder, L. E-64 analogues as inhibitors of cathepsin B. On the role of the absolute configuration of the epoxysuccinyl group. *Bioorg. Med. Chem.* **1997***, 5*, 1789-1797.

(13) Philchenkov, A. Caspases: potential targets for regulating cell death. *J. Cell Mol. Med.* **2004***, 8*, 432-444.

(14) O'Brien, T.; Lee, D. Prospects for Caspase Inhibitors. *Mini-Reviews in Medicinal Chemistry* **2004***, 4*, 153.

(15) Ally, N.; Whisstock, J. C.; Sieprawska-Lupa, M.; Potempa, J.; Le Bonniec, B. F.; Travis, J.; Pike, R. N. Characterization of the specificity of arginine-specific gingipains from *Porphyromonas gingivalis* reveals active site differences between different forms of the enzymes. *Biochemistry* **2003***, 42*, 11693-11700.

(16) Ullmann, D.; Jakubke, H. The specificity of clostripain from *Clostridium hystolyticum*: Mapping the S' subsites via acyl transfer to amino acid amides and peptides. *Eur. J. Biochem.* **1994***, 223*, 865-872.

(17) Powers, J. C.; Asgian, J. L.; Ekici, O. D.; James, K. E. Irreversible inhibitors of serine, cysteine, and threonine proteases. *Chem. Rev.* **2002***, 102*, 4639-4750.

(18) Kitz, R.; Wilson, I. B. Esters of methanesulfonic acid as irreversible inhibitors of acetylcholinesterase. *J. Biol. Chem.* **1962***, 237*, 3245-3249.

(19) Tian, W. X.; Tsou, C. L. Determination of the rate constant of enzyme modification by measuring the substrate reaction in the presence of the modifier. *Biochemistry* **1982***, 21*, 1028-1032.

(20) Bartus, R. T.; Dean, R. L.; Cavanaugh, K.; Eveleth, D.; Carriero, D. L.; Lynch, G. Time-related neuronal changes following middle cerebral artery occlusion: implications for therapeutic intervention and the role of calpain. *J. Cereb. Blood. Flow Metab.* **1995***, 15*, 969-979.

(21) Bartus, R. T.; Elliott, P. J.; Hayward, N. J.; Dean, R. L.; Harbeson, S.; Straub, J. A.; Li, Z.; Powers, J. C. Calpain as a novel target for treating acute neurodegenerative disorders. *Neurol. Res.* **1995***, 17*, 249-258.

(22) Li, Z.; Hogan, E. L.; Banik, N. L. Role of calpain in spinal cord injury: increased mcalpain immunoreactivity in spinal cord after compression injury in the rat. *Neurochem. Int.* **1995***, 27*, 425-432.

(23) Saatman, K. E.; Murai, H.; Bartus, R. T.; Smith, D. H.; Hayward, N. J.; Perri, B. R.; McIntosh, T. K. Calpain inhibitor AK295 attenuates motor and cognitive deficits following experimental brain injury in the rat. *Proc. Natl. Acad. Sci. U. S. A.* **1996***, 93*, 3428-3433.

(24) Kamakura, K.; Ishiura, S.; Sugita, H.; Toyokura, Y. Identification of Ca2+-activated neutral protease in the peripheral nerve and its effects on neurofilament degeneration. *J. Neurochem.* **1983**, *40*, 908-913.

(25) Veeranna; Kaji, T.; Boland, B.; Odrljin, T.; Mohan, P.; Basavarajappa, B. S.; Peterhoff, C.; Cataldo, A.; Rudnicki, A.; Amin, N.; Li, B. S.; Pant, H. C.; Hungund, B. L.; Arancio, O.; Nixon, R. A. Calpain mediates calcium-induced activation of the Erk1,2 MAPK pathway and cytoskeletal phosphorylation in neurons: Relevance to Alzheimer's disease. *Am. J. Path.* **2004**, *165*, 795-805.

(26) Huang, Y.; Wang, K. K. W. The calpain family and human disease. *Trends Mol. Med.* **2001**, *7*, 355-361.

(27) Crocker, S. J.; Smith, P. D.; Jackson-Lewis, V.; Lamba, W. R.; Hayley, S. P.; Grimm, E.; Callaghan, S. M.; Slack, R. S.; Przedborski, S.; Robertson, G. S.; Anisman, H.; Merali, C.; Park, D. S. Inhibition of calpains prevents neuronal and behavioral deficits in an MPTP mouse model of Parkinson's disease. *J. Neurosci.* **2003**, *23*, 4081-4091.

(28) Spencer, M. J.; Croall, D. E.; Tidball, J. G. Calpains are activated in necrotic fibers from mdx dystrophic mice. *J. Biol. Chem.* **1995**, *270*, 10909-10914.

(29) Harris, F.; Chatfield, L.; Singh, J.; Phoenix, D. A. Role of calpains in diabetes mellitus: a mini review. *Mol. Cell. Biochem.* **2004**, *261*, 161-167.

(30) Branca, D. Calpain-related diseases. *Biochem. Biophys. Res. Commun.* **2004**, *322*, 1098-1104.

(31) Wingrave, J. M.; Sribnick, E. A.; Wilford, G. G.; Matzelle, D. D.; Mou, J. A.; Ray, S. K.; Hogan, E. L.; Banik, N. L. Higher calpastatin levels correlate with resistance to calpain-mediated proteolysis and neuronal apoptosis in juvenile rats after spinal cord injury. *J. Neurotrauma* **2004**, *21*, 1240-1254.

(32) Kupina, N. C.; Nath, R.; Bernath, E. E.; Inoue, J.; Mitsuyoshi, A.; Yuen, P.; Wang, K. K. W.; Hall, E. D. The novel calpain inhibitor SJA6017 improves functional outcome after delayed administration in a mouse model of diffuse brain injury. *J. Neurotrauma* **2001**, *18*, 1229-1240.

(33) Moldoveanu, T.; Campbell, R. L.; Cuerrier, D.; Davies, P. L. Crystal structures of the calpain-E64 and -leupeptin inhibitor complexes reveal mobile loops gating the active site. *J. Mol. Biol.* **2004**, *343*, 1313-1326.

(34) Parkes, C.; Kembhavi, A. A.; Barrett, A. J. Calpain inhibition by peptide epoxides. *Biochem. J.* **1985**, *230*, 509-516.

(35) Li, Z.; Ortega-Vilain, A. C.; Patil, G. S.; Chu, D. L.; Foreman, J. E.; Eveleth, D. D.; Powers, J. C. Novel peptidyl alpha-keto amide inhibitors of calpains and other cysteine proteases. *J. Med. Chem.* **1996**, *39*, 4089-4098.

(36) Bartus, R. T.; Hayward, N. J.; Elliott, P. J.; Sawyer, S. D.; Baker, K. L.; Dean, R. L.; Akiyama, A.; Straub, J. A.; Harbeson, S. L.; Li, Z.; et al. Calpain inhibitor AK295 protects neurons from focal brain ischemia. Effects of postocclusion intra-arterial administration. *Stroke* **1994**, *25*, 2265-2270.

(37) Wang, M. S.; Davis, A. A.; Culver, D. G.; Wang, Q.; Powers, J. C.; Glass, J. D. Calpain inhibition protects against Taxol-induced sensory neuropathy. *Brain* **2004**, *127*, 671-679.

(38) Hanada, K.; Tamai, M.; Yamagishi, M.; Ohmura, S.; Sawada, J.; Tanaka, I. Studies on thiol protease inhibitior. Part I. Isolation and characterization of E-64, a new thiol protease inhibitor. *Agric. Biol. Chem.* **1978**, *42*, 523-528.

(39) Lee, T. W.; Cherney, M. M.; Liu, J.; James, K. E.; Powers, J. C.; Eltis, L. D.; James, M. N. G. Crystal structures reveal an induced-fir binding of a substrate-like aza-peptide epoxide to SARS coronavirus main peptidase. *J. Mol. Biol.* **2007**, *366*, 916-932.

(40) Lee, T. W.; Cherney, M. M.; Huitema, C.; Liu, J.; James, K. E.; Powers, J. C.; Eltis, L. D.; James, M. N. G. Crystal structures of the main peptidase from the SARS coronavirus inhibited by a substrate-like aza-peptide epoxide. *J. Mol. Biol.* **2005**, *353*, 1137-1151.

(41) Ganesan, R.; Jelakovic, S.; Campbell, A. J.; Li, Z. Z.; Asgian, J. L.; Powers, J. C.; Grutter, M. G. Exploring the S4 and S1 prime subsite specificities in caspase-3 with aza-peptide epoxide inhibitors. *Biochemistry* **2006**, *45*, 9059-9067.

(42) Ishiura, S.; Nonaka, I.; Sugita, H. Supression of calcium-induced removal of the Z-line by a thiol protease inhibitor, E-64-c. *J. Biochem. (Tokyo)* **1981**, *90*, 283-285.

(43) James, K. E.; Asgian, J. L.; Li, Z. Z.; Ekici, O. D.; Rubin, J. R.; Mikolajczyk, J.; Salvesen, G. S.; Powers, J. C. Design, synthesis, and evaluation of aza-peptide epoxides as selective and potent inhibitors of caspases-1, -3, -6, and -8. *J. Med. Chem.* **2004**, *47*, 1553-1574.

(44) Mori, K.; Iwasawa, H. Stereoselective synthesis of optically active forms of σ-Multistriatin: the attractant for European populations of the smaller European elm bark beetle. *Tetrahedron* **1980**, *36*, 87-90.

(45) Atwell, G. J.; Denny, W. A. Monoprotection of α,ω-alkanediamines with the N-benzyloxycarbonyl group. *Synthesis* **1984**, *12*, 1032-1033.

(46) Thornberry, N. A.; Bull, H. G.; Calacay, J. R.; Chapman, K. T.; Howard, A. D.; Kostura, M. J.; Miller, D. K.; Molineaux, S. M.; Weidner, J. R.; Aunins, J. A novel heterodimeric cysteine protease is required for interleukin-1 beta processing in monocytes. *Nature* **1992**, *356*, 768-774.

(47) Cerretti, D. P.; Kozlosky, C. J.; Mosley, B.; Nelson, N.; Van Ness, K.; Greenstreet, T. A.; March, C. J.; Kronheim, S. R.; Druck, T.; Cannizzaro, L. A. Molecular cloning of the interleukin-1 beta converting enzyme. *Science* **1992**, *256*, 97-100.

(48) Ellis, R. E.; Yuan, J. Y.; Horvitz, H. R. Mechanisms and functions of cell death. *Annu. Rev. Cell. Biol.* **1991**, *7*, 663-698.

(49) Alnemri, E. S.; Livingston, D. J.; Nicholson, D. W.; Salvensen, G.; Thornberry, N. A. Human ICE/CED-3 protease nomenclature. *Cell* **1996**, *87*, 171.

(50) Muzio, M.; Chinnaiyan, A. M.; Kischkel, F. C.; O'Rourke, K.; Shevchenko, A.; Ni, J.; Scaffidi, C.; Bretz, J. D.; Zhang, M.; Gentz, R.; Mann, M.; Krammer, P. H.; Peter, M. E.; Dixit, V. M. FLICE, a novel FADD-homologous ICE/CED-3-like protease, is recruited to the CD95 (Fas/APO-1) death-inducing signalling complex. *Cell* **1996**, *85*, 817-827.

(51) Li, P.; Nijhawan, D.; Budihardjo, I.; Srinivasula, S. M.; Ahmad, M.; Alnemri, E. S.; Wang, X. Cytochrome c and dATP-dependent formation of Apaf-1/caspase-9 complex initiates an apoptotic protease cascade. *Cell* **1997**, *91*, 479-489.

(52) Donepudi, M.; Grutter, M. G. Structure and zymogen activation of caspases. *Biophys. Chem.* **2002**, *101-102*, 145-153.

(53) Nicholson, D. W. Caspase structure, proteolytic substrates, and function during apoptotic cell death. *Cell Death Diff.* **1999**, *6*, 1028-1042.

(54) Wilson, K. P.; Black, J. F.; Thomson, J. A.; Kim, E. E.; Griffith, J. P. Structure and mechanism of interleukin-1β converting enzyme. *Nature* **1994**, *370*, 270-275.

(55) Rotonda, J.; Nicholson, D. W.; Fazil, K. M.; Gallant, M.; Gareau, Y. The three dimensional structure of apopain/CPP32, a key mediator of apoptosis. *Nature Struct. Biol.* **1996**, *3*, 619-625.

(56) Riedl, S. J.; Renatus, M.; Schwarzenbacher, R.; Zhou, Q.; Sun, C. Structural basis for the inhibition of caspase-3 by XIAP. *Cell* **2001**, *104*, 791-800.

(57) Chai, J.; Shiozaki, E.; Srinivasula, S. M.; Wu, Q.; Datta, P. Structural basis of caspase-7 inhibition by XIAP. *Cell* **2001**, *104*, 769-780.

(58) Blanchard, H.; Kodandapani, L.; Mittl, P. R.; Marco, S. D.; Krebs, J. F. The three-dimensional structure of caspase-8: and initiator enzyme in apoptosis. *Structure Fold Des.* **1999**, *7*, 1125-1133.

(59) Renatus, M.; Stennicke, H. R.; Scott, F. L.; Liddington, R. C.; Salvensen, G. S. Dimer formation drives the activation of the cell death protease caspase-9. *Proc. Natl. Acad. Sci. U. S. A.* **2001**, *98*, 14250-14255.

(60) Chereau, D.; Kodandapani, L.; Tomaselli, K. J.; Spada, A. P.; Wu, J. C. Structural and functional analysis of caspase active sites. *Biochemistry* **2003**, *42*, 4151-4160.

(61) Holly, T.; Drinic, A.; Byun, Y.; Nakamura, S.; Harris, K.; Klocke, F.; Cryns, V. Caspase inhibition reduces myocyte cell death induced by myocardial ischemia and reperfusion in vivo. *J. Mol. Cell. Cardiol.* **1999**, *31*, 1709-1715.

(62) Fink, K.; Zhu, J.; Namura, S.; Shimizu-Sasamata, M.; Endres, M.; Ma, J.; Dalkara, T.; Yuan, J. Y.; Moskowitz, M. A. Prolonged therapeutic window for ischemic brain damage caused by delayed caspase activation. *J. Cereb. Blood Flow Metab.* **1998**, *18*, 1071-1076.

(63) Beer, R.; Franz, G.; Krajewski, S.; Pike, B.; Hayes, R.; Reed, J.; Wang, K.; Klimmer, C.; Schmutzhard, E.; Poewe, W.; Kampfl, A. Temporal and spatial profile of caspase 8 expression and proteolysis after experimental traumatic brain injury. *J. Neurochem.* **2001**, *78*, 862-873.

(64) Springer, J.; Azbill, R.; Knapp, P. Activation of the caspase-3 apoptotic cascade in traumatic spinal cord injury. *Nature Med.* **1999**, *5*, 943-946.

(65) Angus, D.; Linde-Zwirble, W.; Lidicker, J.; Clermont, G.; Carcillo, J.; Pinsky, M. Epidemiology of severe sepsis in the United States: analysis of incidence, outcome, and associated costs of care. *Crit. Care Med.* **2001**, *29*, 1303-1310.

(66) Bantel, H.; Ruck, P.; Gregor, M.; Schulze-Osthoff, K. Detection of elevated caspase activation and early apoptosis in liver diseases. *Eur. J. Cell Biol.* **2001**, *80*, 230-239.

(67) Gervais, F.; Xu, D.; Robertson, G. S.; Vaillancourt, J.; Zhu, Y.; Huang, J.; LeBlanc, A.; Smith, D. H.; Rigby, M.; Shearman, M.; Clarke, E.; Zheng, H.; Ploeg, L.; Ruffolo, S.; Thornberry, N. A.; Xanthoudakis, S.; Zamboni, R.; Roy, S.; Nicholson, D. W. Involvement of caspases in proteolytic cleavage of Alzheimer's amyloid-beta precursor protein and amyloidogenic A beta peptide formation. *Cell* **1999**, *97*, 395-406.

(68) Hartmann, A.; Hunot, S.; Michel, P.; Muriel, M.-P.; Vyas, S.; Faucheux, B.; Mouatt-Prigent, A.; Turmel, H.; Srinivasan, A.; Ruberg, M.; Evan, G.; Agid, Y.; Hirsch, E. Caspase-3: A vulnerability factor and final effector in apoptotic death of dopaminergic neurons in Parkinson's disease. *Proc. Natl. Acad. Sci. U. S. A.* **2000**, *97*, 2875-2880.

(69) Gervais, F.; Singaraja, R.; Xanthoudakis, S.; Gutekunst, C. A.; Leavitt, B. R.; Metzler, M.; Hackam, A. S.; Tam, J.; Vaillancourt, J.; Houtzager, V.; Rasper, D. M.; Roy, S.; Hayden, M.; Nicholson, D. W. Recruitment and activation of caspase-8 by the Huntingtin-interacting protein Hip-1 and a novel partner Hippi. *Nature Cell Biol.* **2002**, *4*, 95-105.

(70) Ku, G.; Faust, T.; Lauffer, L.; Livingston, D. L.; Harding, M. Interleukin-1 beta converting enzyme inhibition blocks progression of type II collagen-induced arthritis in mice. *Cytokine* **1996**, *8*, 377-386.

(71) Rozman-Pungercar, J.; Kopitar-Jerala, N.; Bogyo, M.; Turk, D.; Vasiljeva, O.; Stefe, I.; Vandenabeel, P.; Bromme, D.; Puizdar, V.; Fonovic, M.; Trstenjak-Prebanda, M.; Dolenc, I.; Turk, V.; Turk, B. Inhibition of papain-like cysteine proteases and legumain by caspase-specific inhibitors: when reaction mechanism is more important than specificity. *Cell Death Diff.* **2003**, *10*, 881-888.

(72) Neumar, R. W.; Xu, Y. A.; Gada, H.; Guttmann, R. P.; Siman, R. Cross-talk between calpain and caspase proteolytic systems during neuronal apoptosis. *J. Biol. Chem* **2003**, *278*, 14162-14167.

(73) Ekert, P. G.; Silke, J.; Vaux, D. L. Caspase inhibitors. *Cell Death Diff.* **1999**, *6*, 1081-1086.

(74) Garcia-Calvo, M.; Peterson, E. P.; Leiting, B.; Ruel, R.; Nicholson, D. W.; Thornberry, N. A. Inhibition of human caspases by peptide-based and macromolecular inhibitors. *J. Biol. Chem.* **1998**, *273*, 32608-32613.

(75) Ekici, O. D.; Gotz, M. G.; James, K. E.; Li, Z. Z.; Rukamp, B. J.; Asgian, J. L.; Caffrey, C. R.; Hansell, E.; Dvorak, J.; McKerrow, J. H.; Potempa, J.; Travis, J.; Mikolajczyk, J.; Salvesen, G. S.; Powers, J. C. Aza-peptide Michael acceptors: a new class of inhibitors specific for caspases and other clan CD cysteine proteases. *J. Med. Chem.* **2004**, *47*, 1889-1892.

(76) Eichinger, A.; Beisel, H. G.; Jacob, U.; Huber, R.; Medrano, F. J.; Banbula, A.; Potempa, J.; Travis, J.; Bode, W. Crystal structure of gingipain R: an Arg-specific bacterial cysteine proteinase with a caspase-like fold. *EMBO J.* **1999**, *18*, 5453-5462.

(77) Kadowaki, T.; Nakayama, K.; Yoshimura, F.; Okamoto, K.; Abe, N.; Yamamoto, K. Arg-gingipain acts as a major processing enzyme for various cell surface proteins in *Porphyromonas gingivalis*. *J. Biol. Chem.* **1998**, *273*, 29072-29076.

(78) Banbula, A.; Bugno, M.; Kuster, A.; Heinrich, P. C.; Travis, J.; Potempa, J. Rapid and efficient inactivation of IL-6 gingipains, lysine- and arginine-specific proteinases from *Porphyromonas gingivalis*. *Biochem. Biophys. Res. Commun.* **1999**, *261*, 598-602.

(79) Mikolajczyk-Pawlinska, J.; Travis, J.; Potempa, J. Modulation of interleukin-8 activity by gingipains from *Porphyromonas gingivalis*: implications for pathogenicity of periodontal disease. *FEBS Lett.* **1998**, *440*, 282-286.

(80) Imamura, T.; Potempa, J.; Tanase, S.; Travis, J. Activation of blood coagulation factor X by arginine-specific cysteine proteinases (gingipain-Rs) from *Porphyromonas gingivalis*. *J. Biol. Chem.* **1997**, *272*, 16062-16067.

(81) Houle, M. A.; Grenier, D.; Plamondon, P.; Nakayama, K. The collagenase activity of *Porphyromonas gingivalis* is due to Arg-gingipain. *FEMS Microbiol. Lett.* **2003**, *221*, 181-185.

(82) Nishikata, M.; Yoshimura, F. Characterization of *Porphyromonas (bacteroides) gingivalis* hemagglutinin as a protease. *Biochem. Biophys. Res. Commun.* **1991**, *178*, 336-342.

(83) Shah, H. N.; Gharbia, S. E. Lysis of erythrocytes by the secreted cysteine proteinase of *Porphyromonas gingivalis* W83. *FEMS Microbiol. Lett.* **1989**, *52*, 213-217.

(84) Pike, R.; McGraw, W.; Potempa, J.; Travis, J. Lysine- and arginine-specific proteinases from *Porphyromonas gingivalis*. Isolation, characterization, and evidence for the existence of complexes with hemagglutinins. *J. Biol. Chem.* **1994**, *269*, 406-411.

(85) Smalley, J. W.; Birss, A. J. Extracellular vesicle-associated and soluble trypsin-like enzyme fractions of *Porphyromonas gingivalis* W50. *Oral Microbiol. Immunol.* **1991**, *6*, 202-208.

(86) Chen, Z.; Potempa, J.; Polanowski, A.; Wikstrom, M.; Travis, J. Purification and characterization of a 50-kDa cysteine proteinase (gingipain) from *Porphyromonas gingivalis*. *J. Biol. Chem.* **1992**, *267*, 18896-18901.

(87) Kadowaki, T.; Kitano, S.; Baba, A.; Takii, R.; Hashimoto, M.; Katunuma, N.; Yamamoto, K. Isolation and characterization of a novel and potent inhibitor of Arg-gingipain from *Streptomyces sp*. strain FA-70. *Biol. Chem.* **2003**, *384*, 911-920.

(88) Kochalaty, W.; Krejci, L. E. The activation mechanism and physiochemical properties of *Clostridium histolyticum* proteinase. *Arch. Biochem. Biophys.* **1948**, *18*, 1-11.

(89) Cole, P. W.; Murakami, K.; Inagami, T. Specificity and mechanism of clostripain catalysis. *Biochemistry* **1971**, *10*, 4246-4252.

(90) Kembhavi, A. A.; Buttle, D. J.; Rauber, P.; Barrett, A. J. Clostripain: charaterization of an active site. *FEBS Lett.* **1991**, *283*, 277-280.

(91) Bialas, A.; Grembecka, J.; Krowarsch, D.; Otlewski, J.; Potempa, J.; Mucha, A. Exploring the Sn binding pockets in gingipains by newly developed inhibitors: structure-based design, chemistry, and activity. *J. Med. Chem.* **2006**, *49*, 1744-1753.

VITA

The author, Sylvia Shadinger Bridges, was born March 21, 1978 in Nashville, TN, where she graduated from Hume Fogg Academic Magnet High School in 1996. She then attended Mercer University in Macon, GA, where she received a Bachelor of Science Degree in Chemistry with Honors in 2000. Sylvia then began her graduate studies at the Georgia Institute of Technology in Atlanta, GA, in the Department of Chemistry and Biochemistry under the instruction of Dr. James C. Powers. She received her Ph.D. in Chemistry in August 2008.